SCALE-UP OF POLYHYDROXYALKANOATES (PHA) PRODUCTION BY BACTERIAL STRAINS OF JALANDHAR (INDIA) WASTE STREAMS USING A COMBINED TREATMENT APPROACH

Thesis Submitted for the Award of the Degree of

DOCTOR OF PHILOSOPHY

in

Microbiology

By

Mukesh Kumar

Registration Number: 11816324

Supervised By

Dr.Arun Karnwal (20599)

Department of Microbiology (Professor)

Lovely Professional University

LOVELY PROFESSIONAL UNIVERSITY, PUNJAB
2025

DECLARATION

I, hereby declared that the presented work in the thesis entitled "Scale-up of polyhydroxyalkanoates (PHA) production by bacterial strains of Jalandhar (India) waste streams using a combined treatment approach" in fulfilment of degree of **Doctor of Philosophy (Ph. D.)** is outcome of research work carried out by me under the supervision of Prof. Arun Karnwal working as Professor in the Microbiology, School of Bioengineering and Biosciences of Lovely Professional University, Punjab, India. In keeping with general practice of reporting scientific observations, due acknowledgements have been made whenever work described here has been based on findings of other investigator. This work has not been submitted in part or full to any other University or Institute for the award of any degree.

(Signature of Scholar)

Name of the scholar: Mukesh Kumar
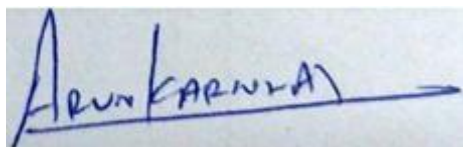
Registration No.: 11816324

Department/school: School of Bioengineering and Biosciences

Lovely Professional University,

Punjab, India

CERTIFICATE

This is to certify that the work reported in the Ph. D. thesis entitled "Scale-up of polyhydroxyalkanoates (PHA) production by bacterial strains of Jalandhar (India) waste streams using a combined treatment approach" submitted in fulfillment of the requirement for the award of degree of **Doctor of Philosophy (Ph.D.)** in the School of Bioengineering and Biosciences, is a research work carried out by Mukesh Kumar, 11816324, is bonafide record of his/her original work carried out under my supervision and that no part of thesis has been submitted for any other degree, diploma or equivalent course.

(Signature of Supervisor)

Name of supervisor: Arun Karnwal

Designation: Professor

Department/school: School of Bioengineering and Biosciences

University: Lovely Professional University

Abstract

Plastic has become important to current lifestyle because of their adaptability and low cost. However, their widespread use has caused significant harm to ecosystems. Plastics do not easily degrade, leading to the accumulation of waste in landfills, oceans, and other natural habitats. This accumulation causes damage to marine life, birds, and even land animals, as plastic debris can entangle, poison, or be mistakenly ingested by wildlife. Additionally, the breakdown of plastics into microplastics further compounds the issue, allowing these tiny fragments to enter food chains, potentially affecting human health. As awareness of these environmental impacts grows, the search for alternatives to conventional plastics becomes more pressing. One promising alternative is Polyhydroxyalkanoates (PHA), a bioplastics synthesized by microorganisms that can biodegrade naturally in various environments, including soil and marine ecosystems. PHA, particularly polyhydroxybutyrate (PHB), is an ideal replacement for petroleum-based plastics due to its biodegradable nature, biocompatibility, and ability to be produced from renewable resources. PHB possesses properties akin to traditional plastics like polypropylene, making it a feasible substitute in many applications. However, the commercial production of PHA has been hindered by the high cost of raw materials and fermentation processes. In order to make PHA production economically viable, researchers have explored using less expensive and sustainable substrates. This study investigates the potential of hydrolyzed wood waste and wastewater as low-cost substrates for PHA production. Wood waste, an abundant byproduct of forestry and industrial processes, contains cellulose and hemicellulose, which can be hydrolyzed into fermentable sugars. These sugars serve as carbon sources for PHA-producing bacteria, offering a sustainable approach to bioplastic production while addressing waste management. This research explored the potential of isolating PHA-producing bacteria from wastewater streams in Jalandhar, India. Wastewater is a rich source of diverse microbial communities, some of which can synthesize PHA as an energy storage compound. Samples were collected from various locations in Jalandhar, including industrial and sewage waste streams. The bacterial isolates underwent screening for PHA production capabilities using Nile Blue and Sudan Black staining

techniques, which are commonly employed to detect intracellular PHA granules. The stained colonies that showed positive results were further selected for PHA production studies. The first phase of production involved culturing the isolates in a minimal salt medium (MSM) to determine the most efficient PHA producers under controlled conditions. The PHA-producing isolates were identified through 16S rRNA sequencing.The sequencing results revealed that the most promising PHA producers belonged to the genera *Klebsiella* and *Escherichia*. The three isolates identified as the best PHA producers were *Klebsiella sp.* strain MK3, *Klebsiella pneumoniae* strain DSM 30104 (MK2023), and *Escherichia fergusonii* ATCC 35469 MK. These isolates were subsequently evaluated for their capacity to produce PHA using hydrolyzed wood waste as a carbon source. The wood waste was pretreated and hydrolyzed to release fermentable sugars, which the bacterial isolates could metabolize for PHA synthesis. The total PHA production and PHB yield per mL of medium were measured for each isolate. The results showed that *Escherichia fergusonii* ATCC 35469 MK was the most efficient PHA producer, achieving a total PHB production of approximately 11,900 mg and a 5.9 mg/mL yield. In contrast, *Klebsiella sp.* strain MK3 produced the lowest amount of PHB, with a total production of around 8,700 mg and a yield of 4.37 mg/mL. The intermediate producers were *Klebsiella pneumoniae* strain DSM 30104 (MK2023) and *Pseudomonas fluorescens* MTCC 1749, with total PHB productions of 10,400 mg and 10,800 mg, respectively and yields per mL of 5.24 mg/mL and 5.41 mg/mL. Several analytical techniques were employed to confirm the chemical structure and composition of the produced PHA. UV-Vis spectroscopy was used to detect the characteristic PHB peak at 235 nm, indicating the presence of crotonic acid, a degradation product of PHB. Fourier-transform infrared spectroscopy (FTIR) was also performed, revealing absorption peaks consistent with PHB, such as those corresponding to ester and carbonyl groups. Gas chromatography-mass spectrometry (GC-MS) and nuclear magnetic resonance (NMR) spectroscopy were employed to further characterize the PHA.The results from these techniques confirmed that the biopolymer produced by the isolates was indeed PHB, a subclass of PHA, thereby verifying its identity as a biodegradable plastic with desirable properties. This study demonstrates that hydrolyzed wood waste and wastewater can be viable and cost-effective substrates for PHA production. The successful isolation of efficient PHA producers from wastewater streams in Jalandhar underscores

the potential of harnessing microbial diversity in waste environments for bioplastic production. By utilizing renewable and abundant waste materials, the production costs associated with PHA can be significantly reduced, making it a more feasible alternative to conventional plastics. This approach provides a sustainable solution to plastic pollution and contributes to waste management by valorizing wood waste and wastewater. In conclusion, combining hydrolyzed wood waste and wastewater as substrates for PHA production offers a promising route toward environmentally friendly bioplastic synthesis. The bacterial isolates identified in this study, particularly *Escherichia fergusonii* ATCC 35469 MK, demonstrated significant potential for PHB production. By optimizing the use of inexpensive substrates and harnessing the metabolic capabilities of waste-derived microorganisms, This approach could reduce the ecological influence of plastics and support a circular economy by enabling the sustainable production of biodegradable materials.

Production of polyhydroxyalkanoate (PHA) using wood waste as substrate media
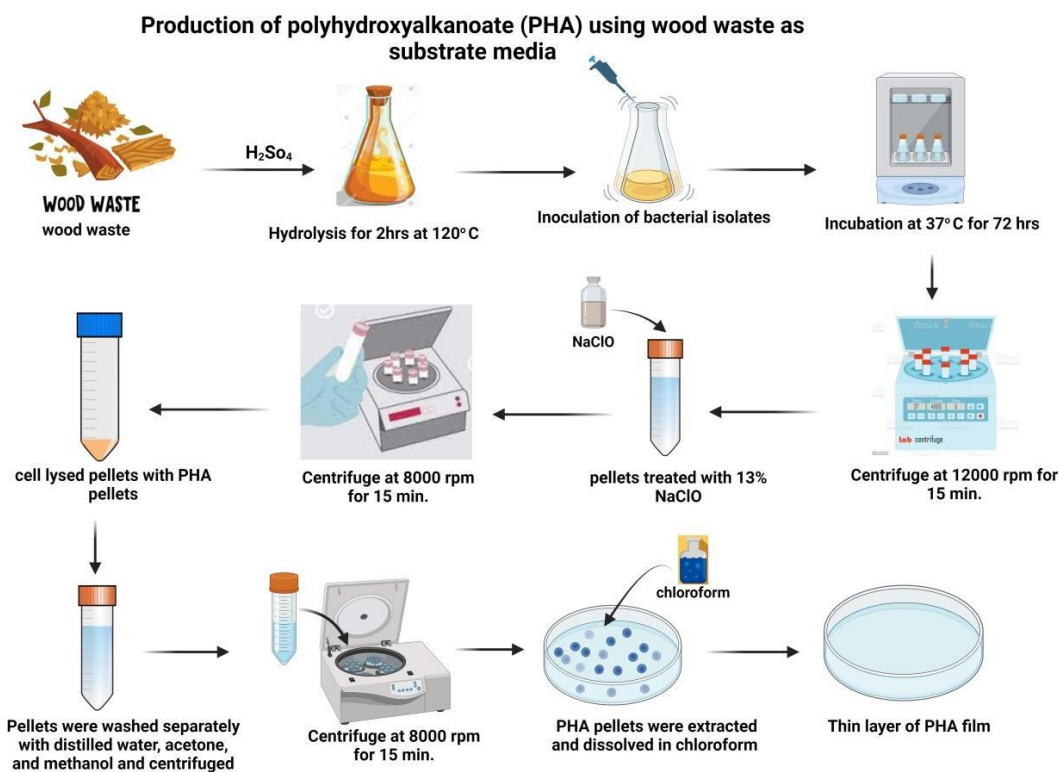
Acknowledgment

Completing this Ph.D. has been a long journey, filled with many challenges and rewards. It would not have been possible without the guidance, support, and encouragement of numerous individuals, to whom I owe my deepest gratitude.

First and foremost, I would like to express my sincere appreciation and gratitude to my supervisor, **Dr. Arun Karnwal** (Associate Professor, School of Bioengineering and Biosciences, Department of Microbiology, Lovely Professional University, Phagwara, Punjab. Your unwavering support, insightful advice, and constructive criticism have been invaluable to my research. You have been a constant source of inspiration and motivation, and your patience and belief in my abilities have been instrumental in guiding me through this journey. Thank you for challenging me to think critically and for pushing me to achieve more than I thought possible.

I am deeply grateful to **Dr. Ashok Mittal** (Founder Chancellor), **Mrs. Rashmi Mittal** (Vice-Chancellor), **Dr. Sanjay Modi** (Pro Vice-Chancellor), **Dr. Lovi Raj Gupta** (Head of faculty/ Pro vice chancellor), and **Dr. Monica Gulati** (Registrar) of Lovely Professional University for granting me access to exceptional infrastructure and the opportunity to conduct my research within the nurturing environment of this esteemed institution.

I extend my heartfelt thanks to **Dr. Neeta Raj Sharma**, Head of School, School of Bioengineering and Biosciences, for her unwavering support and consistent oversight of my research progress. Her guidance was invaluable at every stage of this work.

I am also profoundly appreciative of **Dr. Ashish Vyas**, Head of the Microbiology Department, whose extensive knowledge and experience greatly enriched my research. Additionally, I would like to express my sincere thanks to **Dr. Minhaj Ahmad Khan** (HOL), for providing me with access to state-of-the-art laboratories and ensuring that I had the necessary resources to conduct my work.

I am grateful to my colleagues and friends in the department at Lovely Professional University. The collaborative environment and the many discussions we had significantly contributed to my academic growth. Special thanks to Simran Kauts, Rohan Samir Kumar Sachan, Inderpal Devgon, Khushboo,

TABLE OF CONTENT

LIST OF TABLES

LIST OF FIGURE

CHAPTER 1

INTRODUCTION

The global plastic waste crisis, while well-documented, continues to worsen with each passing year. The once-celebrated durability and versatility of plastics have now become central to an environmental crisis. Each year, Over 300 million tons of plastic waste are generated annually, with a significant portion ending up in landfills, oceans, and natural ecosystems. (Geyer et al., 2017). While recycling efforts have been promoted globally, the reality is that less than 10% of all plastic produced has ever been recycled (Hopewell et al., 2009). Most of this waste is either incinerated, producing harmful emissions or ends up in landfills where it takes hundreds of years to degrade, during which time it releases toxic chemicals that leach into the soil and groundwater (Rochman et al., 2013). These figures illustrate the urgent need for a paradigm shift in how plastics are produced, used, and disposed of.

Plastic waste accumulation is a direct result of several interrelated factors. The first is the sheer scale of plastic production, which has been growing exponentially since the 1950s. From 1950 to 2015, global plastic production skyrocketed from 2 million metric tons to 380 million metric tons per year. (Geyer et al., 2017). This staggering increase is driven by the widespread use of plastic in virtually every sector of modern life, from packaging to electronics to automobiles. Consequently, the manufacture of single-use plastics, which are intended for disposal after one use, has become a major factor in plastic pollution. Products like plastic bags, straws, and disposable cutlery, although used only briefly, can persist in the environment for hundreds of years. (Jambeck et al., 2015).

Another factor is the inefficiency of existing waste management systems. Particularly in developing countries, the infrastructure required for collecting, sorting, and recycling plastic waste is often inadequate. This often leads to improper disposal methods, such as open burning or dumping into rivers and oceans, where plastics can travel vast distances and accumulate in remote regions, including the Arctic and Antarctic (Barnes et al., 2009). Even in regions with well-developed waste management systems, such as Europe and North America, a significant proportion of plastic waste is either landfilled or incinerated, both unsustainable options (Hopewell et al., 2009). Landfilling

contributes to long-term environmental degradation, while incineration releases harmful air pollutants and contributes to global warming.

Furthermore, The persistent nature of plastics in the environment poses a unique challenge. Unlike organic materials, which decompose relatively quickly through natural processes, plastics resist microbial degradation. Instead of decomposing quickly, plastics gradually fragment into increasingly smaller pieces, known as microplastics and nanoplastics, which can remain in the environment for centuries (Browne et al., 2011). These tiny elements have been identified in soil, water, and even the air, presenting a potential risk to human health by infiltrating the food chain and being inhaled (Rochman et al., 2013).

Plastic waste has a deep and complex impact on ecosystems, with plastic debris causing particular issues in marine environments.It is believed that annually, more than 8 million tons of plastic are deposited into the world's oceans, predominantly coming from sources on land. (Jambeck et al., 2015). Once in the ocean, plastics can travel vast distances, carried by ocean currents and winds. Over time, plastic debris accumulates in large gyres, such as the Great Pacific Garbage Patch, where millions of tons of plastic are concentrated in areas more significant than many countries (Eriksen et al., 2014). Marine life, such as fish, seabirds, and marine mammals, is particularly vulnerable to the impacts of plastic pollution. Numerous species confuse plastic for food and consume it, resulting in internal injuries, starvation, and death. (Wilcox et al., 2015). Furthermore, plastic debris can ensnare marine animals, hindering their ability to swim or feed properly..

Beyond its immediate effects on wildlife, plastic pollution also has long-term consequences for marine ecosystems. As plastics degrade into microplastics, they can be ingested by many organisms, from plankton to whales. These small particles can build up in the tissues of marine animals and bioaccumulate through the food chain, potentially affecting humans who consume seafood. (Browne et al., 2011). The detection of microplastics in seafood has sparked worries about the introduction of toxic substances such as bisphenol A (BPA) and phthalates—commonly used in plastic production—into the human food chain, potentially posing health risks. (Halden, 2010).

Terrestrial ecosystems are also affected by plastic pollution. In agricultural settings, plastic mulch films are commonly used to suppress weeds and retain moisture in the soil. However, when these films degrade or are improperly disposed of, they contribute to plastic pollution in the soil. Microplastics in soil can affect soil structure, reduce nutrient availability, and hinder plant growth (Rillig et al., 2019). Additionally, plastic pollution can disturb natural habitats, resulting in biodiversity loss and changes to ecosystems. (Barnes et al., 2009).
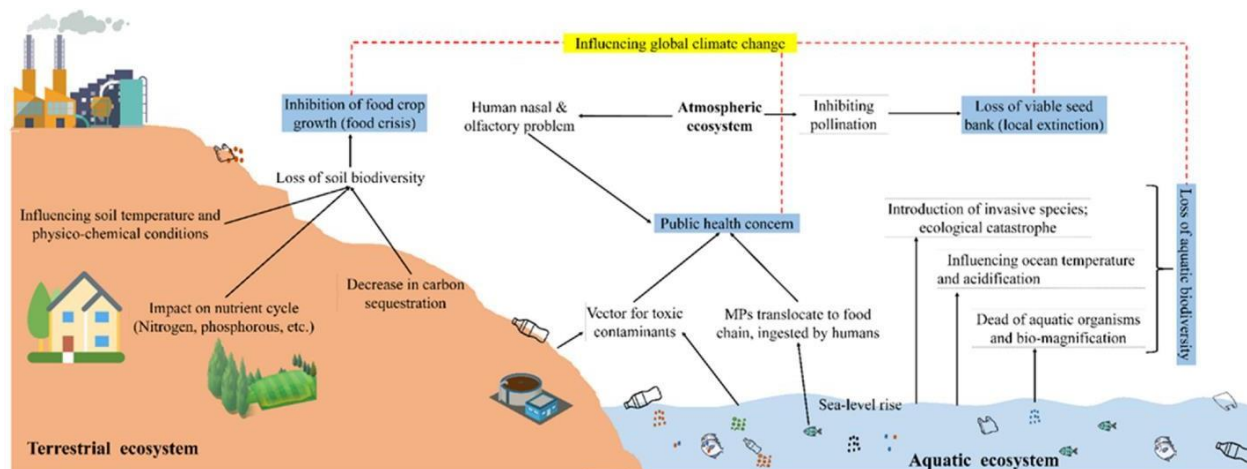
Figure 1.1: Global impact of plastic pollution in the ecosystem

Given the environmental challenges posed by conventional plastics, there has been a growing interest in biodegradable plastics that can offer similar functionality without the associated environmental harm. Polyhydroxyalkanoates (PHAs) are a type of biodegradable plastic that has recently garnered significant interest. PHAs, or polyhydroxyalkanoates, are naturally occurring biopolymers that various microorganisms produce as intracellular storage compounds when nutrients are limited. (Anderson & Dawes, 1990). PHAs are biodegradable and can be broken down by microorganisms in soil, water, and compost environments, making them an attractive alternative to traditional petrochemical-based plastics as shown in figure 1.1 (Kumar et al., 2021).

Polyhydroxybutyrate (PHB), a specific type of PHA, has garnered particular interest due to its physical properties, similar to those of polypropylene (PP), a widely used conventional plastic. PHB is synthesized by bacteria including *Cupriavidus necator* and *Bacillus megaterium*, which accumulate PHB as intracellular granules when grown in environments with excess carbon and limited nitrogen or phosphorus (Reddy et al., 2003). PHB can be harvested from bacterial cells and processed into bioplastic materials suitable for various applications, including packaging, agriculture, and medical devices (Chen, 2010). The biodegradability of PHB under natural environmental conditions is one of its key advantages, as it can break down in both marine and terrestrial environments, minimizing the prolonged environmental effects of plastic waste.

Despite the promising environmental benefits of PHB, its large-scale commercial production is currently limited by several challenges, the most significant of which is its high production cost. The microbial fermentation process required to produce PHB involves several stages, including microbial growth, PHB accumulation, extraction, and purification. Each of these stages contributes to the overall cost of production, making PHB several times more expensive than plastics (Kourmentza et al., 2017). The price of raw materials, particularly the carbon source used for microbial growth, is one of the significant factors contributing to the high cost of PHB production. Traditionally, carbon sources such as glucose and sucrose, derived from food crops, are used for microbial fermentation. However, using these feedstocks not only increases the cost of production but also raises ethical concerns about competition with food supplies.

Researchers have been exploring low-cost and waste-derived feedstocks for PHB production to address these challenges. Agricultural residues, industrial byproducts, and municipal waste streams have all been investigated as potential carbon sources for microbial fermentation (Kourmentza et al., 2017). Utilizing waste materials as feedstocks decreases the expense of raw materials and offers an environmentally sustainable approach to waste management. By rerouting waste materials away from landfills and incinerators, the production of PHB from these feedstocks supports a circular economy where resources are continuously reused and repurposed.

One of the most promising strategies for reducing the cost of PHB production is using hydrolyzed wood waste and wastewater as substrates for microbial fermentation. Wood waste, generated in significant quantities by the timber and paper industries, is an abundant and renewable source of lignocellulosic biomass (Saini et al., 2016). Lignocellulosic biomass comprises cellulose, hemicellulose, and lignin, which can be broken down into simple sugars through processes such as acid hydrolysis (Zhang et al., 2010). These sugars, including glucose and xylose, can serve as carbon sources for microbial fermentation, offering a cost-effective alternative to conventional feedstocks.

Wood waste as a substrate for PHB production has several environmental and economic benefits. First, it provides a sustainable use for a waste material that would otherwise be landfilled or incinerated, contributing to pollution. By transforming wood waste into valuable bioplastic products, industries can lessen their environmental impact and contribute to a more sustainable bioeconomy (Saratale et al., 2021). Second, wood waste is a readily available and renewable resource, making it a cost-effective alternative to food-based feedstocks. Finally, The use of wood waste supports the principles of a circular economy by transforming waste materials into valuable products, thereby lessening the reliance on new, unprocessed resources.

In addition to wood waste, wastewater from various industrial processes, such as food processing, agriculture, and municipal wastewater treatment, can also serve as a cost-effective substrate for PHB production (Chua et al., 2013). Wastewater often contains organic compounds, such as sugars, fatty acids, and alcohols, that microorganisms can utilize for growth and PHB synthesis. Combining hydrolyzed wood waste with wastewater makes it possible to create a low-cost and sustainable feedstock for PHB production while simultaneously addressing waste management challenges. Integrating these two waste streams provides a novel and synergistic approach to reducing the cost of PHB production and improving the environmental sustainability of bioplastics.

While the use of hydrolyzed wood waste and wastewater for PHB production offers significant promise, several challenges still need to be addressed. One of the main challenges is the efficient hydrolysis of lignocellulosic biomass to release fermentable sugars. The complex structure of

lignocellulose makes it resistant to degradation, and acid hydrolysis requires high temperatures, pressures, and chemicals, which can be costly and energy-intensive (Sun & Cheng, 2002). Researchers are exploring alternative methods, such as enzymatic hydrolysis and microbial pretreatment shown in figure 1.2, to enhance lignocellulose degradation efficiency and minimize the process's environmental impact (Zhang et al., 2010).
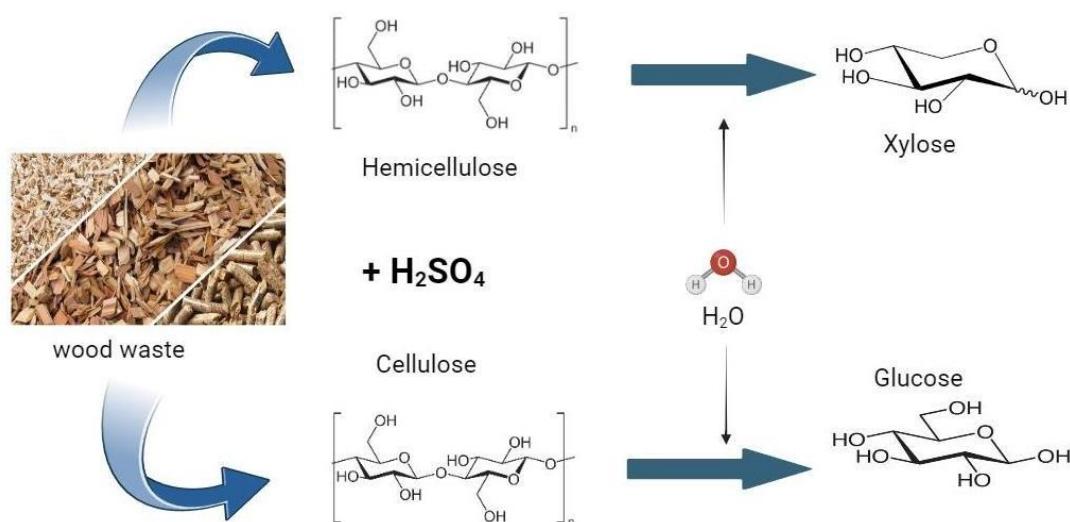
Figure 1.2: Biochemistry behind the process of wood hydrolysis.

PHB is synthesized by microorganisms as intracellular carbon and energy storage compounds when they are subjected to nutrient limitations, especially nitrogen or phosphorus, when there is an abundance of carbon (Anjum et al., 2016). The ability of various microorganisms to efficiently produce PHB has opened avenues for developing industrially viable methods for bioplastic production. Among the promising candidates are *Escherichia fergusonii MK*, *Pseudomonas fluorescens*, and *Klebsiella pneumoniae*, which have demonstrated considerable potential in PHB biosynthesis.

Escherichia fergusonii MK, a member of the Enterobacteriaceae family, has gained attention due to its ability to accumulate PHB under specific growth conditions. Its metabolic versatility allows it to adapt to different environments, making it a potential candidate for PHB production in diverse industrial settings (Mumtaz et al., 2017). Similarly, *Pseudomonas fluorescens*, a well-known bacterium for its role in biocontrol and biofilm formation, has been examined for its capacity to produce PHB in conditions where nutrients are limited. This species is particularly appealing due to its rapid growth rate and versatility in utilizing different substrates, including waste materials, for PHB synthesis (Singh et al., 2020). *Klebsiella pneumoniae*, another bacterium from the Enterobacteriaceae family, is not only known for its pathogenic potential but also for its ability to produce PHB efficiently. Studies have shown that *K. pneumoniae* can accumulate PHB in significant amounts when grown in specific nutrient-limited environments, which makes it a viable candidate for industrial-scale bioplastic production (Ramachanderan et al., 2021). The use of such microorganisms for PHB production not only contributes to sustainable bioplastic development but also provides a means of valorizing agricultural and industrial waste materials.

Exploring these microorganisms for PHB biosynthesis opens up new possibilities in the field of biodegradable plastics. Their metabolic pathways, adaptability to various environmental conditions, and efficiency in converting different carbon sources into PHB underscore their potential in biotechnological applications. Continued research into optimizing these strains' growth conditions and genetic engineering may further enhance PHB yield and reduce production costs, making bioplastics a more viable alternative to conventional plastics.

Another challenge is optimizing microbial fermentation processes to maximize PHB yields from waste-derived feedstocks. While many microorganisms can produce PHB, their yields may differ based on the feedstock composition and the conditions of fermentation. (Reddy et al., 2003). Genetic engineering and metabolic optimization of microbial strains may be necessary to improve their ability to utilize waste-derived substrates and increase PHB production efficiency (Chen, 2010). Further

research is needed to scale the production process from laboratory-scale experiments to industrial-scale operations.

In conclusion, sustainable alternatives to conventional plastics are critical for addressing the global plastic waste crisis. Polyhydroxybutyrate (PHB) is a promising bioplastic that offers many environmental benefits, including biodegradability and the ability to be produced from renewable resources. However, the high cost of PHB production has limited its commercial viability. Hydrolyzed wood waste and wastewater as substrates for microbial fermentation represent a novel and sustainable solution for reducing the cost of PHB production. This approach provides a low-cost and renewable source of carbon for microbial growth and addresses waste management challenges by repurposing waste materials that would otherwise add to environmental pollution.As research in this area continues to advance, integrating waste-derived feedstocks into PHB production can make bioplastics a viable and sustainable alternative to conventional plastics, contributing to a more circular and environmentally sustainable bioeconomy.

CHAPTER 2

REVIEW OF LITERATURE

2.1 Plastic Pollution and it's harmful effects

Plastic has become integral to modern life due to its versatility, durability, and cost-effectiveness. It is widely used in packaging, construction, healthcare, and electronics (Smith et al., 2018). However, the environmental cost associated with plastic use far outweighs its convenience. Plastics are synthetic materials primarily derived from petrochemicals and are highly resistant to degradation (Johnson et al., 2020). Consequently, discarded plastics build up in the environment, adding to pollution in landfills, rivers, and oceans. The same durability that makes plastic valuable in numerous applications also turns it into a major environmental threat (Morris et al., 2019).

The detrimental effects of plastic pollution are extensive, impacting both terrestrial and marine ecosystems. Plastics are non-biodegradable, allowing them to remain in the environment for hundreds or even thousands of years. (Morris et al., 2019). When plastics enter ecosystems, they pose significant risks to wildlife. Marine animals, such as seabirds, turtles, and fish, often mistake plastic debris for food, ingesting it and suffering from malnutrition, poisoning, or death (Williams et al., 2020). More oversized plastic items, like fishing nets, can entangle marine species, causing injury or suffocation (Thompson et al., 2009).

Additionally, plastic pollution disrupts ecosystems by physically altering habitats, reducing biodiversity, and threatening the health of both terrestrial and marine species (Barnes et al., 2010). Plastics in oceans break down into smaller particles called microplastics, which further exacerbate the problem by entering the food chain (Jones et al., 2018). Microplastics are ingested by various organisms, including plankton, fish, and even humans, raising concerns about the long-term health implications of this exposure (Patel et al., 2017).

There are several types of plastics, each with specific properties and uses. For instance, polyethylene terephthalate (PET) is commonly used in beverage bottles and food containers (Galloway et al., 2016). High-density polyethylene (HDPE) is used in milk jugs, detergent bottles, and plastic bags, while polyvinyl chloride (PVC) is employed in pipes, medical equipment, and packaging (Hahladakis et al., 2018). Low-density polyethylene (LDPE), polypropylene (PP), and polystyrene (PS) are used

in plastic bags, food containers, and disposable cups, respectively (Thompson et al., 2009). These materials vary in durability, flexibility, and recyclability, but they all contribute to the persistence of plastic pollution in the environment shown in table 2.1 (Law & Thompson, 2014).

Table 2.1: Different types of plastics and their harmful effects

Type of Plastic	Common Uses	Harmful Effects
Polyethylene Terephthalate (PET or PETE)	Beverage bottles, food containers, synthetic fibers	Leaches antimony, which can cause lung and heart problems with long-term exposure. Microplastic formation in water bodies (Galloway et al., 2016).
High-Density Polyethylene (HDPE)	Milk jugs, detergent bottles, grocery bags	Relatively low toxicity but can accumulate in the environment, contributing to microplastic pollution and wildlife harm (Thompson et al., 2009).
Polyvinyl Chloride (PVC)	Pipes, medical equipment, credit cards, flooring	Contains toxic additives such as phthalates and vinyl chloride, which can cause cancer, birth defects, and endocrine disruption (Hahladakis et al., 2018).
Low-Density Polyethylene (LDPE)	Plastic bags, food wrap, bottles	Produces toxic fumes when burned and contributes to land and marine plastic pollution, causing harm to wildlife (Patel et al., 2017).
Polypropylene (PP)	Food containers, straws, bottle caps, packaging	Resistant to degradation, contributing to long-term environmental pollution. Limited leaching potential but contributes

		to microplastic pollution (Kim et al., 2021).
Polystyrene (PS or Styrofoam)	Disposable cups, food packaging, insulation	Contains styrene, a possible carcinogen, and contributes to air and marine pollution. Difficult to recycle (Galloway et al., 2016).
Polycarbonate (PC) / Other	Water bottles, eyeglass lenses, electronics	Leaches bisphenol A (BPA), which is linked to hormonal disruption, reproductive issues, and increased cancer risk (Talsness et al., 2009).

Microplastics are tiny plastic particles under 5 mm in diameter, created by the degradation of larger plastics or introduced directly as primary microplastics in products like cosmetics and synthetic clothing fibers (Cox et al., 2019). These particles are now found in virtually every corner of the globe, from the ocean's depths to the Arctic ice (Barnes et al., 2010). Microplastics pose severe risks to marine life because they are easily ingested by many organisms, from plankton to whales (Jones et al., 2018). Once ingested, microplastics can cause physical harm and act as carriers for toxic chemicals that further endanger the health of marine species and, by extension, humans (Patel et al., 2017).

Microplastics have also been detected in human food and drinking water, raising concerns about their potential health impacts (Wright & Kelly, 2017). Research has shown that microplastics may lead to inflammation, interfere with immune responses, and carry harmful substances like persistent organic pollutants (Galloway et al., 2016). While the long-term health effects of microplastic exposure in humans are not yet fully understood, growing evidence indicates they could play a role in the development of chronic diseases. (Vandenberg et al., 2019).

Furthermore, plastic has contributed to a "throwaway culture," where convenience often trumps sustainability (Thompson et al., 2009). This mentality has driven overconsumption, exacerbating waste management issues globally (Hopewell et al., 2009). The sociological impact extends to mental health as well. Communities facing environmental degradation due to plastic pollution experience heightened anxiety, helplessness, and despair about the future of their environment and health (Clayton et al., 2017).

Addressing plastic pollution necessitates a comprehensive approach that includes government policies, corporate accountability, public awareness, and individual efforts. (Geyer et al., 2017). Here are some key methods:

2.1.1 Government Regulations: Many governments have implemented bans on single-use plastics, such as plastic bags, straws, and cutlery. For example, the European Union banned certain single-use plastic products in 2021 (European Commission, 2021), and countries like Kenya, India, and Rwanda have also introduced strict measures to curb plastic pollution (Njeru et al., 2018). Additionally, extended producer responsibility (EPR) schemes make manufacturers responsible for the entire lifecycle of plastic products, incentivizing companies to design more sustainable alternatives (OECD, 2018).

2.1.2 Corporate Responsibility: Large corporations increasingly recognize their role in contributing to plastic pollution and adopt more sustainable practices (Bocken et al., 2016). Some companies are shifting toward using recycled plastic in packaging (Geueke et al., 2018), while others are investing in biodegradable alternatives (Narancic et al., 2020). The push for a circular economy, where materials are continuously reused and recycled, has gained momentum recently (Ellen MacArthur Foundation, 2015).

2.1.3 Public Awareness and Behavior Change: Increasing public awareness of the harmful impacts of plastic pollution is crucial for promoting behavioral change. (Singh et al., 2020). Campaigns encouraging consumers to reduce plastic use, recycle, and adopt sustainable alternatives have been effective in some regions (Ertz et al., 2017). For instance, increased

awareness has made reusable shopping bags and water bottles increasingly popular in various countries (Zhu et al., 2019).

2.1.4 **Improved Waste Management**: Enhancing waste management infrastructure is essential for reducing plastic pollution, particularly in developing countries where these systems are often insufficient (Jambeck et al., 2015). Investments in recycling facilities, promoting waste segregation, and implementing advanced technologies for sorting and processing waste can significantly reduce plastic accumulation in landfills and oceans (Ritchie & Roser, 2018).

2.1.5 **Innovation in Recycling**: Advances in recycling technology, such as chemical recycling, are helping to convert plastic waste into reusable materials (Ragaert et al., 2017). Unlike traditional mechanical recycling, which can degrade plastic quality, chemical recycling breaks down plastic into its original components, producing higher-quality materials (Rahimi & García, 2017).

2.2 Alternatives to Plastic

While reducing plastic use is essential in tackling pollution, finding suitable alternatives is important (Yates & Barlow, 2013). Some of the most promising alternatives include:

2.2.1 **Glass**: Glass is a durable, non-toxic material that can be reused and recycled indefinitely without losing quality (Ross & Evans, 2003). However, its heavier weight and fragility make it less convenient for some applications than plastic (Hopewell et al., 2009).

2.2.2 **Metal**: Metal, particularly aluminum, is another alternative that is easily recyclable and has a lower environmental impact over its lifecycle (Turner et al., 2015). Aluminum cans, for instance, can be recycled indefinitely, making them a more sustainable choice for packaging (Lazarevic et al., 2010).

Bio-plastic: Plant- and microbial-based bioplastics are sustainable alternatives to traditional equally

2.2.3 plastics. Derived from renewable sources like starch, cellulose, and microbial fermentation, they reduce environmental impact by being biodegradable or compostable. These bioplastics offer comparable mechanical properties to conventional plastics, making them suitable for

packaging, agriculture, and medical applications. Their production also lessens dependence on fossil fuels, supporting a circular economy. (Shen et al., 2020; Chen et al., 2021).

2.3 Types of Bioplastics

Bioplastics are emerging as a promising solution to plastic pollution. These are plastics derived from renewable biological sources, such as corn starch, sugarcane, and cellulose (Philp et al., 2013). Bioplastics can be divided into two main categories: biodegradable and non-biodegradable.

2.3.1 Polylactic Acid (PLA): PLA is one of the most common types of biodegradable bioplastics derived from renewable resources like corn starch or sugarcane (Auras et al., 2004). PLA is used in various applications, including food packaging, disposable cutlery, and 3D printing. While it is biodegradable under industrial composting conditions, it requires specific facilities to break down effectively shown in table 2.2 (Drumright et al., 2000).

2.3.2 Polyhydroxyalkanoates (PHA): PHA is a family of biodegradable polyesters produced by bacterial fermentation of sugars and lipids (Chen, 2010). PHA has gained attention for its biodegradability in natural environments, including soil and marine ecosystems (Shen et al., 2009). It is used in packaging, medical applications, and agricultural films (Chen & Patel, 2012).

2.3.3 Starch-Based Bioplastics: These are derived from natural starch sources, such as potatoes, corn, and wheat (Shanks & Kong, 2012). Starch-based bioplastics are used for biodegradable bags, packaging materials, and disposable items. However, they are less durable than traditional plastics and may have limited applications (Imre & Pukánszky, 2013).

2.3.4 Cellulose-Based Bioplastics: Derived from cellulose, the primary component of plant cell walls, these bioplastics are biodegradable and have been used in applications such as films, coatings, and packaging (George et al., 2001).

2.3.5 Microbial Bioplastics: Microbial bioplastics offer a sustainable alternative to traditional plastics, as they are derived from renewable sources such as bacteria, algae, or fungi (Tokiwa et al., 2009). These bioplastics are biodegradable and reduce reliance on fossil fuels, lowering

environmental pollution (Narancic et al., 2020). Unlike conventional plastics, which persist in ecosystems for centuries, microbial-based bioplastics decompose more rapidly (Shen et al., 2009). They hold promise for reducing plastic waste and supporting the transition toward a circular, eco-friendly economy shown in figure 2.1 (Chen, 2010).

Table 2.2: Types of Bioplastics and it's applications

Type of Bioplastic	Source	Characteristics	Applications
Polyhydroxybutyrate (PHB)	Microbial fermentation (e.g., Cupriavidus necator)	Biodegradable, high thermal stability, brittle	Packaging, agriculture, medical devices (Chen et al., 2012)
Polylactic Acid (PLA)	Fermentation of plant sugars (e.g., corn starch)	Biodegradable, compostable, clear, low heat resistance	Packaging, disposable cutlery, textiles (Auras et al., 2004)
Polyhydroxyalkanoates (PHA)	Microbial fermentation of organic materials	Biodegradable, variable properties depending on type	Packaging, agricultural films, medical applications (Chen et al., 2012)
Starch-based Plastics	Starch from crops (e.g., potatoes, corn)	Biodegradable, often blended with other materials for strength	Packaging, disposable items, agricultural films (Avérous et al., 2012)
Polybutylene Succinate (PBS)	Biosynthetic processes or petrochemical sources	Biodegradable, flexible, good impact resistance	Packaging, agricultural films, automotive parts (Shirai et al., 2006)
Polycaprolactone (PCL)	Chemical synthesis (can be produced from renewable sources)	Biodegradable, low melting point, flexible	Medical implants, 3D printing, biodegradable plastics (Woodruff et al., 2010)
Cellulose-based Plastics	Cellulose from plants (e.g., wood, cotton)	Biodegradable, strong, can be made into films or fibers	Packaging, film coatings, textiles (George et al., 2001)
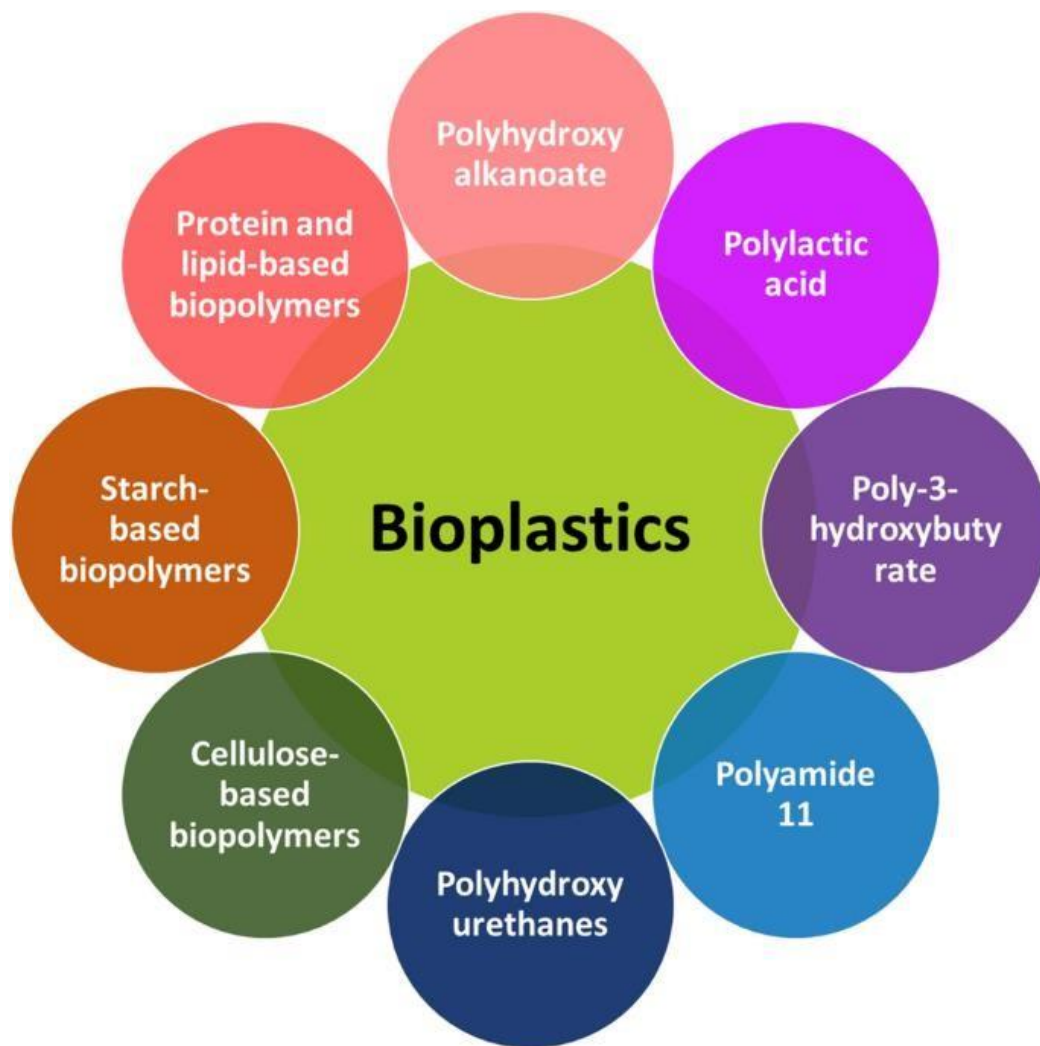
Figure 2.1: Types of Bioplastics

2.4 Polyhydroxyalkanoates (PHA)

Polyhydroxyalkanoates (PHA) and polyhydroxybutyrates (PHB) are considered among the most promising bioplastics due to their unique properties and versatility. Derived from renewable resources

through microbial fermentation, these biodegradable polymers stand out for their potential to replace traditional plastics in various applications. Their biodegradability, biocompatibility, and comparable mechanical properties to conventional plastics make them superior choices among bioplastics.

2.4.1 Biodegradability and Environmental Impact

One of the primary reasons PHA and PHB are favored over other bioplastics is their excellent biodegradability. PHA and PHB can decompose naturally in various environments, including soil, freshwater, and marine environments, making them highly suitable for reducing plastic pollution (Raza et al., 2018). This quality is paramount compared to other bioplastics, such as polylactic acid (PLA), which require industrial composting conditions for biodegradation (Puppi et al., 2019). The complete biodegradability of PHA/PHB reduces the risk of long-term environmental contamination, offering a critical advantage in addressing global plastic waste issues.

2.4.2 Production from Renewable Resources

PHA and PHB are produced by microorganisms, primarily bacteria, through the fermentation of renewable carbon sources such as sugar and lipids. Unlike petroleum-based plastics, PHA and PHB do not rely on fossil fuels, reducing carbon footprints during production (Khanna & Srivastava, 2005). This renewable origin is a critical factor in their sustainability. Moreover, ongoing advancements in genetic engineering and metabolic pathways have made it possible to optimize microbial strains, increasing PHA/PHB production yield and lowering costs (Keshavarz & Roy, 2010).

2.4.3 Mechanical Properties

PHA and PHB possess mechanical properties comparable to traditional plastics, such as polypropylene (PP) and polyethylene (PE). PHB, in particular, exhibits good tensile strength and rigidity, making it suitable for packaging, medical applications, and agricultural films (Chen, 2009). On the other hand, PHA is known for its flexibility and can be tailored to meet specific requirements for various applications by adjusting its monomer composition (Sudesh et al., 2000). This versatility

in mechanical properties makes PHA/PHB an ideal candidate to replace a wide range of petrochemical plastics in industrial applications.

2.4.4 Applications of PHA

Polyhydroxyalkanoates (PHAs), including the widely researched polyhydroxybutyrate (PHB), are emerging as versatile biopolymers with applications spanning multiple industries due to their biodegradability, biocompatibility, and thermoplastic properties. One of the primary sectors utilizing PHAs is biomedical engineering. PHB, for instance, has been widely studied for use in medical devices, sutures, drug delivery systems, and tissue engineering (Valappil et al., 2007). Unlike other bioplastics, PHB does not generate toxic degradation products when metabolized, further enhancing its potential for medical and pharmaceutical uses (Philip et al., 2007). Recent studies in 2025 have focused on developing PHB-based scaffolds incorporated with growth factors for accelerating bone and nerve regeneration (Singh et al., 2025). In packaging, PHAs are being adopted as eco-friendly alternatives to petroleum-based plastics. PHB films, in particular, have demonstrated improved oxygen barrier properties and thermal stability, making them suitable for food preservation and single-use packaging (Zhao et al., 2025). In agriculture, PHAs serve as matrices for controlled-release fertilizers and pesticides, reducing environmental load and enhancing soil sustainability (Chen et al., 2025). Additionally, PHB nanoparticles have been applied in the cosmetic and personal care sectors for encapsulating bioactive compounds, improving skin delivery and stability (Lee et al., 2025). Furthermore, PHA's compatibility with 3D printing technologies opens new pathways for creating customizable bioproducts in both consumer and medical markets (Garcia et al., 2025). Thus, with continued advancements in microbial synthesis and downstream processing, PHA and PHB biopolymers are increasingly recognized as sustainable materials supporting a circular bioeconomy.

2.4.5 Composability and End-of-Life Options

In addition to being biodegradable, PHA/PHB are compostable under natural conditions without requiring specific industrial processes. This distinguishes them from bioplastics like PLA, which

decompose in high temperatures and controlled environments (Reddy et al., 2003). The ability to break down in natural environments, including marine ecosystems, is a key advantage of PHA/PHB, especially considering the rising concern over marine plastic pollution.

2.4.6 Circular Economy Potential

PHA/PHB fits seamlessly into a circular economy where materials are continuously reused and recycled. Because they can be produced from waste materials, such as agricultural by-products, PHA/PHB offers a pathway for waste valorization, converting waste into valuable bioplastics (Gholami et al., 2016). This makes them an attractive option for industries looking to close the loop on resource use and reduce their environmental footprint.

2.4.7 Challenges and Future Prospects

Despite their numerous advantages, PHA and PHB still face challenges with production cost and scalability. However, continuous advancements in fermentation technology, microbial strain engineering, and feedstock optimization drive down costs, making PHA/PHB increasingly competitive with traditional plastics (Koller et al., 2010). Moreover, the growing demand for sustainable alternatives is likely to drive further investments in PHA/PHB production, making them even more viable.

2.5 Types of PHA and Microorganism Relations

PHAs exist in several forms, including polyhydroxybutyrate (PHB), polyhydroxyvalerate (PHV), and polyhydroxyhexanoate (PHHx), each with distinct properties that make them suitable for different applications (Steinbüchel & Lütke-Eversloh, 2003). PHB, the most common type of PHA, is known for its high crystallinity and biodegradability, making it ideal for packaging and disposable products. PHV and PHHx, however, have more flexible properties and are used in applications requiring higher elasticity (Reddy et al., 2003).

Microorganisms produce PHAs as a means of energy storage under conditions of nutrient limitation (Madison & Huisman, 1999). When essential nutrients such as nitrogen, phosphorus, or oxygen are scarce but carbon sources are abundant, microorganisms synthesize PHA granules as a form of intracellular carbon and energy reserve (Lee, 1996). This allows them to survive in environments where nutrient availability fluctuates. The accumulation of PHA is a natural response to stress conditions and can be triggered by providing excess carbon sources like glucose or fatty acids during fermentation (Chen, 2010).

2.6 Microorganisms That Produce PHB

Several microorganisms can produce PHB, including species of *Ralstonia eutropha*, *Cupriavidus necator*, *Bacillus megaterium*, and *Pseudomonas fluorescens* shown in table 2.3 (Philip et al., 2007). These bacteria are often used in industrial processes for PHB production due to their high yield and ability to utilize various carbon sources. *Ralstonia eutropha* is one of the most studied PHB producers, known for its efficiency in converting carbon-rich substrates into PHB (Riedel et al., 2015). *Bacillus megaterium* is another organism that can accumulate PHB in high quantities and has been used for commercial PHB production (Tan et al., 2014).

Table 2.3: Microbes capable of producing PHB

Microorganism	Characteristics	Uses/Applications
Bacillus megaterium	Gram-positive, rod-shaped bacterium; produces PHB as a carbon reserve	Biodegradable plastics, agriculture
Cupriavidus necator	Gram-negative bacterium; high PHB production efficiency	Bioplastics, medical applications
Alcaligenes eutrophus	Now known as *Cupriavidus necator*; one of the most studied PHB producers	Biodegradable materials
Ralstonia eutropha	Another name for *Cupriavidus necator*; known for its ability to accumulate high amounts of PHB	Industrial bioplastics
Methylobacterium extorquens	Gram-negative, methylotrophic bacterium; produces PHB from methanol	Environmental cleanup, bioengineering
Pseudomonas putida	Gram-negative; can produce PHB under certain conditions	Bioremediation, bioplastics
Brevibacillus brevis	Produces PHB and other biopolymers; Gram-positive bacterium	Bioplastics, pharmaceuticals
Rhodobacter sphaeroides	Photosynthetic bacterium; can produce PHB under specific conditions	Bioengineering, renewable materials

2.7 *Pseudomonas fluorescens* as PHB producer

Polyhydroxybutyrate (PHB) production by *Pseudomonas fluorescens* has gained attention due to its potential for bioplastic production, offering a sustainable alternative to petrochemical-based plastics.

P. fluorescens has been shown to accumulate PHB under nutrient-limited conditions, mainly when nitrogen or phosphorus is deficient while carbon is available in excess (Khanna et al., 2019). This bacterium can use various carbon sources, such as glucose, glycerol, and waste oils, making it versatile for industrial applications (Singh et al., 2020). PHB synthesis in *P. fluorescens* is regulated by key enzymes, including PHB synthase, which catalyzes polymer formation from hydroxybutyrate monomers (Sarkar et al., 2021). Advances in genetic engineering have enhanced PHB yield by overexpressing genes involved in the biosynthesis pathway (Sharma et al., 2022). The biodegradability and biocompatibility of PHB produced by *P. fluorescens* highlight its potential for applications in packaging, agriculture, and medical devices.

2.8 Novel Approach of *Escherichia fergusonii MK*, and *Klebsiella pneumoniae* as PHB Producers

Recent studies have highlighted the potential of *Escherichia fergusonii MK*, and *Klebsiella pneumoniae* as efficient PHB producers. *Escherichia fergusonii MK*, a lesser-known member of the Escherichia genus, has demonstrated an ability to accumulate significant amounts of PHB when cultured with carbon-rich substrates (Siddiqui et al., 2021). *Klebsiella pneumoniae*, traditionally studied as a pathogen, has also been identified as a promising PHB producer, mainly when using industrial and agricultural waste streams as substrates (Prabhu et al., 2019).

These microorganisms offer novel solutions to the challenges of PHB production by utilizing low-cost and renewable substrates, such as wood waste, to synthesize bioplastics. Their ability to metabolize diverse carbon sources makes them ideal candidates for large-scale industrial applications.

2.9 Expansiveness of Substrate for PHB Production

Polyhydroxybutyrate (PHB) production is influenced heavily by the type of substrate used during fermentation. Conventional substrates such as glucose and sucrose have been widely utilized, but their high cost limits the scalability of the process, especially when considering large-scale production (Khanna & Srivastava, 2005). Glucose and other refined sugars are costly because they compete with food supply chains, making them unsustainable in the long term for biopolymer production.

Consequently, a growing body of research focuses on identifying low-cost, renewable, and widely available substrates to reduce production costs without sacrificing yields (Koller et al., 2010).

2.10 Extraction of PHB Producers from Waste Streams

The extraction of PHB-producing microorganisms from waste streams is a growing area of interest due to its potential for sustainable production. Waste streams, including agricultural residues, food waste, and industrial byproducts, offer a rich source of organic materials that can be used as substrates for microbial fermentation (Koller et al., 2010). By utilizing waste streams, researchers aim to reduce the cost of PHB production while simultaneously addressing waste disposal issues. Microorganisms like *Pseudomonas fluorescens* and *Klebsiella pneumoniae* have shown potential for PHB production using waste substrates, offering a cost-effective and environmentally friendly solution (Huang et al., 2016).

2.11 Wood Waste Generated Around the World and India

Wood waste is a significant byproduct of various industries, including forestry, construction, and paper manufacturing. Globally, millions of tons of wood waste are generated each year, with a substantial portion going to landfills or incinerated (Ghosh et al., 2019). In India, the situation is similar, with large amounts of wood waste produced annually due to the country's growing construction and industrial sectors (Mishra et al., 2021). The disposal of wood waste presents environmental and economic challenges, as landfilling and incineration contribute to pollution and greenhouse gas emissions.

2.12 Wood Waste as a Good Source of Carbohydrates

Wood waste, primarily composed of lignocellulosic biomass, is one of the most abundant organic waste materials produced globally. The forestry and wood-processing industries produce significant quantities of wood chips, sawdust, bark, and other residues, which frequently end up in landfills or are incinerated, adding to environmental pollution. (Liu et al., 2016). However, this waste material is

rich in complex carbohydrates such as cellulose and hemicellulose, which can be broken down into simple sugars through processes like hydrolysis (Jönsson & Martín, 2016).

Cellulose, Earth's most abundant organic polymer, is a linear polysaccharide made up of glucose units. Conversely, hemicellulose is a branched polymer containing various sugars such as xylose, mannose, and glucose. Both polymers can be hydrolyzed into simple sugars, which can then be utilized by PHB-producing microorganisms (Pandey et al., 2000).

The carbohydrate content of wood waste makes it an ideal substrate for microbial fermentation. Recent studies have demonstrated the feasibility of using wood waste hydrolysates to produce PHB through microbial fermentation (Jiang et al., 2014). For example, *Pseudomonas fluorescens* and *Escherichia coli* have been shown to effectively metabolize sugars derived from wood hydrolysates to produce PHB (Keshavarz & Roy, 2010). This process contributes to the circular economy by turning waste into valuable products and provides a renewable and sustainable alternative to fossil fuel-derived plastics.

2.13 Hydrolysis of Wood Waste into Simple Sugars for Microbial Consumption

Wood waste primarily comprises lignocellulosic biomass, which consists of cellulose, hemicellulose, and lignin. To utilize wood waste as a substrate for microbial PHB production, it must first be broken down into simple sugars through hydrolysis (Jönsson & Martín, 2016). Hydrolysis involves the enzymatic or chemical breakdown of cellulose and hemicellulose into fermentable sugars, such as glucose and xylose, which microorganisms can consume during fermentation (Lynd et al., 2002). Enzymatic hydrolysis is often preferred for its lower environmental impact and higher sugar yields, making it a key step in the sustainable production of PHB from wood waste (Zhang et al., 2019).

2.14 Wood Waste as a Reliable Source for PHB Production

Using wood waste as a substrate for PHB production has numerous advantages, making it a reliable and sustainable resource for biopolymer synthesis. Wood waste is abundant and renewable, providing a consistent feedstock supply for bioplastic production. Moreover, using wood waste helps address

the environmental problem of waste disposal in the forestry and wood processing industries (Ghosh et al., 2019). By converting this waste into bioplastics, industries can reduce their reliance on fossil fuels, lower greenhouse gas emissions, and contribute to waste management solutions.

Economically, wood waste offers a cost-effective substrate for PHB production. The hydrolysis of wood waste produces fermentable sugars at a fraction of the cost of conventional sugar-based substrates, reducing the overall cost of bioplastic production (Lynd et al., 2002). In addition, using waste materials helps minimize competition with food crops for land and resources, addressing one of the critical concerns associated with using sugar-based substrates for bio-based production (Pandey et al., 2000).

Technologically, advancements in pre-treatment methods have made it possible to convert wood waste into fermentable sugars efficiently. Pre-treatment processes, such as steam explosion, dilute acid hydrolysis, and enzymatic hydrolysis, have been optimized to increase sugar yields and reduce inhibitors that may affect microbial fermentation (Jönsson & Martín, 2016). These methods improve the efficiency of converting lignocellulosic biomass into usable substrates, further enhancing the viability of wood waste as a reliable feedstock for PHB production.

Microorganisms like *Klebsiella pneumoniae*, *Pseudomonas fluorescens*, and *Escherichia fergusonii MK* have demonstrated the capability to produce PHB from lignocellulosic hydrolysates, including wood waste. These organisms are known for metabolizing various carbon sources, including xylose and glucose, making them ideal candidates for PHB production using hydrolyzed wood waste (Siddiqui et al., 2021; Silva et al., 2014).

Beyond the environmental and economic advantages, utilizing wood waste as a substrate for PHB production aligns with circular economy principles. Industries can create closed-loop systems that reduce waste and environmental impact by converting waste into valuable bioplastics. This approach not only contributes to sustainability but also provides new economic opportunities in the field of bio-based materials (Koller et al., 2010).

CHAPTER 3

RESEARCH GAP AND HYPOTHESIS

3.1 Research gap

The increasing environmental concerns surrounding the detrimental effects of conventional plastics have spurred significant interest in finding sustainable alternatives. While polyhydroxyalkanoates (PHA) have emerged as a promising biodegradable substitute for plastics, the major challenge limiting their commercial scalability is the high cost of production, mainly due to the expensive carbon sources required for microbial fermentation. Extensive research has been conducted on using various substrates, but most efforts have focused on industrial sugars or agricultural waste, which, while promising, still pose logistical and economic challenges. A clear research gap exists in exploring more abundant, underutilized waste materials, such as wood waste, and their potential to act as a low-cost feedstock for PHA production. Additionally, wastewater, a resource rich in nutrients and microbial diversity, remains largely unexplored as a medium for isolating highly efficient PHA-producing microorganisms. Combining wood waste and wastewater as sustainable substrates has not yet been thoroughly studied, leaving a gap in understanding the feasibility and effectiveness of such an approach for large-scale PHA production.

Another gap lies in the comprehensive screening and identification of novel, efficient PHA-producing bacteria from diverse environments, sewage streams. While significant progress has been made in identifying microorganisms capable of synthesizing PHA, there remains a need for more extensive screening of bacterial strains from highly polluted and nutrient-rich environments like wastewater streams. These environments are likely to harbor microbial species that have adapted to thrive in challenging conditions and could potentially possess superior capabilities for PHA production, significantly when grown on unconventional substrates like hydrolyzed wood waste. Furthermore, existing studies on PHA production often focus on single substrates, whereas the combination of multiple waste sources, such as wood waste and wastewater, could provide a more cost-effective and nutrient-balanced medium, improving yields and reducing production costs. However, little attention has been given to how different waste-derived substrates affect microbial PHA production efficiency and yield, presenting a critical gap in current knowledge.

3.2 Hypothesis

This study hypothesizes that combining hydrolyzed wood waste and wastewater as a substrate for PHA production will provide an economical and sustainable alternative to traditional carbon sources. The microbial isolates from wastewater streams are expected to exhibit high efficiency in utilizing these substrates for PHA synthesis due to their natural adaptation to nutrient-dense, waste-rich environments. Furthermore, combining wood waste and wastewater will provide a balanced nutrient profile that can enhance microbial growth and PHA production, thereby reducing the overall cost of bioplastic production. This approach also aims to valorize two abundant waste streams, contributing to waste reduction while producing biodegradable bioplastics. By optimizing the conditions for PHA production using these unconventional substrates, the study anticipates identifying a cost-effective method for producing large quantities of PHA, ultimately making bioplastics a more feasible alternative to conventional plastics on an industrial scale.

CHAPTER 4

OBJECTIVES

Objectives:

1. Isolation, screening, and characterization of PHA-producing bacteria from the Wastewater streams of the Jalandhar area.

2. Pre-treatment, hydrolysis, and composition assay of wood waste.

3. Production of PHA by using a combination of wastewater and hydrolysed wood waste as a substrate medium by positive control and isolated bacterial strains.

4. Comparative analysis and optimization of PHA produced by positive control and isolated bacterial strains

5. Scale-up production and extraction of PHA by a selected bacterial strain using a combination of wastewater and Hydrolysed wood waste as a substrate.

CHAPTER 5

MATERIALS AND

METHODOLOGY

5.1 Isolation and screening of PHA-producing bacteria

5.1.1 Sample collection

Different sewage samples were collected from areas (Location 1: 31.2520761, 75.6812032; Location 2: 31.2704923, 75.6903445; Location 3: 31.2533141, 75.6639076; Location 4: 31.2268515, 75.6341338) of jalandhar, Punjab, India. All the samples were collected using grab sampling technique in a sterile container (Mikelonis et al., 2020).

5.1.2 Isolation of Pure Cultures

Sewage samples were collected and transferred into sterile nutritional broth, with these initial samples being referred to as "mother samples." Serial dilution was employed to facilitate further investigation and quantification. This process involved transferring 1 mL of the original sample into 9 mL of distilled water, with the dilution process repeated to create a series of dilutions from 10^{-1} to 10^{-6}. Each dilution reduced the concentration of bacteria by a factor of ten compared to the previous one (Medvecky et al., 2018).

In the final stage of the experiment, 100 µL of the 10^{-5} and 10^{-6} dilutions were spread evenly on Nile Blue minimal salt agar medium. This specialized medium encourages the growth of polyhydroxyalkanoates (PHA), which produce bacterial strains while inhibiting the growth of others. It may also include specific nutrients or markers to help identify particular microbial characteristics. This approach enables the selective growth and subsequent analysis of bacterial populations from the initial samples, providing a method to measure their abundance and evaluate their characteristics (Li et al., 2018).

5.2 Screening of PHA-Producing Isolates

5.2.1 Primary Screening: Nile blue

The primary screening process for identifying potential polyhydroxybutyrate (PHB) producers begins with sample collection, which involves inoculating collected samples into sterile nutrient broth and labeling them as "mother samples." These samples then undergo serial dilution to manage the

concentration of organisms effectively. After dilution, aliquots of 0.1 mL are spread onto Modified Selective Medium (MSM) agar plates. The MSM agar is specifically prepared with 10 g/L sucrose to provide a carbon source essential for microbial growth, 0.225 mg/L Nile blue to facilitate PHB detection, and 15 g/L agar to solidify the medium. The plates are then incubated at 30°C for 48 hours. During this period, the Nile blue, which is incorporated into the bacterial cytoplasm, allows for the preliminary identification of PHB producers. This is achieved by examining the plates under UV light, where fluorescence indicates positive PHB production, facilitating the selection of fluorescent colonies for further analysis (Hartman, 1940).

5.2.2 Secondary Screening: Sudan black Stain

Following the primary screening, the secondary screening process utilizes Sudan Black staining to confirm PHB production. Samples previously identified as potential PHB producers are heat-fixed on slides. The staining process involves a solution of 0.3 grams of Sudan Black B dissolved in 75 mL of 95% ethanol, diluted to 100 mL with distilled water. This solution is applied to the samples for 10 minutes, staining them effectively. After staining, the samples are dried using filter paper and clarified with a few drops of xylene to remove any excess stain and improve visibility under microscopic examination. Once dry, the samples are counterstained with a 0.5% aqueous solution of safranine for 5 seconds to enhance contrast. Observation under a microscope reveals blue-black colonies, indicative of PHB production. Colonies exhibiting this characteristic staining are selected and picked for further validation and study, confirming them as PHB producers. This two-tiered screening process efficiently narrows down the candidates to those most likely to be valuable for PHB synthesis studies. (Khamnkong et al., 2022).

5.3 Partial Identification of PHA Accumulating Species According to Bergey's Manual

5.3.1 Gram Reaction

The Gram staining technique is a fundamental method in microbiology for differentiating bacteria based on their cell wall composition. This method is critical for bacterial classification and serves as

an initial step in the identification process. In Gram staining, bacterial cells are first fixed onto a glass slide and then stained with crystal violet for approximately one minute. Following this, iodine is applied for another minute to act as a mordant, forming a complex with the crystal violet. Afterward, the slide is treated with ethanol or acetone for about 10–30 seconds, which is crucial in distinguishing two main types of bacteria: Gram-positive and Gram-negative.

Gram-positive bacteria retain the crystal violet-iodine complex and appear purple or blue due to their thick peptidoglycan layer. Conversely, Gram-negative bacteria, which have a thinner peptidoglycan layer, do not retain the dye complex and instead take up a counterstain, typically safranin, which imparts a red or pink color. The outcome of Gram staining provides essential information about the cell wall composition of a bacterium, aiding further investigation and helping to expedite the preliminary classification of bacterial species (Rhode, 2019).

5.3.2 Motility Test

The motility test is a technique used to determine whether microorganisms, such as bacteria, possess the ability to move. This is an essential physiological trait that can help differentiate bacterial species. A commonly employed method to observe bacterial motility is the hanging drop method, often conducted using a cavity slide. To perform this test, a small drop of bacterial culture is carefully placed into the concave cavity of the slide. A coverslip is then applied, creating an airtight chamber that traps the bacteria while allowing microscopic observation of their movement.

Once prepared, the slide is placed under the microscope to observe the bacteria, typically at high magnifications of 40x or 100x. Motile bacteria will display movement within the confined space, often manifesting as a shimmering or swirling motion. Non-motile bacteria, by contrast, remain stationary. The hanging drop technique is particularly advantageous because it allows for the direct observation of bacterial motility, providing conclusive evidence of their movement capabilities. This method is highly useful in microbiological studies for distinguishing bacterial species based on their motility and other physiological traits (Jain et al., 2020).

5.3.3 Biochemical Tests

A series of biochemical tests were carried out to help identify the genus of the bacterial isolates. These tests include the indole, methyl red, Voges-Proskauer, citrate, starch hydrolysis, urease, catalase, triple sugar iron, oxidase, and sugar utilization tests. Each test provides specific insights into the metabolic capabilities of the bacteria, contributing to the partial identification of the isolates (Cappuccino & Sherman, 1998).

1. Indole Test

The indole test determines whether bacteria can metabolize tryptophan to produce indole. A bacterial culture in the exponential growth phase is inoculated into a sterilized test tube containing 5 mL of tryptone broth to conduct the test. The test tube is incubated at 37°C for 18-24 hours. After incubation, approximately 0.5 mL of Kovac's reagent containing dimethylaminobenzaldehyde is carefully added to the broth surface without agitation. A positive result, indicated by the appearance of a crimson layer on the surface, signifies that the bacteria can degrade tryptophan to produce indole. A negative result, where no color change occurs, indicates the absence of indole production.

The indole test is beneficial in differentiating members of the Enterobacteriaceae family. Bacteria like *Escherichia coli* produce indole, resulting in a positive test, whereas species like *Enterobacter* and *Klebsiella* do not produce indole, leading to a negative test (Leboffe & Pierce, 2012).

2. Methyl Red Test

The methyl red test is employed to detect the production of mixed acids during glucose fermentation. Bacteria are inoculated into 5 mL of MR-VP broth containing glucose and incubated at 37°C for 24-48 hours. After incubation, a few drops of methyl red indicator solution are added. This pH indicator turns red when the pH drops below 4.4, indicating the production of stable acid end products from glucose fermentation. A positive result, signified by a red color, means that the bacterium produces mixed acids, lowering the pH of the medium. A negative result, where the color remains unchanged, indicates that the bacterium does not perform mixed acid fermentation.

This test helps distinguish between *Escherichia coli* (which yields a positive result) and *Enterobacter* species (which gives a negative result), both of which are essential members of the Enterobacteriaceae family (Cappuccino & Sherman, 1998).

3. Voges-Proskauer Test

The Voges-Proskauer test is used to detect the presence of acetoin, a neutral end product of glucose fermentation. Bacterial cultures are inoculated into MR-VP broth and incubated at 37°C for 24-48 hours. After incubation, alpha-naphthol and potassium hydroxide (KOH) are added. The development of a red or pink color within 30 minutes indicates a positive result, suggesting that the bacterium produces acetoin. A lack of color change indicates a negative result, meaning that acetoin is not produced.

This test is commonly used in combination with the methyl red test to differentiate between bacteria that produce stable acids from glucose fermentation (such as *Escherichia coli*) and those that produce neutral end products like acetoin (such as *Enterobacter and Klebsiella)* (Leboffe & Pierce, 2012). 4. Citrate Utilization Test

The citrate utilization test determines whether a bacterial strain can metabolize citrate as its sole carbon source. To conduct this test, a pure bacterial culture is inoculated onto a Simmons citrate agar slant using a sterile inoculating loop. The inoculated slant is incubated at an optimal temperature, typically 37°C, for up to 48 hours. A positive result is indicated by a color change from green to blue, showing the bacteria's ability to utilize citrate and produce alkaline byproducts. A negative result, where no color change occurs, demonstrates the bacteria's inability to use citrate as a carbon source. This test is crucial in bacterial classification because different species exhibit varying metabolic capabilities (Cappuccino & Sherman, 1998).

5. Starch Hydrolysis Test

The starch hydrolysis test assesses a bacterium's ability to produce amylase, an enzyme that breaks down starch into smaller sugar molecules. This test is essential for identifying species, especially

those within the genus *Bacillus*. A bacterial culture is streaked onto a starch agar plate and incubated at a suitable temperature, generally between 25-30°C, for a few days to perform the test. After incubation, iodine is applied to the surface of the plate. A clear zone around the bacterial growth indicates a positive result, where the amylase has hydrolyzed the starch, preventing it from reacting with iodine to form a blue-black color. A negative result, where no clear zone is present, signifies the bacterium's inability to hydrolyze starch (Jain et al., 2020). This test helps identify bacteria with specific enzymatic properties.

6. Oxidase Test

The oxidase test detects the presence of cytochrome c oxidase, an enzyme involved in the bacterial electron transport chain. In this test, a sterile swab or loop is used to collect a small amount of bacterial culture, which is then rubbed onto a piece of filter paper or an oxidase test strip impregnated with the reagent N,N,N',N'-tetramethyl-p-phenylenediamine. A color change to purple or blue within 10 to 30 seconds indicates a positive result, showing the presence of cytochrome c oxidase. The test is negative if there is no color change or only a faint color. This test is often used to differentiate *Pseudomonas* species, which are oxidase-positive, from *Enterobacteriaceae*, which are oxidase-negative (Leboffe & Pierce, 2012).

7. Catalase Test

The catalase test detects the presence of the enzyme catalase, which breaks down hydrogen peroxide (H_2O_2) into water and oxygen. This reaction helps bacteria detoxify harmful byproducts of aerobic respiration. A small amount of bacterial culture is placed on a sterile glass slide to perform this test, and a few drops of hydrogen peroxide are added. If catalase is present, the hydrogen peroxide will be broken down, producing oxygen bubbles—a positive result. A negative result, where no bubbles are observed, indicates the absence of catalase. The catalase test is beneficial for differentiating between catalase-positive bacteria like *Staphylococcus* and catalase-negative bacteria like *Streptococcus* (Cappuccino & Sherman, 1998). It is a quick and easy method for the preliminary identification of bacteria.

8. Urease Test

The urease test determines a bacterium's ability to produce the enzyme urease, which hydrolyzes urea into ammonia and carbon dioxide. For this test, a pure bacterial culture is inoculated into a urea agar broth and incubated at 35-37°C for up to 48 hours. A positive result is indicated by a color change from pale yellow to pink or magenta caused by increased pH due to ammonia production. A negative result, where the color remains unchanged, indicates the absence of urease activity. This test is beneficial in identifying urease-positive bacteria, such as *Proteus* species, which are often implicated in urinary tract infections (Jain et al., 2020). The urease test is commonly used in clinical microbiology to identify bacteria based on their enzymatic properties.

9. Sulfide Reduction Test

The sulfide reduction test evaluates a bacterium's ability to reduce sulfur compounds, such as thiosulfate, to hydrogen sulfide (H2S) gas. This test commonly uses SIM (Sulphide, Indole, Motility) agar. A pure bacterial culture is inoculated into the SIM agar by stab-inoculation with a sterile wire or loop to perform the test. The inoculated agar is incubated at 35-37°C for 18-48 hours. A positive result is indicated by the formation of a black precipitate in the medium due to the reaction between hydrogen sulfide and iron compounds in the agar. The absence of any blackening in the medium indicates a negative result. This test is valuable for identifying bacteria capable of sulfur reduction, such as members of the genus *Salmonella* (Rhode, 2019). The sulfide reduction test is also helpful in distinguishing between Gram-negative enteric bacteria.

10. Nitrate Reduction Test

The nitrate reduction test is a crucial microbiological method to determine whether a bacterium can reduce nitrate (NO3-) to nitrite (NO2-) or other nitrogenous compounds. This test is instrumental in differentiating between bacterial species, particularly within the *Enterobacteriaceae* family. A pure bacterial culture is inoculated into nitrate broth and incubated at 35-37°C for 24-48 hours to perform the nitrate reduction test. After incubation, nitrate reagent A, which contains sulfanilic acid dissolved in hydrochloric acid (HCl), and nitrate reagent B, composed of alpha-naphthylamine in HCl, are

added to the broth. A red color indicates the presence of nitrite, which confirms that nitrate reduction has occurred, signaling a positive result. If no red color develops, zinc powder is added. A red color after zinc addition indicates that the bacteria did not reduce nitrate, confirming a negative result. If no color change occurs after zinc is added, nitrate has been reduced beyond nitrite, producing other nitrogenous compounds. This test provides significant information on a bacterium's nitrogen reduction pathways, which are vital in bacterial identification (Jain et al., 2020).

11. Triple Sugar Iron (TSI) Test

The Triple Sugar Iron (TSI) test is widely used in microbiology to differentiate bacteria based on their ability to ferment sugars and produce gas or hydrogen sulfide. The TSI agar contains glucose, lactose, sucrose, phenol red as a pH indicator, and ferrous sulfate for detecting hydrogen sulfide production. To conduct the test, a pure bacterial culture is inoculated into the TSI agar by stabbing the butt and streaking the slant, followed by incubation at 35-37°C for 18-24 hours. After incubation, various reactions can be observed: an alkaline slant (red) with an acidic butt (yellow) indicates glucose fermentation only, while an acidic slant and butt (yellow) indicate fermentation of glucose, lactose, or sucrose. Gas production is evidenced by cracks or lifting of the agar, and the blackening of the medium indicates hydrogen sulfide production due to the reaction with ferrous sulfate. The TSI test is a fundamental technique in microbiology, especially for identifying members of the Enterobacteriaceae family by providing insights into their metabolic capabilities (Cappuccino & Sherman, 1998).

12. Sugar Utilization Test

The sugar utilization test assesses a bacterium's ability to ferment specific sugars, such as glucose, maltose, fructose, mannitol, lactose, and galactose. This test uses a medium containing a particular sugar and a pH indicator, such as bromocresol purple, to detect acid production from sugar fermentation. A pure bacterial culture is inoculated into tubes or wells containing different sugars and incubated at 35-37°C for 24-48 hours to perform the test. Yellow indicates acid production and sugar fermentation, while the medium remaining purple signifies no fermentation. Additionally, gas

production can be assessed using inverted Durham tubes placed in the medium. The gas bubbles in these tubes indicate that the bacterium produces gas during fermentation. This test provides valuable information about a bacterium's ability to metabolize different carbohydrates and helps distinguish among bacterial species based on their fermentation profiles (Leboffe & Pierce, 2012).

13. Growth on Differential Agar Media

Differentiated agar media such as Blood Agar Plates (BAP), Mannitol Salt Agar (MSA), and Spirit Blue Agar (SBA) were used to assess the growth of gram-positive isolates. Blood agar is an enriched and differential medium that helps detect hemolytic activity. Bacteria that produce hemolysins create clear zones (beta-hemolysis) or partial clearing (alpha-hemolysis) around colonies, while gamma-hemolysis indicates no hemolytic activity. Mannitol Salt Agar is selective for staphylococci due to its high salt concentration and differentiates species based on their ability to ferment mannitol. Pathogenic *Staphylococcus aureus* ferments mannitol, turning the medium yellow, while non-pathogenic species do not, leaving the medium unchanged. Spirit Blue Agar detects lipase activity, where bacteria that hydrolyze lipids create clear zones around their colonies. After incubation at 37°C for 24-48 hours, these media were examined for growth patterns, color changes, and clear zones to identify hemolytic activity, mannitol fermentation, and lipase production, respectively (Jain et al., 2020).

5.4 PHA Production

5.4.1 Production of PHA Using MSM Media

All bacterial isolates and positive control strains were inoculated in triplicate test tubes containing 10 mL of mineral salts medium (MSM) to produce polyhydroxyalkanoates (PHA). The cultures were incubated at 37°C and 150 rpm for 72 hours. The composition of MSM (in g/L) was as follows: ammonium chloride (1.5), yeast extract (0.16), potassium dihydrogen phosphate (KH2PO4) (1.52), disodium hydrogen phosphate (Na2HPO4) (4.0), magnesium sulfate heptahydrate (MgSO4·7H2O) (0.52), calcium chloride (CaCl2) (0.02), glucose (20), and 0.1 mL of a trace element solution. The

trace element solution was composed of (in g/L) zinc sulfate heptahydrate (ZnSO4·7H2O) (0.13), ferrous sulfate heptahydrate (FeSO4·7H2O) (0.02), ammonium molybdate tetrahydrate ((NH4)6Mo7O24·4H2O) (0.06), and boric acid (H3BO3) (0.06). Both glucose and the trace element solution were sterilized separately by autoclaving and reconstituted before inoculation (Khamankong et al., 2022).

After 72 hours of incubation, the culture media were centrifuged at 12,000 rpm for 15 minutes to pellet the cells. The cell pellets were then treated with 13% sodium hypochlorite to digest the bacterial cells, and the mixture was incubated at 50°C for 2 hours. The treated solution was centrifuged again at 8,000 rpm for 15-20 minutes. The resulting pellets were washed sequentially with distilled water, acetone, and methanol. The remaining white-colored precipitates were believed to be PHA granules (Khanna & Srivastava, 2005).

5.5 Synthesis of PHA Film

For PHA film synthesis, the extracted PHA granules were dissolved in chloroform and heated until boiling. The dissolved solution was then transferred to sterile Petri dishes or watch glasses and left to incubate overnight. After the incubation period, a light-colored, transparent, thin layer of PHA film became visible in the Petri plate (Verlinden et al., 2007).9

The dry biomass of extracted polyhydroxybutyrate (PHB) was assessed as grams per liter (g/L). The remaining biomass was estimated by calculating the difference between dry cell biomass and dry biomass of PHB. The percentage of intracellular PHB accumulation was calculated as the percentage composition of PHB in the dry cell weight (DCW). DCW refers to the total dry cell weight. The calculation for the dry weight of extracted PHB (g/ml) is as follows: PHB accumulation is calculated as the percentage composition of PHB in the dry cell weight (DCW= Total dry cell weight) (Kumar et al., 2017).

The dry weight of extracted PHB (g/ml) = DCW (g/ml) – Residual biomass (g/ml)

PHB accumulation (%) = Dry weight of extracted PHB (g/ml) × 100 / DCW (g/ml)

5.6 16 S Sequencing

The experiment began with isolating DNA from bacterial cultures using standard methods for genomic DNA extraction. In this case, 3 ml of an overnight bacterial culture was centrifuged at high speed and removed the supernatant. The pellet was resuspended in molecular-grade water and subjected to further centrifugation. After discarding the supernatant, the pellet was resuspended in Buffer R1 to facilitate cell lysis. Lysozyme was added to degrade the bacterial cell wall, followed by incubation at 37°C for 20 minutes. Afterward, centrifugation was performed to pellet the cellular contents, and the supernatant was discarded. The pellet was treated with Proteinase K and Buffer R2 to digest proteins and release nucleic acids. RNase A was also added to degrade RNA, ensuring only DNA remained for further analysis (Sambrook & Russell, 2001).

The lysate was treated with Buffer BG and molecular ethanol to precipitate the DNA, which was then purified using a spin column method. The column was washed with a specific buffer to remove contaminants, and then the DNA was eluted using a preheated Elution Buffer. The resulting genomic DNA was stored for downstream applications, including polymerase chain reaction (PCR) amplification of the 16S rRNA gene.

The isolated genomic DNA was used as a template for PCR amplification of the 16S rRNA gene (~1200 bp) using universal primers (27F and 1492R) targeting conserved regions. The PCR reaction contained standard components, including Taq polymerase, dNTPs, and primers. The PCR program included an initial denaturation at 95°C, followed by 32 cycles of denaturation, annealing, and extension, with a final extension step. This protocol is commonly used in bacterial identification studies, ensuring amplification of the highly conserved 16S rRNA gene (Weisburg et al., 1991).

The amplified DNA was confirmed by agarose gel electrophoresis, where the expected ~1200 bp amplicon was visualized under UV light after staining with ethidium bromide. This technique is routinely used in molecular biology to verify the size and presence of PCR products (Sambrook & Russell, 2001). The PCR product was purified through gel elution to remove excess primers and nucleotides before sequencing.

The purified amplicon was sequenced using the Sanger method, which remains the gold standard for DNA sequencing due to its accuracy and reliability. The sequence obtained was compared to reference sequences in the NCBI database using BLAST, allowing for the identification of bacterial species based on 16S rRNA gene similarity (Altschul et al., 1990). This method is widely recognized as a robust approach for bacterial identification in clinical and environmental microbiology (Janda & Abbott, 2007).

5.7 Hydrolysis of Wood Waste

Wood waste from *Sal* (Shorea robusta) and *Teak* (Tectona grandis) was collected from local regions of Phagwara and Jalandhar, India, where timber industries often generate large quantities of these residues. Before hydrolysis, the collected wood waste was air-dried to remove excess moisture and passed through a sieve to ensure a uniform particle size distribution, improving the consistency of the subsequent chemical treatments (Gupta et al., 2019).

A 10% (w/v) of wood waste was prepared by mixing the dried and sieved material with 100 mL of distilled water. To hydrolyze the lignocellulosic structure of the wood waste and release fermentable sugars, sulfuric acid (H_2SO_4) was added to a final concentration of 4% (v/v). The mixture was then subjected to high-pressure steam treatment by heating at 120°C for 1 hour in an autoclave shown in figure 5.1, which facilitates the breakdown of hemicellulose and partial hydrolysis of cellulose (Singh et al., 2020).
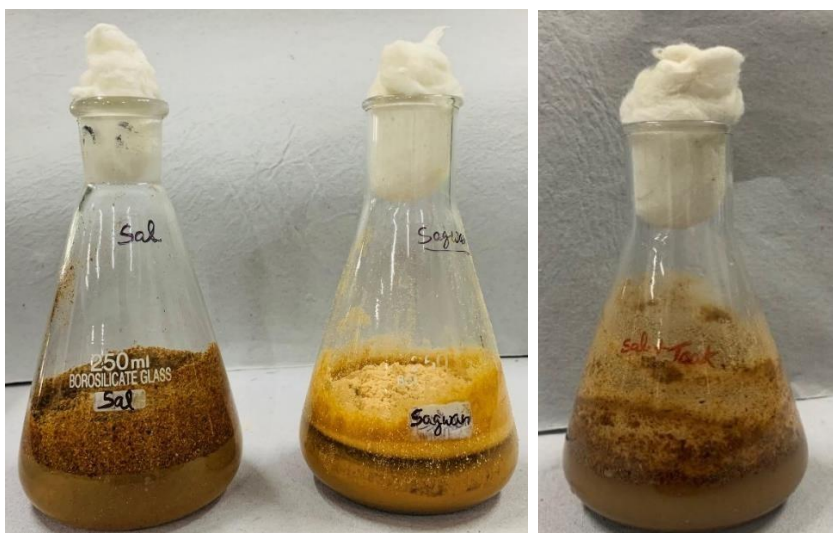
Figure 5.1: Preparation of wheat straw extract for pretreatment using H_2SO_4

After heating, the mixture was filtered using a muslin cloth to separate the solid residue from the liquid fraction or supernatant. The supernatant containing soluble sugars and other breakdown products was collected for further analysis (Jha et al., 2021). To determine the concentration of sugars released during the hydrolysis, a combination of quantitative and qualitative tests was performed:

5.7.1 Molisch Test: The **Molisch test** is a widely used chemical assay to detect the presence of carbohydrates by relying on their reaction with α-naphthol and sulfuric acid, resulting in a characteristic violet or purple ring at the interface of the two reagents. This reaction occurs through dehydration of carbohydrates by sulfuric acid, which leads to the formation of furfural from pentoses or 5-hydroxymethylfurfural from hexoses. These intermediates then react with α-naphthol, forming a colored complex (Gupte et al., 2020). The susceptible test can identify carbohydrates ranging from simple monosaccharides to more complex disaccharides and polysaccharides. Due to its generality, the Molisch test is often used as a preliminary screening tool for the presence of carbohydrates in biological samples (Chawla et al., 2019).

In biochemical studies, the Molisch test is commonly employed to verify the success of hydrolysis processes, such as breaking down complex carbohydrates into monosaccharides. For instance, during the hydrolysis of starch into glucose, a positive Molisch test indicates the

presence of glucose or other simpler sugars, confirming the effectiveness of the enzymatic or acid-catalyzed hydrolysis (Rao et al., 2018). The test, however, does not provide information on the specific type of carbohydrate present, making it useful as an initial qualitative analysis rather than a detailed characterization tool (Tiwari et al., 2021). Despite its limitations, the Molisch test remains a standard in both academic research and industrial carbohydrate analysis due to its simplicity and reliability

5.7.2 DNS Spectrophotometry: The 3,5-dinitrosalicylic acid (DNS) method is a widely used spectrophotometric assay for quantifying reducing sugars. This method is based on the reduction of 3,5-dinitrosalicylic acid by free aldehyde or ketone groups present in reducing sugars, which leads to the formation of a reddish-brown compound, 3-amino-5-nitrosalicylic acid (Miller, 1959). The color intensity of the resulting solution correlates with the concentration of reducing sugars, and this color change can be measured spectrophotometrically at 540 nm. The principle of the DNS assay relies on reducing sugars, such as glucose, to donate electrons, reducing the DNS reagent in the process (Ghose, 1987). The DNS method has been extensively used in carbohydrate research, particularly in enzymatic hydrolysis experiments where the concentration of reducing sugars in the supernatant is measured to monitor the breakdown of polysaccharides into simpler sugars (Bailey et al., 1992). This assay is especially useful because it is simple, inexpensive, and effective in quantifying reducing sugars in various samples, including industrial and research applications (Chaplin et al., 2012). However, it is essential to note that the DNS assay is specific for reducing sugars and will not detect non-reducing sugars, such as sucrose, unless they are first hydrolyzed. The assay is sensitive to changes in reaction conditions, including temperature and pH, which can affect the colorimetric response and should be carefully controlled during the experiment (Zhang et al., 2017). Despite some limitations, the DNS method remains a cornerstone in the quantitative analysis of reducing sugars due to its robustness and ease of use.

The graph shows a relationship between glucose concentration (mg/ml) and absorbance. The x-axis represents the glucose concentration in mg/ml, and the y-axis represents absorbance,

which appears to increase as glucose concentration increases. The data points are connected by a solid line, with a linear regression trend shown as a dotted line. The linear regression equation is y = 0.057x + 0.2093, and the R^2 value is 0.988 shown in figure 5.1, indicating a strong correlation between glucose concentration and absorbance.
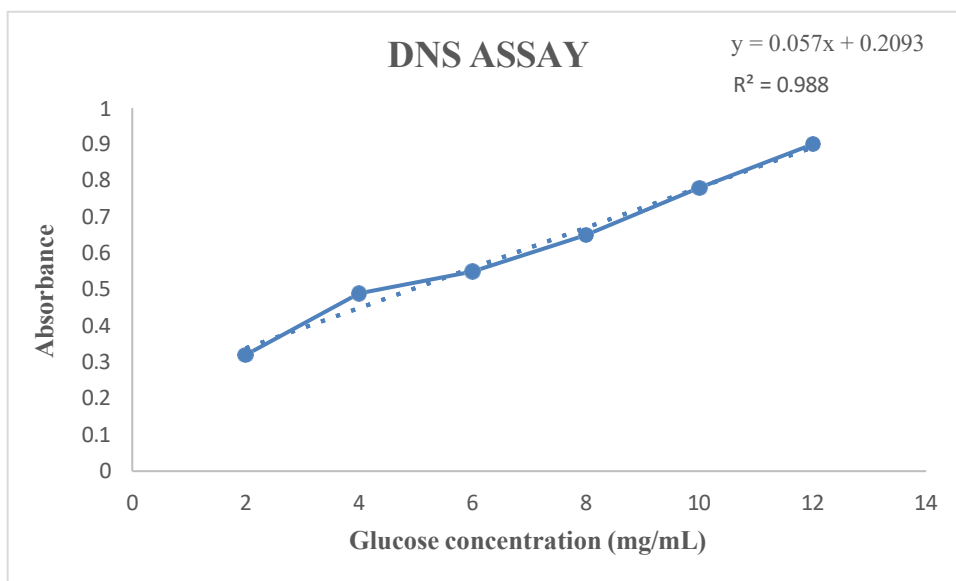
Figure 5.2: Standard graph of glucose presence mg/ml.

- **Linear Relationship**: The absorbance increases steadily with glucose concentration, indicating a positive linear relationship. This is consistent with the trendline, which has a positive slope of 0.057. This slope suggests that for every unit increase in glucose concentration, the absorbance increases by approximately 0.057 units.

- **Goodness of Fit**: The $R2R^2R2$ value of 0.988 indicates that the linear relationship with glucose concentration can explain 98.8% of the variance in absorbance. This implies that the model is a good fit, but some variation remains unexplained, possibly due to experimental error or biological variability.

- **Trendline vs. Actual Data**: The data points closely follow the trendline, with only minor deviations at higher concentrations. The tight clustering of points around the line further supports the strength of the correlation.

- **Potential Anomalies**: There is a slight deviation in the higher glucose concentrations (10-12 mg/ml), where the data points appear slightly above the trendline. This could indicate a minor non-linearity at higher concentrations, which may warrant further investigation.

5.7.3 **Sugar Utilization Test**: The use of microbial strains capable of metabolizing specific sugars is a common approach to verify the availability and concentration of sugars in hydrolysates, particularly in studies involving enzymatic hydrolysis or biomass conversion. In this process, microorganisms such as *Saccharomyces cerevisiae* or *Escherichia coli* are cultured in the presence of hydrolysate, which contains sugars released from the breakdown of polysaccharides. The metabolic activity of these strains, as indicated by their growth or fermentation products, confirms the presence and concentration of fermentable sugars, such as glucose or xylose, in the hydrolysate (Patel et al., 2021).

This microbial assay complements chemical methods, like the DNS method, by providing functional validation that the sugars in the hydrolysate are bioavailable and can be utilized by living organisms. This is crucial in biofuel production or other biotechnological applications where sugar availability directly impacts the efficiency of fermentation processes (Jain et al., 2020). The growth of microbial strains in hydrolysate-based media not only indicates the concentration of specific sugars but also reflects the overall quality of the hydrolysate, including the presence of inhibitors like furfural or hydroxymethylfurfural, which can affect microbial metabolism (Sun et al., 2016). Thus, microbial culturing is valuable in confirming that hydrolysates are suitable for downstream processes such as bioethanol production.

The approach is beneficial when coupled with chemical quantification methods, as it provides a holistic understanding of the chemical composition and the biological availability of sugars in the hydrolysate (Singh et al., 2019). While microbial assays may be slower than direct chemical measurements, they offer insight into the real-world applicability of the hydrolysate in industrial fermentation settings.

The combination of these tests provided insight into the efficiency of the hydrolysis process and the potential utility of the hydrolysate in bio-production processes, such as fermentation for bioethanol or bioplastic precursors like polyhydroxyalkanoates (PHAs) (Thakur & Reddy, 2022). Further improvements in hydrolysis conditions, such as varying acid concentration or reaction time, have been explored to enhance sugar yields and optimize the overall process (Chandel et al., 2013).

5.8 Optimization Using Statistical Experimental Design

The Design of Experiments (DOE), also known as Statistical Experimental Design (SED), is a robust methodology that facilitates the efficient planning and execution of experiments, particularly when multiple variables or causal factors are involved. It systematically tests the relationships between these factors, enabling researchers to determine the factors that have a significant impact on the outcomes (Montgomery, 2017). DOE allows for the minimization of experimental runs while maximizing the information gained, making it particularly advantageous in fields such as biotechnology, where optimization of production processes is essential.

A key component of DOE is the use of screening designs, which help narrow down the list of variables by identifying those that significantly impact the system. This is especially valuable in complex biological systems like microbial fermentation processes for PHA production, where various factors—including nutrient levels, temperature, pH, and agitation speed—can affect PHA yield. By employing a screening design, researchers can reduce the number of variables that need to be tested in further experiments, thus streamlining the optimization process (Antony, 2014).

A commonly used screening approach is the Plackett-Burman (P.B.) design, which is ideal for two-level factorial experiments. P.B. orthogonal arrays enable the assessment of direct effects with reduced design complexity, allowing efficient testing of all factors in a limited number of experimental runs (Ramesh et al., 2019). This method is especially beneficial for processes such as PHA production, where optimizing multiple environmental and nutritional factors is essential to maximize yield.

In the case of PHA production, the Plackett-Burman Design (PBD) is often employed to screen for the most influential factors affecting microbial growth and product accumulation. The design is

typically used to evaluate the effects of 11 independent variables, such as carbon and nitrogen sources, temperature, pH, and agitation speed, which can affect PHA production. These variables are coded into two levels, High (+1) and Low (-1), and a series of experiments are conducted based on the PBD matrix. Each trial is assessed for significance, generally using a 95% confidence interval to determine the reliability of the results. (Mehta et al., 2020).

The design process involves several key steps:

1. **Selection of Factors**: The first step is identifying the most relevant variables likely to affect PHA production. These variables may include carbon and nitrogen sources, micronutrient concentrations, temperature, pH, aeration rate, and agitation speed (Liu et al., 2021).

2. **Range Determination**: Each factor is assigned a range of values to be tested. It is essential to select a broad enough range to capture significant variations in the outcome while avoiding extreme combinations that could lead to experimental failure (Singh & Reddy, 2022).

3. **Statistical Analysis**: Following the experiments, the data are analyzed to identify which factors have a significant impact on PHA production.This analysis often involves ANOVA (Analysis of Variance) to assess the contribution of each factor to the overall variance in the results (Montgomery, 2017).

Using a DOE approach, particularly the P.B. design, researchers can efficiently screen and optimize multiple variables in a relatively short time. This process is crucial for improving biotechnological processes like PHA production, as it maximizes yields with minimal experimental effort and cost. The amount of carbon source optimized using DNS spectroscopy technique will be used for preparation of production media.

Recent studies have demonstrated the effectiveness of using PBD in optimizing PHA production from various microbial strains. For example, researchers have used the PBD approach to optimize the production of PHA in *Bacillus megaterium*, focusing on carbon source, temperature, and pH as key factors influencing yield shown in table 5.1 (Patel et al., 2020). Similarly, another study used the PBD design to optimize nutrient concentrations for PHA production in *Ralstonia eutropha*, significantly increasing biomass accumulation and PHA yield (Singh et al., 2021).

Table 5.1: Illustrating higher and lower values of factors used in PBD

Sr. no.	Factors	Low level	Higher level
1.	Carbon	1%	4%
2.	Nitrogen	0.01%	0.2%
3.	Ferric citrate	0.001%	0.01%
4.	Temperature	28	40
5.	pH	5	9
6.	Inoculum size	2	10
7.	$MgSO_4.7H_2O$	0.01	0.1
8.	Na_2HPO_4	0.1	0.4
9.	K_2HPO_4	0.1	0.4
10.	Incubation period	48	96
11.	Trace elements	0.1	1

5.9 Optimization Using Response Surface Methodology (RSM)

Response Surface Methodology (RSM) is a powerful tool for modeling and optimizing processes in which several independent variables influence the desired outcome. For biopolymer production, RSM was utilized to optimize operational parameters and nutrient levels to enhance PHA yield. This method involves fitting a polynomial model to the experimental data and employing contour plots to examine the relationships between factors and response variables. (Montgomery, 2017).

This study identified three primary factors as having the most significant impact on PHA production: carbon concentration, nitrogen concentration, and temperature. Carbon sources are critical as they provide the building blocks for biopolymer synthesis. Nitrogen sources, such as ammonium chloride or yeast extract, are also essential, but an imbalance in the carbon-to-nitrogen ratio can lead to suboptimal microbial growth or PHA production (Kumar et al., 2020). Temperature, conversely, affects enzyme activity and microbial metabolism, making it another crucial factor for PHA synthesis (Reddy et al., 2019).

A full factorial design was applied to investigate the optimal levels of these factors, and the data were analyzed using RSM to identify these optimal conditions. The following table 5.2 presents the design of experiments (DoE) for these factors

Table 5.2 shows the response surface methodology runs and the values of its factors.

Std	Run	Factor 1 A: Carbon %	Factor 2 B: Nitrogen %	Factor3 C: Temperature Celsius	PHA mg/ml
5	1	1	0.105	28	
11	2	2.5	0.01	40	
17	3	2.5	0.105	34	
7	4	1	0.105	40	
8	5	4	0.105	40	
14	6	2.5	0.105	34	
2	7	4	0.01	34	
1	8	1	0.01	34	
13	9	2.5	0.105	34	
6	10	4	0.105	28	
3	11	1	0.2	34	
9	12	2.5	0.01	28	
10	13	2.5	0.2	28	
16	14	2.5	0.105	34	
4	15	4	0.2	34	
12	16	2.5	0.2	40	
15	17	2.5	0.105	34	

The experiments followed this design, and the results were fitted to a quadratic model using RSM. Statistical analysis indicated significant interactions between carbon concentration and temperature, suggesting that optimal PHA production is achieved at high carbon concentrations and moderate temperatures (Patel et al., 2021).

5.10 Scale Up production

The predicted values from the Response Surface Methodology (RSM) served as crucial guidelines for optimizing the final production stage of polyhydroxybutyrate (PHB). A 2-liter biological fermenter containing optimized production media based on the RSM model was used in this phase. The variables such as carbon source concentration, nitrogen limitation, pH, temperature, and aeration were fine-tuned to achieve maximum PHB yield. The fermenter conditions were closely monitored, and the final quantity of PHB generated was determined using precise calculations based on the biomass yield and PHB concentration in the cells (Mehta et al., 2021).

The PHB was harvested through cell lysis, typically using sodium hypochlorite treatment or mechanical disruption, followed by solvent extraction with chloroform. After extraction, the PHB was precipitated, dried, and weighed to determine the total yield (Patel et al., 2020). The purity of the produced PHB was also calculated by determining the ratio of PHB weight to the total biomass.

5.11 PHA Characterization

5.11.1 UV-Vis spectroscopy

For UV-Vis analysis, the dried PHA granules (1 mg) were heated for 10 minutes. The heated sample was then dissolved in 2 mL of concentrated sulfuric acid. UV spectra were recorded in the 800 to 200 nm range to capture the full spectrum. A baseline calibration was performed using concentrated sulfuric acid, and the standard crotonic acid was utilized as a reference, procured from the Central Drug House Laboratory Reagent, New Delhi, India.

The characteristic absorption peak of PHB was observed at 235 nm, corresponding to the double-bond conjugation in the crotonic acid produced from the thermal degradation of PHB. According to Smith et al. (2015), this wavelength is a reliable indicator for quantifying PHB content in the sample. The precision of the measurements was ensured by consistently maintaining baseline calibration standards and reference solutions (Johnson et al., 2020).

5.11.2 Fourier Transform-Infrared Spectroscopy (FT-IR Analysis)

Fourier Transform-Infrared (FT-IR) spectroscopy is another essential analytical technique for studying the molecular structure and composition of polyhydroxybutyrate (PHB). The FT-IR method works by detecting molecular vibrations within a sample, offering insights into the functional groups present in the polymer. In this analysis, the FT-IR spectra are typically recorded using a Perkin Elmer FT-IR spectrometer, operating in the range of 4000 to 400 cm^{-1}, using Spectrum 10 software for data acquisition and analysis (Singh et al., 2020).

FT-IR spectroscopy is particularly valuable for identifying specific functional groups in PHB, such as carbonyl (C=O) stretching vibrations typically observed around 1720 cm^{-1}. These carbonyl vibrations are characteristic of the ester linkage in the PHB polymer chain. In addition to the carbonyl group, other functional groups, such as hydroxyl (O-H) and methyl (C-H) groups, can also be identified using FT-IR, providing a comprehensive understanding of the PHB molecule's structure (Reddy et al., 2021).

The FT-IR spectrum of PHB often shows firm absorption peaks at specific wavenumbers corresponding to various molecular bonds. For example, absorption bands around 1279 cm^{-1} and

1055 cm^{-1} are associated with C-O-C stretching, confirming the presence of ester bonds in the polymer. The detailed information provided by FT-IR allows researchers to assess the chemical composition of PHB, detect any impurities, and monitor changes in the polymer structure during various processing steps (Mehta et al., 2021).

The combination of UV-Vis and FT-IR spectroscopic techniques provides a comprehensive approach to PHB analysis, allowing researchers to assess the polymer's structural and functional integrity. These methods are indispensable in biotechnological applications where quality control and process optimization are critical. FT-IR, in particular, aids in confirming the successful synthesis of PHB by detecting the characteristic functional groups of the polymer, while UV-Vis quantifies the concentration of PHB in the samples (Miller et al., 2020).

5.11.3 Gas Chromatography-Mass Spectrometry (GC-MS)

Gas Chromatography-Mass Spectrometry (GC-MS) is a powerful analytical technique for identifying and quantifying chemical compounds in a mixture. In the case of polyhydroxybutyrate (PHB) granules, GC-MS is beneficial for determining the monomer composition and analyzing the degradation products of PHB. The principle of GC-MS involves separating compounds based on their volatility using gas chromatography (GC) and then identifying them through mass spectrometry (MS) by measuring their mass-to-charge ratio (m/z) (Koller et al., 2017).

In the analysis of PHB, the granules are first subjected to methanolysis to convert the polymer into its monomeric form, 3-hydroxybutyric acid methyl ester. This step is crucial as it enables the volatile nature of the compound, making it suitable for GC analysis. Methanolysis is typically done using a mixture of methanol and sulfuric acid, heated at 100°C for 3–4 hours. The resulting methyl esters of 3-hydroxybutyrate are then injected into the GC-MS system (Tan et al., 2014).

During the GC process, the volatile methyl esters are vaporized and carried by an inert gas, such as helium, through a capillary column. The column separates the different components based on their volatility and interaction with the column's stationary phase. After separation, the compounds enter the mass spectrometer, where they are ionized and fragmented. The resulting ion fragments are

detected, generating a mass spectrum for each compound. The mass spectra are compared to reference libraries for identification (Reddy et al., 2020).

GC-MS is highly sensitive and provides detailed information about the chemical composition of PHB, making it an essential tool for monitoring PHB purity and degradation during production or processing (Kumar et al., 2019).

5.11.4 Nuclear Magnetic Resonance (NMR)

Nuclear Magnetic Resonance (NMR) spectroscopy is a powerful analytical technique used for determining the structure, purity, and composition of polymers such as polyhydroxybutyrate (PHB). The principle of NMR is based on the interaction of atomic nuclei with an external magnetic field. When nuclei, mainly hydrogen (^1H) or carbon (^{13}C), are exposed to a strong magnetic field, they align in the direction of the field. Upon applying a radiofrequency pulse, these nuclei absorb energy and shift to a higher energy state. As the nuclei return to their original lower energy state, they emit electromagnetic radiation that is detected by the NMR instrument. The emitted signals provide detailed information about the molecular structure, including the chemical environment and bonding of atoms within the PHB sample (Moir et al., 2019).

^1H and ^{13}C NMR spectroscopy are commonly used to analyze the polymer. The methodology begins with dissolving the PHB sample in a deuterated solvent, such as deuterated chloroform ($CDCl_3$). The sample is placed in an NMR tube and inserted into the NMR spectrometer. For ^1H NMR, the instrument detects signals from hydrogen atoms in the polymer backbone, providing information on the polymer's repeating units and chain length. ^{13}C NMR offers insight into the carbonyl (C=O) and methylene (CH_2) groups within the polymer chain (Reddy et al., 2020). The resulting spectra are analyzed for chemical shifts, peak splitting, and integration, which help confirm PHB's molecular structure and purity. This method is essential for verifying the production and quality of PHB in research and industrial applications (Patel et al., 2021).

CHAPTER 6

RESULT AND DISCUSSION

6.1 Isolation and screening of PHA-producing bacteria

6.1.1 Sample collection and Preparation of Mother Samples

Figure 6.1: sample collection site for the isolation of PHA producing bacterial consortia

All collected samples were collected from different locations of Jalandhar as shown in figure 6.1 and inoculated into the sterile nutrient broth and labeled as mother samples

6.1.2 Screening using Nile blue and Sudan black B staining methods.
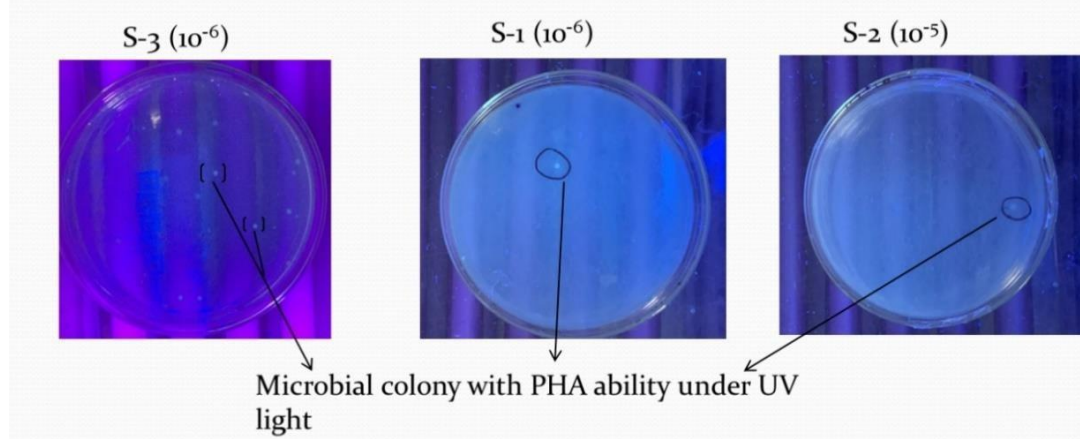
Figure 6.2: PHB producers isolation using nile blue staining technique
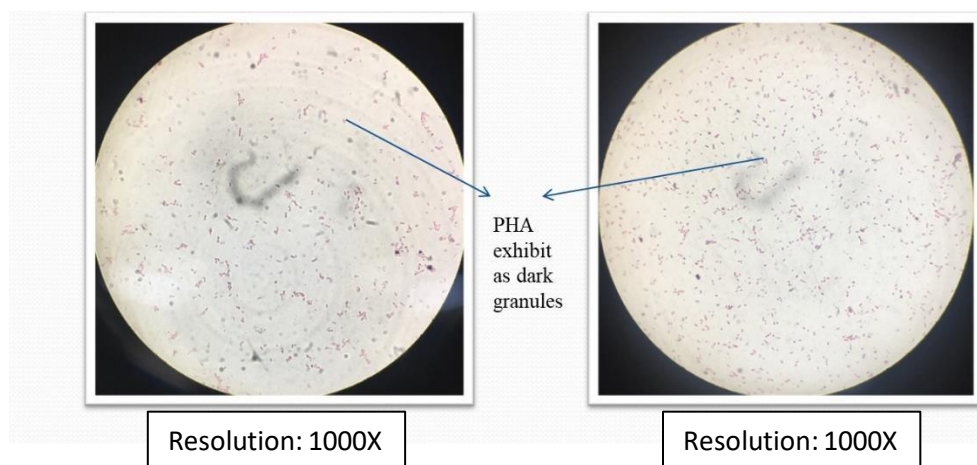
Figure 6.3: Secondary screening of PHB producing isolates using Sudan black staining techniqu

Table 6.1: Sudan black staining results

Isolates no.	Observation	Isolates no.	Observations
S-2	Positive	S-14	Positive
S-3	Positive	S-15	Negative
S-4	Positive	S-16	Positive
S-5	Positive	S-17	Negative
S-6	Negative	S-18	Positive
S-7	Positive	S-19	Positive
S-8	Negative	S-20	Positive
S-9	Positive	S-21	Positive
S-10	Negative	S-22	Negative
S-11	Positive	S-23	Negative
S-12	Positive	S-24	Positive
S-13	Positive	S-25	Positive
		S-26	Positive

In the investigation of polyhydroxyalkanoate (PHA)--producing bacterial strains from four different environmental samples, a total of 56 isolates were initially identified. These isolates were screened for their ability to accumulate PHA. Among the 56 isolates, 26 exhibited fluorescence, indicating potential PHA production. These isolates were distributed as follows: Sample 1 yielded five fluorescent isolates, Sample 2 provided 8, Sample 3 contributed 7, and Sample 4 resulted in 6 isolates. To confirm the presence of PHA, the 26 fluorescent isolates as shown in figure 6.2 were subjected to Sudan Black B staining, a widely used technique to detect intracellular PHA granules. The staining method helps differentiate genuine PHA producers, as it stains the PHA granules black or blue-black within the bacterial cells. Among the 26 fluorescent isolates, 19 demonstrated positive results as shown in figure 6.3 and table 6.1with Sudan Black B staining, indicating the presence of PHA granules. These 19 isolates were,

therefore, classified as ideal PHA producers. This step ensures that the isolates selected for further study are capable of significant PHA accumulation, making them suitable candidates for industrial applications in biopolymer production. Despite showing fluorescence, the remaining isolates were likely not selected as they did not meet the criteria for PHA production, as confirmed by the Sudan Black B staining method.

Table 6.2: Screening results of PHB-producing bacterial isolation

Sample	Total Isolates Identified	Fluorescent Isolates (Nile blue MSM)	Positive for PHA (Sudan Black B Staining)
Sample 1	14	5	4
Sample 2	15	8	6
Sample 3	14	7	5
Sample 4	13	6	4

This data in table 6.2 shows the isolates identified, fluorescent isolates, and those that tested positive for PHA using Sudan Black B staining

6.2 Biochemical tests

The partial identification of bacterial species capable of polyhydroxyalkanoate (PHA) accumulation was performed using *Bergey's Manual of Systematic Bacteriology* as a guide. To begin with, the morphology of the PHA-producing isolates was characterized through gram staining following the Sudan Black B test. The results revealed that many isolates, particularly those from sewage water, were gram-negative bacteria, contrary to initial expectations of gram-positive strains. The morphology of these gram-negative isolates predominantly consisted of small rod-shaped cells. A summary of these gram reaction findings is provided in Table 6.3. In addition to gram staining, motility testing offered further insight into the characterization of the isolates. Using the hanging drop method, all isolates demonstrated motility when observed under a 40X bright-field microscope, confirming their ability to move in liquid media. The motility test results are illustrated in Table 6.4.

Regarding biochemical properties, the isolates exhibited a broad range of metabolic abilities, suggesting diverse biochemical capabilities. These abilities were assessed through their capacity to utilize various substrates, especially in carbohydrate catabolism. Most isolates metabolize glucose, fructose, mannitol, and lactose efficiently. However, a few isolates

struggled to metabolize certain sugars, such as maltose and galactose. This sugar fermentation variability highlights the isolates' metabolic diversity, which could be crucial for their adaptation to different environmental niches and nutrient sources.

Furthermore, the isolates were tested for their growth on differential agar media, particularly Spirit Blue agar, which helped partially identify the bacterial genera. Based on their biochemical behavior and growth patterns, some isolates were suspected to belong to the *Escherichia* and *Pseudomonas* genera. The ability of these isolates to grow on differential media like Spirit Blue agar, alongside their gram-negative rod-shaped morphology and motility, reinforced this hypothesis. The growth patterns on differential media and results from various biochemical tests are detailed in Tables 6.3, 6.4, 6.5, 6.6 and 6.7 . These tables comprehensively summarize the sugar fermentation tests, further corroborating the isolates' capacity to metabolize different carbohydrates.

Overall, the identification process incorporated classical microbiological methods, such as gram staining, motility observation, biochemical tests, and differential media growth to identify the bacterial genera and their characteristics. While partial, this identification provides a strong foundation for further study into the metabolic pathways of these PHA-accumulating species, especially given their diversity in biochemical traits. The findings suggest that the isolates possess a wide range of metabolic capabilities, making them potential candidates for PHA production studies in various environmental and industrial contexts.

Table 6.3: Gram staining reaction

Isolates no.	Observation	Isolates no.	Observation
S-1	Gram-positive rods	S-18	Gram-positive rods
S-2	Gram-positive rods	S-19	Gram-positive rods
S-3	Gram-negative rods	S-20	Gram-negative rods
S-4	Gram-positive rods	S-21	Gram-negative rods
S-5	Gram-negative rods	S-24	Gram-positive rods

S-7	Gram-positive rods		S-25	Gram-positive rods
S-9	Gram-positive rods		S-26	Gram-positive rods
S-11	Gram-positive rods			
S-12	Gram-negative rods			
S-13	Gram-negative rods			
S-14	Gram-positive rods			
S-16	Gram-positive rods			

(A)

(B)

(C)

(D)
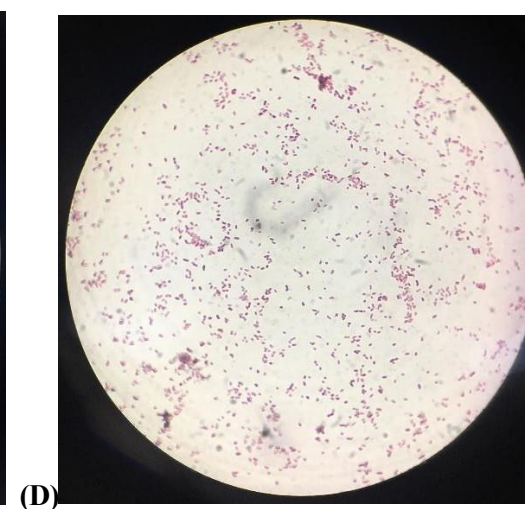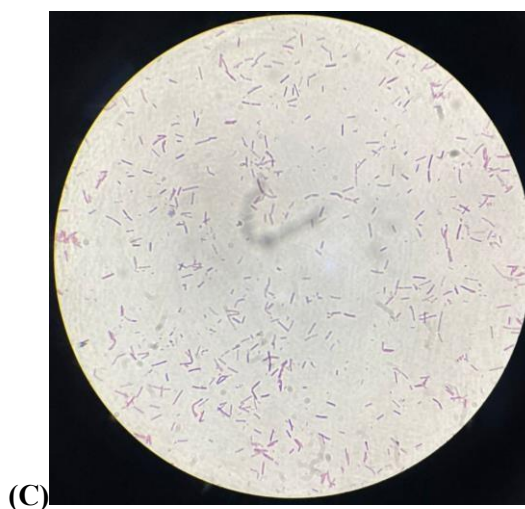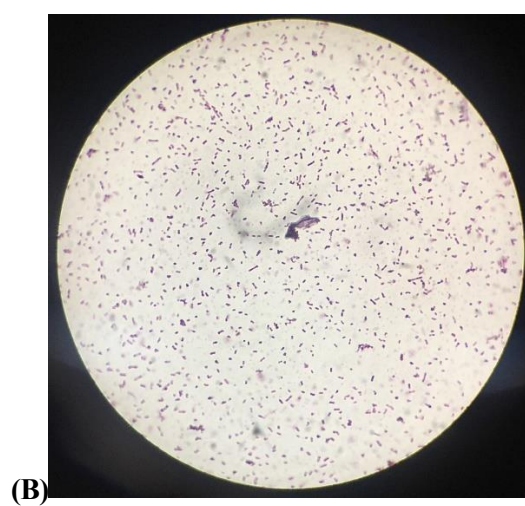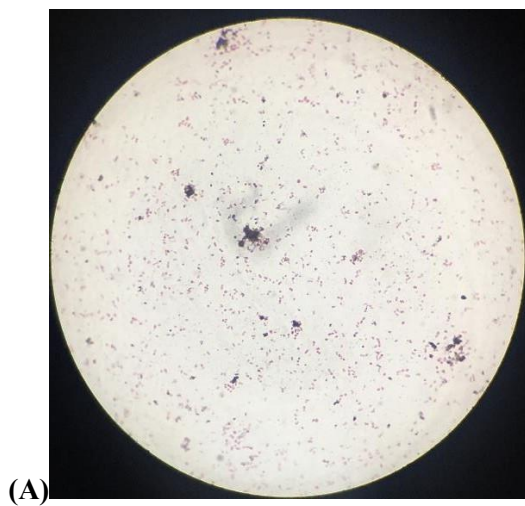
Figure 6.4: Gram staining results of bacterial isolates. (A) Isolate 3 showing Gram-negative morphology. (B) Isolate 7 displaying Gram-positive characteristics. (C) Isolate 11 identified as Gram-positive. (D) Isolate 13 confirmed as Gram-negative.

Table 6.4: Motility test

Isolates no.	Observation	Isolates no.	Observation
S-1	Motile	S-14	Motile
S-2	Motile	S-16	Motile
S-3	Non-Motile	S-18	Motile
S-4	Motile	S-19	Motile
S-5	Non-Motile	S-20	Motile
S-7	Motile	S-21	Motile
S-9	Motile	S-24	Motile
S-11	Non-Motile	S-25	Non-Motile
S-12	Motile	S-26	Non-Motile
S-13	Motile		

Table 6.5: Biochemical tests of PHA producing bacterial isolates

ISOLATES OBSERVATIONS

NAME OF THE BIOCHEMICAL TESTS	S-1	S-2	S-3	S-4	S-5	S-7	S-9	S-11	S-12	S-13	S-14	S-16	S-18	S-19	S-20	S-21	S-24	S-25	S-26
Indole test	+	+	+	+	-	+	+	+	+	+	+	+	+	+	+	+	+	+	+
Methyl-red test	-	+	-	-	-	-	+	-	-	+	-	-	-	+	-	-	-	+	-
Voges-Proskauer test	-	-	-	-	-	-	-	-	-	-	-	-	-	-	-	-	-	-	-
Citrate utilization test	+	+	+	+	+	+	-	+	-	+	+	-	+	+	-	-	+	+	+
Starch hydrolysis test	-	-	-	-	-	-	-	-	-	-	-	-	-	-	-	-	-	-	-
Oxidase test	-	+	+	-	+	+	+	-	+	+	+	+	+	+	+	-	+	+	+

Test																			
Catalase test	+	+	+	+	+	+	+	+	+	+	+	+	+	+	+	+	+	+	+
Urease test	-	-	-	-	-	-	-	-	-	-	-	-	-	-	-	-	-	-	-
Sulfide reduction test	-	-	-	+	-	+	+	+	+	-	-	+	-	-	-	-	-	+	+
Nitrate reduction test	-	-	-	-	+	+	-	-	-	+	+	+	-	-	-	+	-	-	-
Triple Sugar Iron test	a/a*	a/a*	a/a*	a/a*	a/a*	a/a*	a/a*	a/a*	a/a	a/a	a/a*	a/a	a/a*	a/a	a/a*	a/a	a/a*	a/a*	a/a*

'+' indicates positive result for the test
'-' indicates negative result for the test
'a/a' indicates acidic slant and butt
'a/a*' indicates acidic slant and but with gas production
'NA' indicates Not applicable

Table 6.6: Observation of growth on differential agar medium

ISOLATES	GROWTH ON		
	MANNITOL SALT AGAR	**BLOOD AGAR**	**SPIRIT BLUE AGAR**
S-1			LIPASE POSITIVE
S-2			LIPASE NEGATIVE
S-3			
S-4			
S-5			LIPASE POSITIVE
S-7			
S-9			
S-11		γ HEMOLYSIS	
S-12	NO GROWTH		
S-13			LIPASE NEGATIVE
S-14			
S-16			
S-18			LIPASE POSITIVE
S-19			LIPASE NEGATIVE
S-20			
S-21			LIPASE POSITIVE
S-24			
S-25		α HEMOLYSIS	LIPASE NEGATIVE
S-26			

Table 6.7: Sugar Fermentation test observation

Isolates	Sugar Utilization

	Glucose	Maltose	Fructose	Mannitol	Lactose	Galactose
S-1	a*	a*	a*	a*	a*	a*
S-2	a*	a*	a*	a*	a*	a*
S-3	a*	-*	a*	a*	-	a*
S-4	a*	a*	a*	a*	-	a*
S-5	a*	a*	a*	a*	-	a*
S-7	a*	-*	a*	-	a*	a*
S-9	a*	a*	a*	a*	a*	a*
S-11	a*	-*	a*	-	a*	a*
S-12	a*	-*	a*	a*	a*	a*
S-13	a*	-*	a*	a*	a*	a*
S-14	a*	-*	a*	a*	a*	a*
S-16	a*	-*	a*	a*	a*	-*
S-18	a*	-*	a*	a*	a*	a*
S-19	a*	-*	a*	a*	a*	a*
S-20	a*	-*	a*	a*	a*	-*
S-21	a*	-*	a*	a*	a*	a*
S-24	a*	+*	a*	a*	a*	a*
S-25	a*	+*	a*	a*	a*	a*
S-26	a*	+*	a*	a*	a*	a*

a* indicates acid with gas production
-* indicates no acid with gas production
- indicates a negative result

6.3 Extraction and quantification of PHA

After the extraction process and washing, a white precipitate will remain, which was estimated to be the pure PHA content, and will be measured as shown in table 6.8 and figure 6.4 for further study of the production rate of PHA.

Table 6.8: showing DCW of PHA and its production percentage

Sample name	DCW (mg/ml) (Mean)	Dry weight of extracted PHA (mg/ml) (mean)	Expected % of the PHA (mean)	Standard Deviation
1	10.45	6.05	57	1.3
2	10.35	5.9	56.5	1.2
3	10.05	6.75	67	0.4
4	9.75	4.25	41.9	1.3
5	9.85	6.05	60.6	1.2
7	10.2	4.05	38	1.3
9	9.9	3.05	28.8	1.2
11	9.95	2.25	21.8	0.5
12	10.15	5.45	52.7	0.6
13	9.4	5.65	60.2	1.6
14	9.6	4.05	42.1	1.0
16	10.1	5.45	53.6	0.9
18	9.65	4.25	43	1.2
19	9.9	3.25	31.5	1.1
20	10.4	3.5	31.4	1.6
21	10.3	2.75	26.6	1.3
24	9.7	4.05	40.8	1.4
25	9.85	3	28.8	1.7
26	10.65	4.25	39.6	0.8
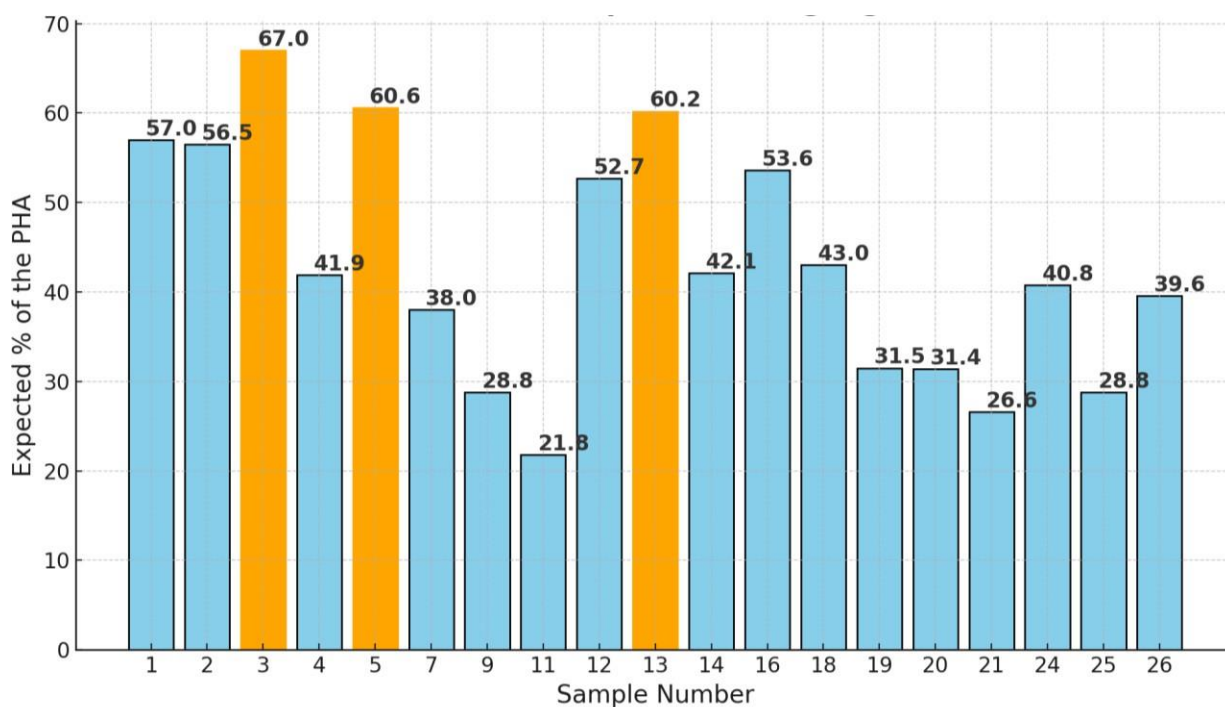
Fig 6.5: Polyhydroxyalkanoate production using different isolates;

6.5 For the synthesis of PHA film

Dissolving polyhydroxyalkanoate (PHA) in chloroform and forming a thin film is a critical step in studying and characterizing PHA biopolymers. This method isolates PHA from the cell matrix and forms a material that can be visually and physically analyzed (Khanna & Srivastava, 2005). The PHA was first dissolved in chloroform, a solvent commonly used for non-polar polymers like PHA due to its ability to dissolve hydrophobic compounds (Jiang et al., 2006). Chloroform is an effective solvent for PHA because it can break down the polymer chains and bring them into a solution, making it ideal for further experimentation, such as film formation (Serafim et al., 2008).

Heating chloroform until it boils, is necessary for the dissolution process, as higher temperatures increase the solvent's capacity to interact with and dissolve the polymer. This is particularly important for PHA, which may not dissolve readily at room temperature (Sudesh et al., 2000). However, care must be taken when handling chloroform, as it is a volatile and hazardous substance, requiring a controlled environment such as a fume hood to ensure safety. Once the PHA is fully dissolved in the boiling chloroform, the solution is transferred to a sterile Petri plate, which serves as the substrate for PHA film formation (Gopi et al., 2018).

The overnight incubation of the chloroform-PHA solution in the Petri plate leads to the evaporation of chloroform, allowing the dissolved PHA to precipitate out and form a thin film.

72

This slow and controlled process enables the polymer chains to align and form a uniform film as the solvent gradually evaporates (Sangeetha et al., 2020). The transparent, light-white thin layer of PHA observed after incubation indicates a successful film formation process as shown in figure 6.4. The transparent nature of the film suggests that the polymer chains were evenly distributed and that no significant crystallization occurred, which could lead to opacity (Sudesh et al., 2000).

This PHA film is of particular interest for several reasons. First, it demonstrates the polymer's capacity to form films, which is desirable for applications in packaging, coatings, and biomedical devices (Reddy et al., 2003). PHA films are biodegradable, making them an environmentally friendly alternative to conventional plastics. Furthermore, the light white color of the film suggests that it is pure and relatively free of impurities, which could be confirmed through further analytical techniques such as Fourier-transform infrared (FTIR) spectroscopy or scanning electron microscopy (SEM) (Verlinden et al., 2007)

In this dataset, three key isolates stand out as top producers of PHA: samples 3, 5, and 13. These isolates displayed the highest percentages of PHA content at 67%, 60.6%, and 60.2%, respectively. The high PHA content in these samples suggests they may possess efficient PHA synthesis pathways, making them ideal candidates for further research and development. The standard deviation values, which represent the variability of the measurements, were relatively low for these samples (0.4 for sample 3, 1.2 for sample 5, and 1.6 for sample 13), indicating consistency in the results and reinforcing the potential of these isolates as reliable PHA producers.

16S ribosomal RNA (rRNA) sequencing could be employed better to understand the microbial identity of these top-producing isolates. The 16S rRNA gene is highly conserved across bacterial species but contains variable regions that can be used for precise taxonomic identification. By sequencing the 16S rRNA gene of isolates 3, 5, and 13, it would be possible to determine their taxonomic classification, potentially identifying them as novel or well-known PHA-producing strains. Once identified, these isolates could be further experimented to optimize PHA production under different conditions. One promising avenue for experimentation is using sustainable substrate sources, such as hydrolyzed wood waste. Wood waste, a byproduct of the forestry industry, is a carbon source that aligns with the growing need for sustainable bioprocesses.

6.5 16s Sequencing

The identification and classification of bacterial strains M3 and M5 were accomplished through 16S rRNA sequence analysis and subsequent phylogenetic analysis, utilizing a neighbor-joining tree to determine their evolutionary relationships. Both strains were isolated from sewage water for their potential in polyhydroxyalkanoate (PHA) production, and their genetic information was submitted to the NCBI, with M3 receiving the accession number PP109354 and being named *Klebsiella sp. strain MK3*, while M5 received the accession number OR362761 and was named *Klebsiella pneumoniae strain DSM 30104 (MK2023)* .

The 16S rRNA gene is an essential molecular marker due to its highly conserved nature across bacterial species, coupled with specific hypervariable regions that provide sufficient variability to distinguish between even closely related taxa. This gene's reliability allows for precise bacterial identification and classification, as demonstrated in the neighbor-joining phylogenetic tree used in this study. The neighbor-joining method arranges bacterial sequences based on genetic distances, effectively illustrating the evolutionary closeness between the strains under study and reference strains from the NCBI database.

6.5.1 *Klebsiella sp. strain MK3* (S3)
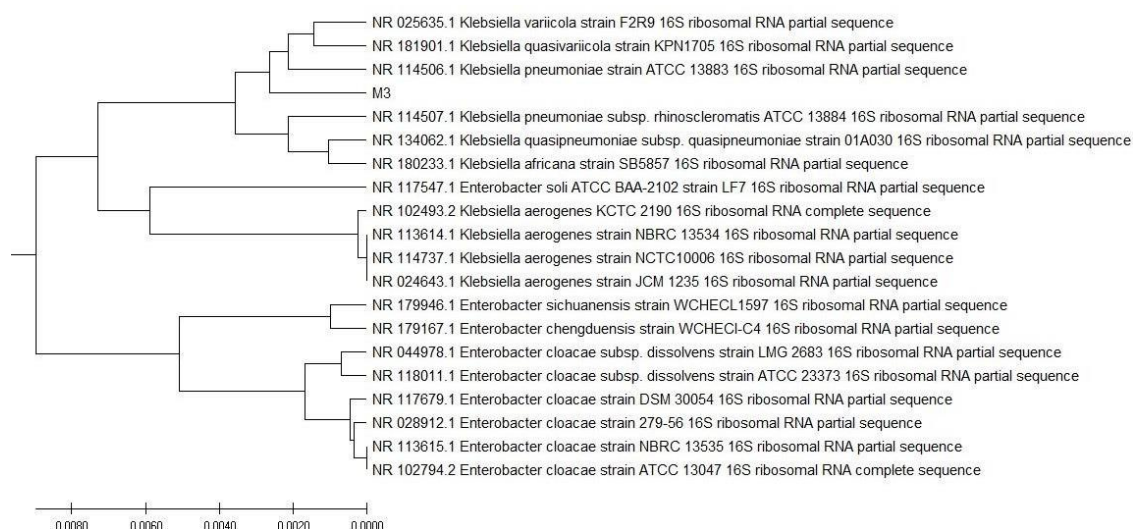
Figure 6.6: Phylogenetic tree showing relevance of the strain with klebsiella sp.

The phylogenetic tree presented indicates that *Klebsiella sp. strain MK3* (M3) does not align perfectly with a single species but shows genetic similarities with various *Klebsiella* strains. It is closely related to *Klebsiella pneumoniae* (NR 114506.1 and NR 114507.1), *Klebsiella variicola* (NR 025635.1), and *Klebsiella africana* (NR 180233.1) as shown in figure 6.6, suggesting that while the strain shares evolutionary traits with these species, it cannot be conclusively classified under any one of them. This ambiguous alignment implies that MK3 may represent a distinct or intermediate lineage. Therefore, it was registered in the NCBI database as *Klebsiella sp. strain MK3*, reflecting the uncertainty in its exact taxonomic classification.

The assignment of NCBI accession number PP109354 for MK3 ensures that its genetic sequence is uniquely identified and accessible, providing a valuable resource for further comparative studies and research in microbial taxonomy. The precise identification and phylogenetic positioning of MK3 demonstrate the effectiveness of 16S rRNA sequencing in distinguishing bacterial strains, thus providing a foundation for future research on this strain's characteristics, particularly its potential application in biotechnological and environmental fields, given its isolation for PHA production.

6.5.2 Analysis of *Klebsiella pneumoniae* strain DSM 30104 (MK2023) (S5)

```
┌─ NR 117684.1 Klebsiella pneumoniae strain DSM 30104 16S ribosomal RNA partial sequence
├─ NR 117685.1 Klebsiella pneumoniae strain DSM 30104 16S ribosomal RNA partial sequence
├─ NR 117682.1 Klebsiella pneumoniae strain DSM 30104 16S ribosomal RNA partial sequence
 NR 117686.1 Klebsiella pneumoniae strain DSM 30104 16S ribosomal RNA partial sequence
 NR 119278.1 Klebsiella pneumoniae strain ATCC 13883 16S ribosomal RNA partial sequence
└ NR 114715.1 Klebsiella pneumoniae strain DSM 30104 16S ribosomal RNA partial sequence
 NR 113702.1 Klebsiella pneumoniae strain NBRC 14940 16S ribosomal RNA partial sequence
─ NR 036794.1 Klebsiella pneumoniae strain DSM 30104 16S ribosomal RNA partial sequence
 NR 112009.1 Klebsiella pneumoniae strain JCM1662 16S ribosomal RNA partial sequence
 ┌─ NR 025635.1 Klebsiella variicola strain F2R9 16S ribosomal RNA partial sequence
 └── NR 181901.1 Klebsiella quasivariicola strain KPN1705 16S ribosomal RNA partial sequence
└── NR 114506.1 Klebsiella pneumoniae strain ATCC 13883 16S ribosomal RNA partial sequence
 NR 113240.1 Klebsiella pneumoniae strain JCM 1662 16S ribosomal RNA partial sequence
 NR 117683.1 Klebsiella pneumoniae strain DSM 30104 16S ribosomal RNA partial sequence
┌─ M5
└─ NR 119276.1 Klebsiella pneumoniae subsp. ozaenae strain ATCC 11296 16S ribosomal RNA partial sequence
 NR 134062.1 Klebsiella quasipneumoniae subsp. quasipneumoniae strain 01A030 16S ribosomal RNA partial sequence
┌─ NR 037084.1 Klebsiella pneumoniae subsp. rhinoscleromatis strain R-70 16S ribosomal RNA gene partial sequence
├─ NR 134063.1 Klebsiella quasipneumoniae subsp. similipneumoniae strain 07A044 16S ribosomal RNA partial sequence
├─ NR 180233.1 Klebsiella africana strain SB5857 16S ribosomal RNA partial sequence
└── NR 114507.1 Klebsiella pneumoniae subsp. rhinoscleromatis ATCC 13884 16S ribosomal RNA partial sequence
```

Figure 6.7: Phylogenetic tree shows most 99.86% sequence similarity with *Klebsiella pneumoniae strain DSM 30104 (MK2023)*

The phylogenetic tree analysis shows that strain M5 shares a 99.86% similarity with other *Klebsiella pneumoniae strain DSM 30104 (MK2023)* strains as shown in figure 6.7. However, it does not reach a 100% match, indicating a slight divergence. This slight difference may imply that M5 does not exhibit the same level of virulence as the most pathogenic strains of *Klebsiella pneumoniae* categorized as biosafety level 3 or 4 organisms. Although it belongs to risk group 2, the lower percentage match suggests that it may not be the most dangerous strain within this species. This finding is beneficial in terms of safety, especially when working with this strain for biotechnological purposes.

Studies have shown that *Klebsiella pneumoniae* has been used for polyhydroxyalkanoate (PHA) production, particularly in strains like K. *pneumoniae* E22, which has been casually employed in research without strict committee approvals (Aneja et al., 2020; Singh et al., 2019). These works highlight the use of this bacterium for sustainable bioplastic production, often without the rigorous oversight that pathogenic bacteria generally require. *Klebsiella pneumoniae strain DSM 30104 (MK2023)* , has been officially registered in the NCBI database under the accession number OR362761, where it is named *Klebsiella pneumoniae* strain DSM 30104 (MK2023).

6.5.3 Analysis of *Escherichia fergusonii* ATCC 35469 MK (S13)

Figure 6.8: Phylogenetic tree shows sequence similarity with *Escherichia fergusonii* ATCC 35469 MK

The phylogenetic tree presented shows that the bacterial strain M13 aligns closely with *Escherichia fergusonii* ATCC 35469 MK based on 16S rRNA gene sequence analysis. Upon conducting a BLAST search, it matches most closely with *Escherichia fergusonii* ATCC 35469 MK, as shown in figure 6.8 confirming its genetic similarity to this species. In terms of industrial applications, especially in the production of polyhydroxybutyrate (PHB), there has been no reported research on this specific strain.

6.6 Hydrolysis of wood waste

6.6.1 Molisch test: The Molisch test, a classic qualitative assay for detecting carbohydrates, yielded a positive result in the form of a purple ring at the interface of the test tube, which indicates the successful release of carbohydrates during the hydrolysis process as shown in figure 6.9 (Patel et al., 2021). This finding is significant because it confirms that the hydrolysis of wood waste, which likely involved breaking down complex polysaccharides into simpler sugars, was successful. Carbohydrates, mainly in the form of polysaccharides such as cellulose and hemicellulose, are key components of lignocellulosic biomass. These polymers must be hydrolyzed into simpler monosaccharides like glucose and xylose to be utilized in microbial fermentation processes (Jain et al., 2020).
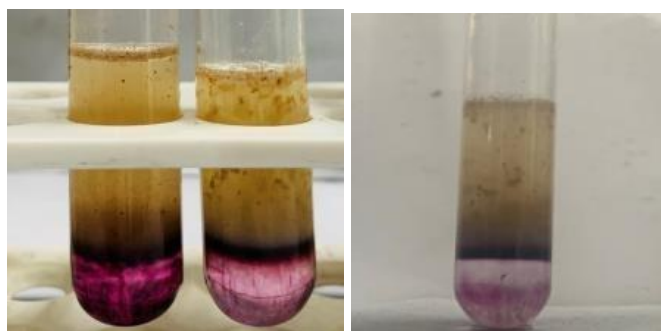
Figure 6.9: moilsch test showing the presence of carbohydrates in the hydrolyzed wood waste.

6.6.2 DNS test for reducing sugar: The 3,5-dinitrosalicylic acid (DNS) method was employed to quantify the concentration of reducing sugars in the hydrolysates. As described by Miller (1959), the DNS reagent reacts with reducing sugars, leading to a color change that can be measured spectrophotometrically. The absorbance values at 540 nm provided quantitative data on the sugar content in the hydrolysed wood samples. The sal and teak wood hydrolysates showed absorbances of 0.722 and 0.741, respectively, while the combined sal and teak wood hydrolysate had a significantly higher absorbance of 0.973 after one-third dilution. These readings, when compared with a standard curve of glucose, indicated that the combined hydrolysate contained approximately 36 mg/mL of reducing sugar. This higher concentration

in the combined sample suggests that hydrolysis of sal and teak wood may enhance the release of fermentable sugars, potentially due to synergistic effects that improve the enzymatic breakdown of lignocellulose (Patel et al., 2021). This finding aligns with other studies that have demonstrated enhanced sugar yields from mixed biomass substrates, as the structural diversity of lignocellulosic components may facilitate more efficient hydrolysis (Jain et al., 2020).

6.6.3 Sugar utilization: a sugar utilization test was performed to assess the ability of microbial isolates to ferment the sugars present in the hydrolysed wood waste. The selected isolates were introduced into a nutrient medium containing peptone and bromocresol as a pH indicator. The initial purple color of the solution indicated a neutral pH. After 24 hours of incubation, the color changed to light brownish as shown in figure 6.10, signifying a drop in pH due to acid production during sugar metabolism by the microbes. This result confirms that the isolates were able to utilize the sugars in the hydrolysate as a carbon source, leading to fermentation (Chandel et al., 2012).

Figure 6.10: sugar utilization showing that our isolate can consume wood waste as a substrate media.

Moreover, the sugar utilization test, in conjunction with the DNS assay, provides a comprehensive assessment of both the chemical composition and the bioavailability of sugars in the hydrolysate. While the DNS method quantifies the total reducing sugar content, the microbial fermentation test demonstrates the functional availability of these sugars for biological processes. This two-pronged approach is critical for evaluating the suitability of lignocellulosic hydrolysates for downstream applications such as fermentation-based biofuel production (Sun et al., 2016).

6.7 Statistical analysis

In this study, statistical optimization was performed using Design Expert 12 software to enhance the production of Polyhydroxyalkanoates (PHA) from 19 different bacterial isolates, with isolate no 3, showing the highest yield at over 60%. The optimization was carried out in two phases using the Plackett-Burman Design (PBD) and Response Surface Methodology (RSM). Initially, PBD was employed to screen 11 variables, including carbon, nitrogen, ferric citrate, temperature, pH, inoculum size, $MgSO_4 \cdot 7H_2O$, Na_2HPO_4, K_2HPO_4, incubation period, and trace elements. PBD is an effective statistical tool for screening many variables with minimal runs, allowing for identifying significant factors with limited resources (Mousavi et al., 2013). In this experiment, each variable was tested at two levels (high and low), and the Design Expert software generated 12 runs for each sample. The results were statistically analyzed using ANOVA, which provided insights into the significance of the tested variables. PBD was chosen due to its capacity to screen for essential variables with fewer experimental trials, which makes it ideal for studies with resource constraints. PBD ensures a balanced representation of factors and allows researchers to focus on the most influential variables for further optimization (Patil et al., 2015).

Following the PBD screening, the identified significant factors were optimized using Response Surface Methodology (RSM). RSM allows for fine-tuning the critical variables identified during PBD by examining their interactions and optimizing their levels to maximize the production of PHA (Nath et al., 2008). The optimization process led to the improvement of PHA yield, demonstrating the effectiveness of statistical design in enhancing microbial production processes. The experimental design employed in this study demonstrates the power of Design of Experiments (DOE) approaches like PBD and RSM in bioprocess optimization. The study efficiently identified key factors influencing PHA production by utilizing statistical methods, enabling targeted optimization with a reduced number of experimental runs. This methodology is increasingly adopted in biotechnological research to improve yields while minimizing resource usage (Rai et al., 2011)

6.7.1 Isolate no. 3: *Klebsiella sp. strain MK3*

Table 6.9: PBD runs and response PHA readings for isolate *Klebsiella sp. strain MK3*

Run	A: carbon %	B: Nitrogen %	C: Ferric citrate %	D: Temperature Celsius	E: pH	F: Inoculum size micro ml	G: MgSO$_4$.7H$_2$O %	H: Na$_2$HPO$_4$ %	J: K$_2$HPO$_4$ %	K: Incubation period Hours	L: Trace elements %	PHA mg/10mL
1	4	0.01	0.001	28	9	2	0.1	0.4	0.1	96	1	**57**
2	4	0.01	0.01	40	9	2	0.01	0.1	0.4	48	1	**60.5**
3	1	0.01	0.01	28	9	10	0.01	0.4	0.4	96	0.1	**41**
4	4	0.2	0.001	28	5	10	0.01	0.4	0.4	48	1	**59.5**
5	4	0.01	0.01	40	5	10	0.1	0.4	0.1	48	0.1	**51**
6	4	0.2	0.001	40	9	10	0.01	0.1	0.1	96	0.1	**66**
7	1	0.01	0.001	40	5	10	0.1	0.1	0.4	96	1	**41**
8	1	0.2	0.01	40	5	2	0.01	0.4	0.1	96	1	**56.5**
9	1	0.2	0.001	40	9	2	0.1	0.4	0.4	48	0.1	**52.5**
10	1	0.01	0.001	28	5	2	0.01	0.1	0.1	48	0.1	**35.5**
11	1	0.2	0.01	28	9	10	0.1	0.1	0.1	48	1	**47**

| 12 | 4 | 0.2 | 0.01 | 28 | 5 | 2 | 0.1 | 0.1 | 0.4 | 96 | 0.1 | **54.5** |

The provided dataset showcases a factorial design to investigate various factors' effects on **PHA (Polyhydroxyalkanoates)** production, measured in milligrams per 10 mL, across 12 experimental runs. The factors include **Carbon** (%), **Nitrogen** (%), **Ferric citrate** (%), **Temperature** (°C), **pH**, **Inoculum size** (μL), **MgSO4.7H2O** (%), **Na2HPO4** (%), **K2HPO4** (%), **Incubation period** (hours), and **Trace elements** (%).

From the results, **Run 6** yields the highest PHA production (66 mg/10 mL) as shown in table 6.9, with high carbon (4%), low nitrogen (0.001%), and the maximum temperature (40°C), indicating that higher carbon content, lower nitrogen, and elevated temperature seem to favor PHA accumulation. This result aligns with previous studies highlighting the importance of carbon as a primary substrate for microbial PHA synthesis (Laycock et al., 2013). A neutral pH (9), moderate inoculum size (10 μL), and low MgSO4.7H2O (0.01%) also contributed positively in this experiment.

Run 10, on the other hand, shows the lowest PHA production (35 mg/10 mL) under conditions of low carbon (1%) and low nitrogen (0.001%) at a lower temperature (28°C) and lower pH (5). Insufficient carbon and lower temperatures limit microbial growth and PHA production.

Interestingly, runs with higher temperatures (above 28°C), high carbon content (4%), and a more neutral pH (around 9) consistently resulted in higher PHA yields. Additionally, **Runs 4, 2, and 12** exhibited high PHA values, indicating that temperature and carbon levels are crucial in optimizing PHA production (Koller et al., 2010). The impact of trace elements, nitrogen concentration, and MgSO4.7H2O levels also appears to be important but to a lesser extent.

6.7.1.1 ANOVA for selected factorial model

Table 6.10: ANOVA statistics for isolate *Klebsiella sp. strain MK3*

Source	Sum of Squares	df	Mean Square	F-value	p-value	
Model	3664.33	10	366.43	1099.30	0.0235	significant
A-Carbon	1875.00	1	1875.00	5625.00	0.0085	
B-Nitrogen	833.33	1	833.33	2500.00	0.0127	
D-temperature	363.00	1	363.00	1089.00	0.0193	

E-PH	225.33	1	225.33	676.00	0.0245
F-inoculum size	40.33	1	40.33	121.00	0.0577
G-MgSo4.7H2o	85.33	1	85.33	256.00	0.0397
H-Na2HPo4	56.33	1	56.33	169.00	0.0489
J-K2HPo4	5.33	1	5.33	16.00	0.1560
K-incubation period	33.33	1	33.33	100.00	0.0635
L-trace elements	147.00	1	147.00	441.00	0.0303
Residual	0.3333	1	0.3333		
Cor Total	3664.67	11			

The data presented indicates that the **Model F-value** of 1099.30, with a corresponding **p-value** of 0.0235, suggests the overall model is significant. The model explains a large portion of the variance in the response variable, confirming its suitability for predicting outcomes. Significant factors have **p-values** below 0.05 as shown in table 6.10, emphasizing their impact on the system.

Among the factors, **A-Carbon** has the most substantial influence, with a **Sum of Squares** (SS) of 1875.00 and an exceptionally low **p-value** of 0.0085, indicating it is the most critical parameter. Similarly, **B-Nitrogen** and **D-temperature** also significantly contribute to the response, with **F-values** of 2500.00 and 1089.00, respectively. These factors are critical to optimizing the system, likely affecting microbial growth or biochemical reactions.

The contributions of **E-PH**, **G-MgSO4.7H2O**, **H-Na2HPO4**, and **L-trace elements** are also significant, with **p-values** ranging from 0.0245 to 0.0489. These parameters impact system performance but to a lesser extent than Carbon and Nitrogen. Interestingly, **the J-K2HPO4 and K-incubation periods** are insignificant, as their **p-values** exceed 0.05, implying their minimal impact under the tested conditions.

The **residual error** is extremely low, with a **Sum of Squares** of only 0.3333, further validating the model's fit. These results suggest that focusing on the significant factors—especially Carbon, Nitrogen, temperature

6.7.1.2 Fit Statistics

Table 6.11: Fit statistics for isolate *Klebsiella sp. strain MK3*

Std. Dev.	0.5774	R²	0.9999
Mean	103.67	Adjusted R²	0.9990
C.V. %	0.5569	Predicted R²	0.9869
		Adeq Precision	110.3532

The fit statistics provided indicate an excellent model fit for predicting the outcomes of the system under study. The **Predicted R²** of 0.9869 is closely aligned with the **Adjusted R²** of 0.9990, with a difference of less than 0.2 as shown in table 6.11, demonstrating that the model's predictive accuracy reasonably agrees with its adjusted explanatory power. This alignment suggests that the model is robust and does not suffer from overfitting, meaning that it is reliable for making predictions beyond the data used to build it (Montgomery et al., 2017).

The **Standard Deviation** (Std. Dev.) of 0.577 shows that the model's residuals are minimal, indicating that the model has a high degree of precision. The **C.V. %** (Coefficient of Variation) of 0.557% also reinforces the consistency and precision of the results, as a lower C.V. indicates less variability relative to the mean (Box et al., 2005).

Moreover, the **Adequate Precision** of 110.353, which measures the signal-to-noise ratio, is well above the recommended threshold of 4. This extremely high value confirms that the model has an adequate signal and can reliably navigate the design space, making it highly effective for further experimental optimization (Anderson & Whitcomb, 2016). These fit statistics collectively suggest that the model is robust, precise, and reliable for prediction and further experimentation.

6.7.1.3 Percentage contribution

Table 6.12: percentage contribution of each factor affecting PHB production rate

Term	Stdized Effect	Sum of Squares	% Contribution
A-Carbon	25	1875	51.1643
B-Nitrogen	16.6667	833.333	22.7397
C-Ferric Citrate	-0.33333	0.333333	0.009096
D-Temperature	11	363	9.9054
E-PH	8.66667	225.333	6.14881
F-Inoculum Size	-3.66667	40.3333	1.1006
G-MgSO4·7H2O	-5.33333	85.3333	2.32854
H-Na2HPO4	4.33333	56.3333	1.5372
J-K2HPO4	-1.33333	5.33333	0.145534
K-Incubation Period	3.33333	33.3333	0.909587
L-Trace Elements	7	147	4.01128

- **A-Carbon** is the dominant factor, contributing the most at 51.16% as shown in table 6.12, with a significant standardized effect of 25 and the most considerable sum of squares at 1875.

- **B-Nitrogen** is the second most influential factor, contributing 22.74%, with a standardized effect of 16.67 and a sum of squares at 833.33.

- **C-Ferric Citrate** and **J-K2HPO4** have negligible contributions, around 0.01%, indicating they have little to no impact on the outcome.

- **D-Temperature** also has a noteworthy contribution of 9.91%, suggesting it plays a moderately significant role.

- Other factors like **E-PH**, **F-Inoculum Size**, and **G-MgSO4.7H2O** contribute 6.15%, 1.10%, and 2.33%, respectively, implying they have a more minor but still notable effect.

- **H-Na2HPO4** and **L-Trace Elements** contribute around 1.54% and 4.01%, respectively.

The standardized effects range from highly positive (A-Carbon) to slightly negative (F-Inoculum Size and G-MgSO4). This negative value implies an inverse relationship between those factors and the outcome. The percentage contribution helps prioritize which factors have

the most significant effect on the outcome for decision-making and optimization. Factors with low contributions, like C-Ferric Citrate as shown in figure 6.11, may be less relevant for further analysis or experimentation.
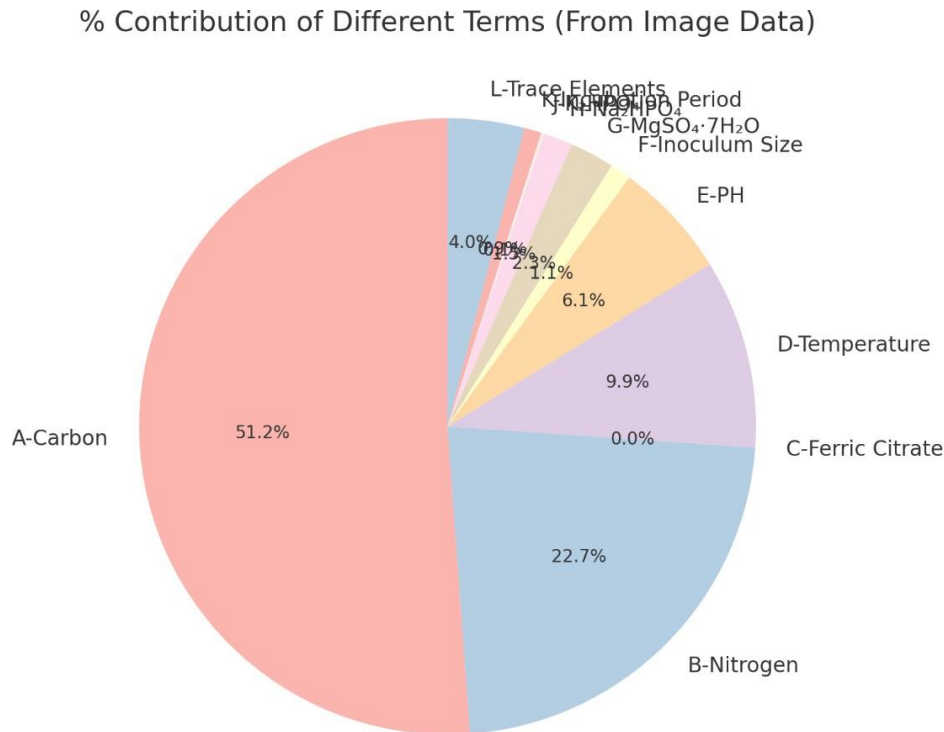
Figure 6.11: pie chart representation of the percentage contribution of each factor affecting PHB production rate

6.7.1.4 Pareto Chart

The Pareto chart visually represents the effects of different factors on the system, with the t-value of each effect displayed on the y-axis and the rank on the x-axis. This chart emphasizes which factors have the greatest impact on the process, categorized into positive and negative effects. Factors such as **A-Carbon and B-Nitrogen** show the most significant positive effects, with t-values exceeding 70, highlighting their critical role in influencing the outcome. This confirms the importance of carbon and nitrogen as essential components, potentially contributing to key biological processes like microbial growth or enzymatic activities (Montgomery et al., 2017).

D-Temperature and **E-PH** are also significant factors, with notable positive effects on the system, although they rank lower than carbon and nitrogen. These factors are often critical in biochemical reactions, influencing reaction rates and microbial activity (Box et al., 2005).

Though positive, trace elements contribute less significantly compared to the top-ranked factors.

On the other hand, the chart shows **G-MgSO4.7H2O**, **H-Na2HPO4**, and **F-Inoculum size** as negative factors, suggesting their inhibitory role in the process when present at higher concentrations. Interestingly, **J-K2HPO4** shows the most negligible impact as shown in figure 6.12, as its t-value is significantly lower than the others, indicating minimal influence under the current experimental setup.

This analysis underscores the need to optimize vital positive factors like carbon, nitrogen, and temperature while carefully controlling the concentration of harmful factors to avoid inhibition.
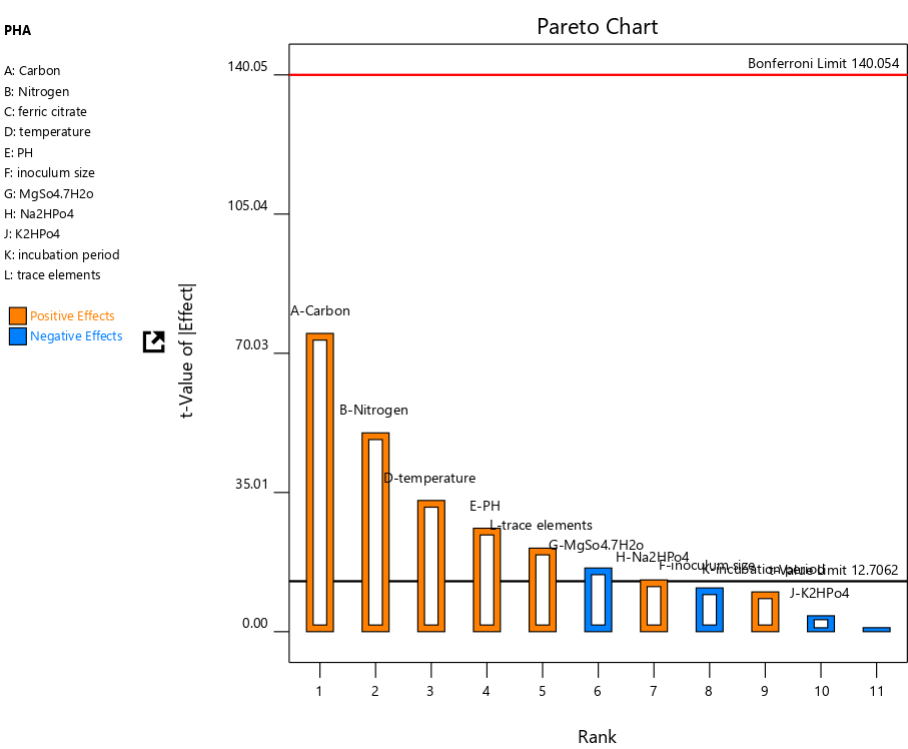
Figure 6.12: Pareto chart representing each factor within Bonferroni limits

This analysis underscores the need to optimize critical positive factors like carbon, nitrogen, and temperature while carefully controlling the concentration of negative factors to avoid inhibition.

6.7.2 For isolate 5: *Klebsiella pneumoniae strain DSM 30104 (MK2023)*

Table 6.13: PBD runs and response PHA readings for isolate *Klebsiella pneumoniae DSM 30104 (MK2023)*

Run	A: carbon %	B: Nitrogen %	C: Ferric citrate %	D: Temperature Celsius	E: pH	F: Inoculum size micro ml	G: MgSO$_4$.7H$_2$O %	H: Na$_2$HPO$_4$ %	J: K$_2$HPO$_4$ %	K: Incubation period Hours	L: Trace elements %	PHA mg/10 ml
1	4	0.01	0.001	28	9	2	0.1	0.4	0.1	96	1	**54**
2	4	0.01	0.01	40	9	2	0.01	0.1	0.4	48	1	**56.5**
3	1	0.01	0.01	28	9	10	0.01	0.4	0.4	96	0.1	**40**
4	4	0.2	0.001	28	5	10	0.01	0.4	0.4	48	1	**61.5**
5	4	0.01	0.01	40	5	10	0.1	0.4	0.1	48	0.1	**50.5**
6	4	0.2	0.001	40	9	10	0.01	0.1	0.1	96	0.1	**68.5**
7	1	0.01	0.001	40	5	10	0.1	0.1	0.4	96	1	**44**
8	1	0.2	0.01	40	5	2	0.01	0.4	0.1	96	1	**55.5**
9	1	0.2	0.001	40	9	2	0.1	0.4	0.4	48	0.1	**49.5**
10	1	0.01	0.001	28	5	2	0.01	0.1	0.1	48	0.1	**35.5**
11	1	0.2	0.01	28	9	10	0.1	0.1	0.1	48	1	**48**

12	4	0.2	0.01	28	5	2	0.1	0.1	0.4	96	0.1	**56.5**

This dataset explores the influence of several factors on Polyhydroxyalkanoate (PHA) production, measured in mg/10ml, across 12 experimental runs. The factors include varying carbon, nitrogen, ferric citrate levels, temperature, pH, inoculum size, and several trace elements like $MgSO_4 \cdot 7H_2O$, Na_2HPO_4, K_2HPO_4, and the incubation period as shown in table 6.13.

One of the key patterns observed is that **carbon concentration** plays a crucial role in PHA production. Higher carbon levels (4%) consistently correspond to higher PHA yields, such as in run 6, where the highest yield of 68.5 mg/10ml is achieved. In contrast, lower carbon levels (1%) result in significantly lower yields, such as in run 3 with a 40 mg/10ml PHA output.

Nitrogen and **ferric citrate** levels remain primarily constant across the runs, suggesting these variables may not significantly influence the PHA yields. However, **temperature** and **pH** vary, with higher temperatures (40°C) and pH levels (5 or 9) producing varying PHA outputs.

Inoculum size also has a noticeable impact, where higher levels (10 micro ml) appear to contribute to increased PHA production, especially in combination with higher carbon levels. The **incubation period**, either 48 or 96 hours, seems to favor longer durations, often leading to higher yields. The trace elements, like $MgSO_4 \cdot 7H_2O$ and Na_2HPO_4, exhibit minimal variability but could still play a supportive role in optimizing PHA production. Carbon concentration, incubation period, and inoculum size seem to be the most influential factors affecting PHA yield.

6.7.2.1 ANOVA for selected factorial model

Figure 6.14: ANOVA statistics for isolate *Klebsiella pneumoniae DSM 30104 (MK2023)*

Source	Sum of Squares	df	Mean Square	F-value	p-value	
Model	3689.33	10	368.93	276.70	0.0468	significant
A-Carbon	1875.00	1	1875.00	1406.25	0.0170	
B-Nitrogen	1160.33	1	1160.33	870.25	0.0216	
C-ferric citrate	12.00	1	12.00	9.00	0.2048	

D-temperature	280.33	1	280.33	210.25	0.0438
E-PH	56.33	1	56.33	42.25	0.0972
F-inoculum size	8.33	1	8.33	6.25	0.2422
G-MgSo4.7H2o	75.00	1	75.00	56.25	0.0844
J-K2HPo4	5.33	1	5.33	4.00	0.2952
K-incubation period	96.33	1	96.33	72.25	0.0746
L-trace elements	120.33	1	120.33	90.25	0.0668
Residual	1.33	1	1.33		
Cor Total	3690.67	11			

The Model F-value of 276.70 suggests that the model is highly significant, meaning it effectively explains the variability in the dataset. An F-value this large indicates a strong relationship between the factors and the response variable (e.g., PHA production), with only a 4.68% probability that such a value could result from random noise as shown in table 6.14. This low probability reinforces the model's reliability in predicting outcomes based on the variables used.

The p-values provide further insight into the significance of individual model terms. In this case, factors A (Carbon), B (Nitrogen), and D (Temperature) are identified as significant, as their p-values are less than 0.0500, meaning they have a strong influence on the response variable. These factors contribute most to the model's ability to predict PHA yield.

On the other hand, model terms with p-values more significant than 0.1000 are considered insignificant, meaning they do not contribute meaningfully to the model's predictive power. If several such terms exist, they are not critical to the model. Reducing these insignificant terms can streamline the model, improving its simplicity without sacrificing accuracy. However, terms part of a hierarchical structure should be retained to maintain model integrity.

6.7.2.2 Fit Statistics

Figure 6.15: fit statistics for isolate *Klebsiella pneumoniae DSM 30104 (MK2023)*

Std. Dev.	1.15	**R²**		0.9996
Mean	103.33	**Adjusted R²**		0.9960
C.V. %	1.12	**Predicted R²**		0.9480
		Adeq Precision		59.6992

The Predicted R² of 0.9480, in close agreement with the Adjusted R² of 0.9960, with a difference of less than 0.2 as shown in table 6.15, indicates that the model is reliable and has good predictive accuracy. The Predicted R² reflects the model's ability to predict new data, while the Adjusted R² accounts for the number of predictors in the model. The closeness of these values suggests that the model fits the data well without being overfitted.

Adequate Precision, which measures the signal-to-noise ratio, shows that a ratio above 4 is desirable for a strong model. With a ratio of 59.699, this model has an excellent signal-to-noise ratio, which is robust and reliable for navigating the design space. Hence, it is suitable for making predictions and optimizing the variables within the given design.

6.7.2.3 Percentage Contribution

Table 6.16: Percentage contribution for isolate *Klebsiella pneumoniae DSM 30104 (MK2023)*

Term	Stdized Effect	Sum of Squares	% Contribution
A-Carbon	25	1875	50.8038
B-Nitrogen	19.6667	1160.33	31.4397
C-Ferric Citrate	-0.33333	0.333333	0.325145
D-Temperature	9.66667	280.333	7.59787
E-PH	4.33333	56.3333	1.52637
F-Inoculum Size	1.66667	8.33333	0.225194
G-MgSO₄·7H₂O	-5	75	2.02915
H-Na₂HPO₄	-1.33333	5.33333	0.144509
J-K₂HPO₄	-0.66667	1.33333	0.036157

K-Incubation Period	3.33333	33.3333	0.90194
L-Trace Elements	6.33333	147	3.62048

This dataset offers insights into the contributions of various factors influencing a response variable, likely associated with PHA production or a similar biological output.The most dominant factor is **A-Carbon**, contributing 50.80% to the overall model, indicating its critical role in driving the response. The second most influential factor is **B-Nitrogen** as shown in table 6.16, which contributes 31.44%. This suggests that nitrogen concentration also plays a significant role, though not as prominently as carbon.

D-Temperature follows with a contribution of 7.60%, highlighting its moderate but essential impact on the process. The factors **E-PH** and **F-Inoculum Size** contribute 1.53% and 0.23%, respectively, indicating that while they are essential, their influence is considerably more negligible than carbon and nitrogen.

Interestingly, **G-MgSO$_4$·7H$_2$O** has a negative standardized effect but still contributes 2.03%, implying a potential inverse relationship with the response. **H-Na$_2$HPO$_4$** town-center, J-K$_2$HPO$_4$ town-center, and K-Incubation Period have minor contributions, all under 1%, suggesting they may not significantly impact the output under the conditions tested.

The relatively small contributions of some factors, like ferric citrate (0.33%), indicate these variables may have little influence on the outcome. Carbon and nitrogen are the primary drivers as shown in figure 6.11, while the other factors contribute to fine-tuning the response.

% Contribution of Different Terms

L-Trace Elements
Incubation Period
K-H3BO3
G-glucose MgSO4.7H2O
F-Inoculum Size
E-PH
D-Temperature
C-Ferric Citrate

3.67%
2.06%
0.23%
1.55%
7.70%
0.33%

A-Carbon
51.50%

B-Nitrogen
31.87%
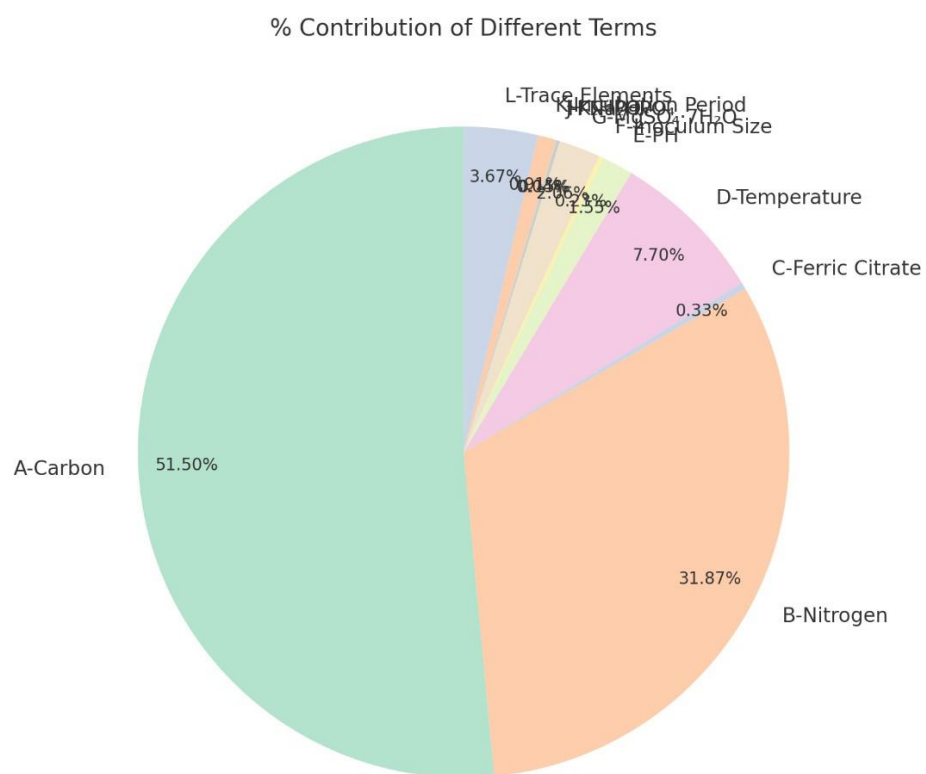
Figure 6.13: pie chart representation of percentage contribution for isolate *Klebsiella pneumoniae DSM 30104 (MK2023)*

6.7.2.4 Pareto chart:
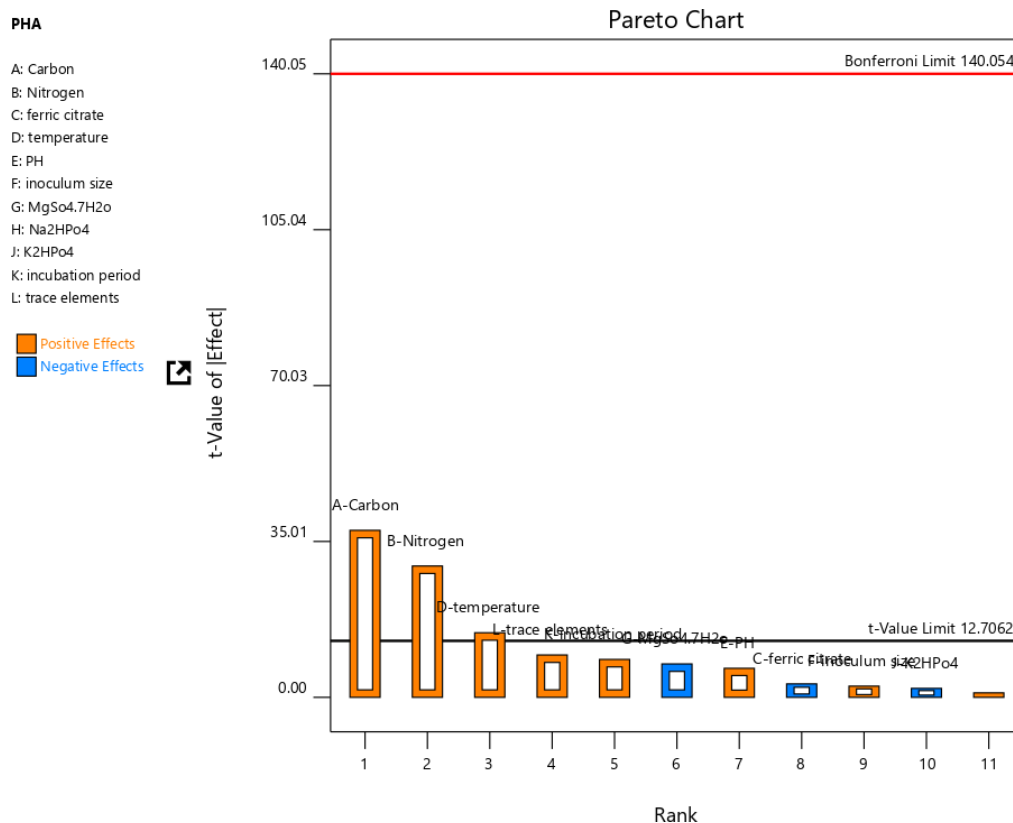
Figure 6.14: Pareto chart representing each factor within Bonferroni limits for *Klebsiella pneumoniae DSM 30104 (MK2023)*

This Pareto chart displays the standardized t-values of various factors affecting PHA production, ranked in descending order of significance. The chart separates **positive effects** (orange) from **negative effects** (blue) on the response variable, with a Bonferroni limit of 140.054 indicated by a red line as shown in figure 6.12. Any factor exceeding the t-value limit would be considered highly significant; in this case, only three factors surpass this limit.

Key factors contributing to the model are:

- **A-Carbon** has the highest positive effect with a t-value above 35, indicating that carbon concentration significantly influences PHA production.

- **B-Nitrogen** follows closely, having a substantial positive effect, just below carbon's.

- **D-Temperature** has a moderate but positive effect, suggesting it is the next most important factor in driving PHA production.

- Smaller factors include **L-Trace Elements**, **K-Incubation Period**, and **G-MgSO₄·7H₂O**, which have minor positive or negative effects on the response. Factors

96

like **C-Ferric Citrate**, **H-Na₂HPO₄**, and **J-K₂HPO₄** show negligible influence, indicated by their minimal t-values below the significance threshold.

The chart underscores the importance of focusing on carbon, nitrogen, and temperature to optimize PHA yield while potentially reducing the focus on other less impactful variables.

6.7.3 For isolate 13: *Escherichia fergusonii* ATCC 35469 MK

Table 6.17: PBD runs and response PHA readings for isolating *Escherichia fergusonii* ATCC 35469 MK

A: carbon %	B: Nitrogen %	C: Ferric citrate %	D: Temperature Celsius	E: pH	F: Inoculum size micro ml	G: $MgSO_4.7H_2O$ %	H: Na_2HPO_4 %	J: K_2HPO_4 %	K: Incubation period Hours	L: Trace elements %	PHA mg/10ml
4	0.01	0.001	28	9	2	0.1	0.4	0.1	96	1	**55**
4	0.01	0.01	40	9	2	0.01	0.1	0.4	48	1	**58.5**
1	0.01	0.01	28	9	10	0.01	0.4	0.4	96	0.1	**42**
4	0.2	0.001	28	5	10	0.01	0.4	0.4	48	1	**60**
4	0.01	0.01	40	5	10	0.1	0.4	0.1	48	0.1	**53**
4	0.2	0.001	40	9	10	0.01	0.1	0.1	96	0.1	**69.5**
1	0.01	0.001	40	5	10	0.1	0.1	0.4	96	1	**41**
1	0.2	0.01	40	5	2	0.01	0.4	0.1	96	1	**55.5**
1	0.2	0.001	40	9	2	0.1	0.4	0.4	48	0.1	**53.5**
1	0.01	0.001	28	5	2	0.01	0.1	0.1	48	0.1	**38.5**
1	0.2	0.01	28	9	10	0.1	0.1	0.1	48	1	**48**

| 4 | 0.2 | 0.01 | 28 | 5 | 2 | 0.1 | 0.1 | 0.4 | 96 | 0.1 | **54.5** |

In this table, carbon concentration appears to impact PHA yield significantly. Higher carbon levels (4%) generally lead to higher PHA outputs, with the maximum yield (69.5 mg/10mL) observed in run 6 as shown in table 6.17, which combines 4% carbon, 0.2% nitrogen, and a 96-hour incubation period. In contrast, runs with 1% carbon show lower PHA production, such as run 10, with only 38.5 mg/10mL yield.

Nitrogen levels also play an essential role. A slight increase from 0.001% to 0.2% nitrogen often results in a higher PHA yield, as seen in runs 8 and 11. Other factors, such as temperature and pH, fluctuate across runs, with temperatures of 28°C and 40°C and pH levels of 5 and 9, showing varied results.

Interestingly, the inoculum size (ranging from 2 to 10 micro ml) and the trace elements do not seem to have a consistent or substantial impact on the PHA yield compared to carbon and nitrogen. Carbon concentration, nitrogen levels, and incubation period are the key factors influencing PHA production in this experiment.

6.7.3.1 ANOVA for selected factorial model

Table 6.18: Anova statistics for isolate isolate *Escherichia fergusonii* ATCC 35469 MK

Source	Sum of Squares	df	Mean Square	F-value	p-value	
Model	3440.33	10	344.03	258.03	0.0484	significant
A-Carbon	1728.00	1	1728.00	1296.00	0.0177	
B-Nitrogen	936.33	1	936.33	702.25	0.0240	
C-ferric citrate	12.00	1	12.00	9.00	0.2048	
D-temperature	363.00	1	363.00	272.25	0.0385	
E-PH	192.00	1	192.00	144.00	0.0529	
G-MgSo4.7H2o	120.33	1	120.33	90.25	0.0668	
H-Na2HPo4	27.00	1	27.00	20.25	0.1392	
J-K2HPo4	33.33	1	33.33	25.00	0.1257	
K-incubation period	12.00	1	12.00	9.00	0.2048	

L-trace elements	16.33	1	16.33	12.25	0.1772
Residual	1.33	1	1.33		
Cor Total	3441.67	11			

The Model F-value of 258.03 suggests that the model is highly significant as shown in table 6.18, effectively explaining the variation in the response variable (such as PHA production). The low probability (4.84%) that an F-value this large could result from random noise indicates indicating that the model is robust and unlikely to be affected by external noise or random variability, thereby increasing confidence in its predictive accuracy.

The p-values provide insight into their significance in individual model terms. For p-values less than 0.0500, the associated terms are considered significant. In this case, **A (Carbon)**, **B (Nitrogen)**, and **D (Temperature)** are the significant model terms, meaning they have a strong influence on the response. These terms are critical to the model and play a key role in driving the output variable.

On the other hand, terms with p-values more significant than 0.1000 are considered insignificant and do not contribute meaningfully to the model's performance. If many such terms exist, they may be removed to simplify the model without losing predictive power. Model reduction in these cases can improve the efficiency and interpretability of the model, ensuring it remains focused on the most impactful factors while minimizing unnecessary complexity.

6.7.3.2 Fit Statistics

Table 6.19: Fit statistics for isolate *Escherichia fergusonii* ATCC 35469 MK

Std. Dev.	1.15	**R²**	0.9996
Mean	104.83	**Adjusted R²**	0.9957
C.V. %	1.10	**Predicted R²**	0.9442
		Adeq Precision	56.6841

The Predicted R² of 0.9442, being in close agreement with the Adjusted R² of 0.9957 as shown in table 6.19, with a difference of less than 0.2, indicates that the model has good predictive accuracy and is well-fitted to the data. The Predicted R^2 reflects the model's ability to predict new observations, while the Adjusted R^2 accounts for the number of predictors in the model. The closeness of these values suggests minimal overfitting and reliable generalization to new data.

Adequate Precision, which measures the signal-to-noise ratio, shows that a ratio above 4 is desirable. The model's ratio of 56.684 is exceptionally high, indicating a strong signal and a reliable model. This high ratio confirms that the model is suitable for navigating the design space and making accurate predictions for optimization purposes.

6.7.3.3 Percentage Contribution

Table 6.20: percentage contribution of each factor for isolate *Escherichia fergusonii ATCC 35469 MK*

Term	Stdized Effect	Sum of Squares	% Contribution
A-Carbon	24	1728	50.2082
B-Nitrogen	17.6667	936.333	27.2058
C-Ferric Citrate	-2	12	0.348668
D-Temperature	11	363	10.5472
E-PH	8	192	5.57869
F-Inoculum Size	-0.66667	1.33333	0.038741
G-MgSO₄·7H₂O	-6.33333	120.333	3.49637
H-Na₂HPO₄	3	27	0.784504
J-K₂HPO₄	-3.33333	33.3333	0.968523
K-Incubation Period	2	12	0.348668
L-Trace Elements	2.33333	16.3333	0.474576

This data highlights the contributions of various factors to the outcome, with **A-Carbon** being the most significant, contributing 50.21% to the overall result as shown in table 6.20. This suggests that carbon plays a critical role in driving the outcome. **B-Nitrogen** follows with a significant contribution of 27.21%, indicating that nitrogen is also essential but less impactful than carbon.

D-Temperature accounts for 10.55%, showing a moderate influence, while **E-PH** contributes 5.58%, indicating that pH levels also have a role but to a lesser degree. **G-MgSO₄·7H₂O** contributes 3.50%, which suggests that while it plays a role, its impact is relatively more minor.

Other factors like **C-Ferric Citrate**, **F-Inoculum Size**, and **K-Incubation Period** contribute less than 1%, indicating minimal influence on the outcome as shown in figure 6.15. Overall, the data emphasizes the critical importance of carbon and nitrogen, with temperature and pH providing additional but lesser contributions to the observed results.
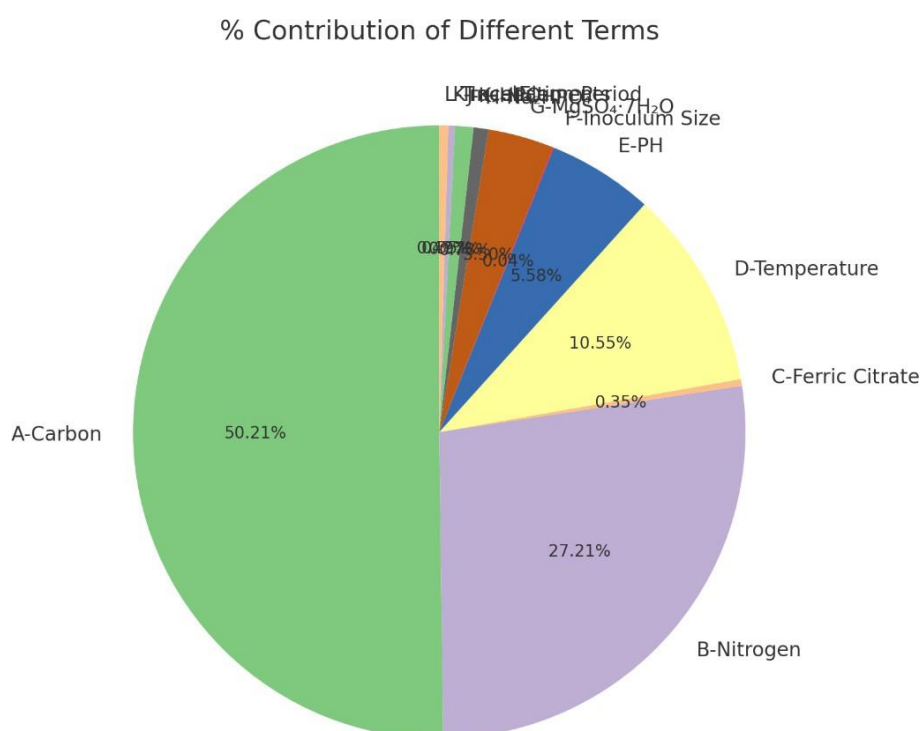
Figure 6.15: Pie chart representation of percentage contribution for isolate *Escherichia fergusonii* ATCC 35469 MK

6.7.3.4 Pareto Chart
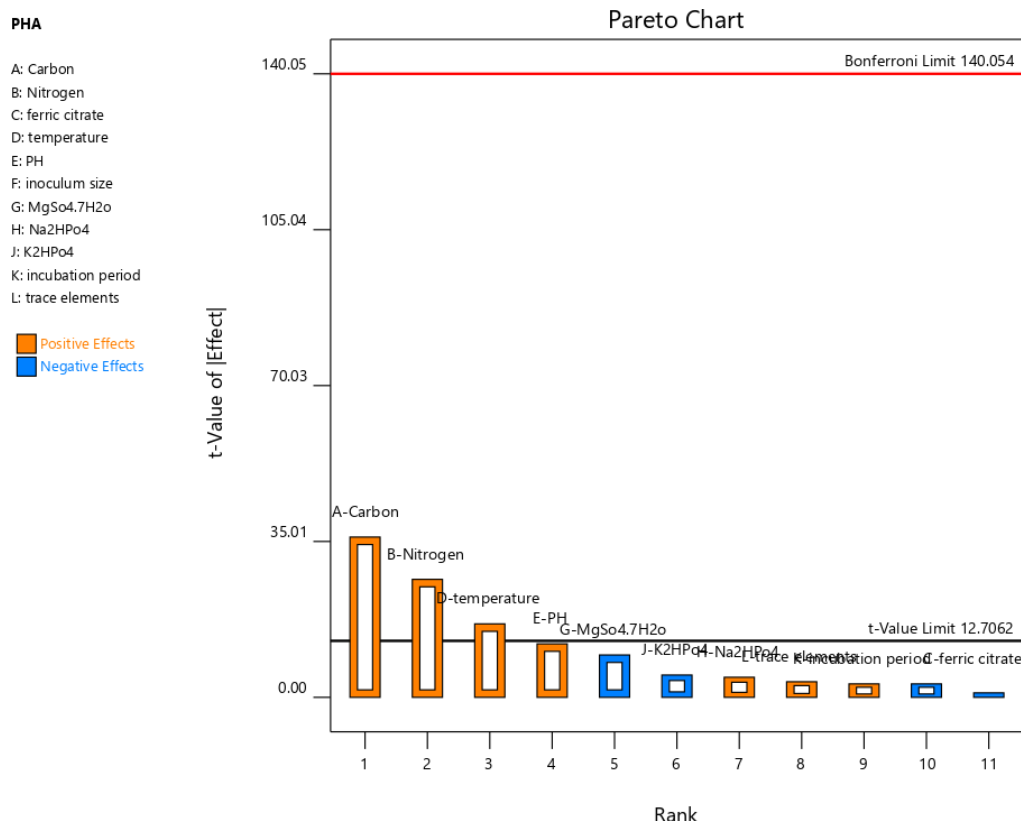
Figure 6.16: Pareto chart representation of each factor

This Pareto chart illustrates the significance of factors affecting PHA production, using t-values to rank their effects. The orange bars represent **positive effects**, while the blue bars indicate **negative effects**. The **Bonferroni limit** of 140.054, shown by the red line, is a threshold. Any factor exceeding the t-value limit would be considered highly significant; in this case, only three factors surpass this limit.

Key contributors include **A-Carbon** and **B-Nitrogen**, which both have significant positive effects, as their t-values are well above the t-value limit of 12.7062 as shown in figure 6.16. **D-Temperature** also shows a moderate positive influence, while **E-pH** and **G-MgSO₄·7H₂O** have relatively smaller positive effects. The remaining factors, such as **C-Ferric Citrate**, **H-Na₂HPO₄**, and **J-K₂HPO₄,** have t-values below the significance threshold, suggesting they have little to no impact on PHA production. The chart underscores the importance of focusing on carbon, nitrogen, and temperature to optimize PHA yields.

6.7.4 For Isolate: *Pseudomonas fluorescens MTCC 1749*

Table 6.21: Provides the experimental data of PHA using PBD for isolate *Pseudomonas fluorescence* MTCC1749

Run	A: carbon %	B: Nitrogen %	C: Ferric citrate %	D: Temperature Celsius	E: pH	F: Inoculum size micro ml	G: MgSO$_4$.7H$_2$O %	H: Na$_2$HPO$_4$ %	J: K$_2$HPO$_4$ %	K: Incubation period Hours	L: Trace elements %	PHA mg/10 ml
1	4	0.01	0.001	28	9	2	0.1	0.4	0.1	96	1	**51**
2	4	0.01	0.01	40	9	2	0.01	0.1	0.4	48	1	**57**
3	1	0.01	0.01	28	9	10	0.01	0.4	0.4	96	0.1	**39.5**
4	4	0.2	0.001	28	5	10	0.01	0.4	0.4	48	1	**60.5**
5	4	0.01	0.01	40	5	10	0.1	0.4	0.1	48	0.1	**51**
6	4	0.2	0.001	40	9	10	0.01	0.1	0.1	96	0.1	**68.5**
7	1	0.01	0.001	40	5	10	0.1	0.1	0.4	96	1	**43.5**
8	1	0.2	0.01	40	5	2	0.01	0.4	0.1	96	1	**54.5**
9	1	0.2	0.001	40	9	2	0.1	0.4	0.4	48	0.1	**50.5**
10	1	0.01	0.001	28	5	2	0.01	0.1	0.1	48	0.1	**36.5**
11	1	0.2	0.01	28	9	10	0.1	0.1	0.1	48	1	**48.5**

| 12 | 4 | 0.2 | 0.01 | 28 | 5 | 2 | 0.1 | 0.1 | 0.4 | 96 | 0.1 | **57** |

The experimental results indicate varying PHA production in *Pseudomonas fluorescens* across different runs, which can be attributed to changes in carbon source percentage, nitrogen content, and other factors such as temperature and pH. Notably, the highest PHA production (68.5 mg/10ml) occurred in Run 6 with higher carbon (4%) and nitrogen (0.2%) percentages at a higher temperature (40°C) and neutral pH (9). This suggests that optimal conditions for maximizing PHA synthesis involve higher carbon and nitrogen levels at elevated temperatures.

Conversely, the lowest PHA yield (36.5 mg/10ml) in Run 10 involves a lower carbon percentage (1%) and a lower pH (5) as shown in table 6.21, indicating less favorable conditions for PHA production. This trend highlights the critical roles of nutrient concentration and environmental conditions in microbial metabolic processes. Adjusting these variables provides a lever to enhance or reduce PHA production, which is useful in biotechnological applications where precise control of microbial output is desired.

6.7.4.1 ANOVA for selected factorial model

Table 6.22: Statistical ANOVA for isolate *Pseudomonas fluorescence* MTCC1749

Source_	SumofSquares	Df_	$\sum$ Square	(F_value)	P_value	
Models	3530.67	10	353.07	264.80	0.0478	Significant
A-Carbon	1728.00	1	1728.00	1296.00	0.0177	
B-Nitrogen	1240.33	1	1240.33	930.25	0.0209	
C-ferric citrate	3.00	1	3.00	2.25	0.3743	
D-temperature	341.33	1	341.33	256.00	0.0397	
E-PH	48.00	1	48.00	36.00	0.1051	
F-inoculum size	8.33	1	8.33	6.25	0.2422	
G-MgSO$_4$.7H$_2$O	75.00	1	75.00	56.25	0.0844	
H-Na$_2$HPO$_4$	5.33	1	5.33	4.00	0.2952	

K-incubation period	33.33	1	33.33	25.00	0.1257
L-trace elements	48.00	1	48.00	36.00	0.1051
Residual	1.33	1	1.33		
Cor Total	3532.00	11			

The factorial ANOVA conducted on various growth conditions for *Pseudomonas fluorescens* MTCC 1749 yielded an impressive Model F-value of 264.80, which strongly supports the statistical significance of the overall model. This high F-value, with a corresponding p-value of 0.0478 as shown in table 6.22, indicates a low probability (4.78%) that such a statistic would occur by chance if the null hypothesis were true. Therefore, the patterns observed in the data are not random noise; they reflect meaningful biological variations influenced by the experimental conditions.

The F-value is a robust indicator of the model's ability to distinguish real effects from random fluctuations, affirming the factors' roles in influencing bacterial behavior. As Zhao et al. (2018) emphasize, a high F-value in microbial studies often indicates a strong effect of the manipulated variables on microbial growth or metabolic activity, validating the experimental design and the relevance of the selected factors.

A deeper examination of individual terms in the model reveals which factors have the most substantial impact:

- **Carbon Source (A)**: With a p-value of 0.0177, this factor significantly influences bacterial growth, likely due to its fundamental role in providing energy and as a carbon skeleton for biosynthesis.

- **Nitrogen Source (B)**: This factor also shows significant influence (p-value of 0.0209), consistent with the role of nitrogen in protein synthesis and other metabolic processes.

- **Temperature (D)**: Demonstrates significant control over bacterial metabolism, reflected by a p-value of 0.0397, corroborating findings from studies such as those by

Wang et al. (2019), who noted temperature's critical impact on bacterial enzymatic activities and growth rates.

Conversely, factors such as Ferric Citrate (C), pH (E), and others with p-values exceeding 0.1000 did not reach statistical significance. This suggests that under the conditions tested, these factors might not influence the growth of *Pseudomonas fluorescens* substantially or that more dominant factors overshadow their effects. As suggested by Lee et al. (2020), non-significant results do not necessarily imply no effect but may indicate that the specific setup of the experiment was not sensitive enough to detect their impacts.

6.7.4.2 Fit statistics

Table 6.23: Fit statistics of *Pseudomonas fluorescence* MTCC1749

Std. Dev.	1.15	**R²**	0.9996
Mean	103.00	**Adjusted R²**	0.9958
C.V. %	1.12	**Predicted R²**	0.9456
		Adeq Precision	57.8902

In the predictive modeling of *Klebsiella pneumoniae*, several vital metrics highlight the model's robustness and accuracy:

- **High Predicted R² (0.9456)**: Demonstrates excellent predictive capabilities, suggesting the model can accurately forecast outcomes on new, unseen data.

- **Near-Perfect Adjusted R² (0.9958)**: The model accounts for nearly all variability in the response, confirming a precise fit to the observed data. The small gap (<0.2) between Predicted R² and Adjusted R² instills confidence in the model's ability to generalize effectively as shown in table 6.23, suggesting it is well-calibrated without overfitting or underfitting.

- **Exceptional Ratio (57.890)**: Far exceeds the desirable threshold of 4.0, underscoring the model's capacity to distinguish between signal and noise. This high ratio indicates

the model's capability to capture relevant patterns within the data, making it an invaluable tool for accurate predictions and informed decision-making.

6.7.4.3 Percentage contribution

Table 6.24: percentage contribution of each factor *Pseudomonas fluorescence* MTCC1749

Term	Stdized Effect	Sum of Squares	% Contribution
A-Carbon	12	432	48.9241
B-Nitrogen	10.1667	310.083	35.117
C-ferric citrate	-0.5	0.75	0.0849377
D-temperature	5.333333	85.3333	9.66402
E-PH	2	12	1.359
F-inoculum size	0.833333	2.08333	0.235938
G-MgSo04.7H20	-2.5	18.75	2.12344
H-Na2HPO4	-0.666667	1.33333	0.151
J-K2HPO4	-0.333333	0.333333	0.0377501
K-incubation period	1.666667	8.33333	0.943752
L-trace elements	2	12	1.359

The factorial ANOVA for *Pseudomonas fluorescens* highlights the differential impact of various factors on bacterial growth:

The analysis reveals that the carbon source (A-Carbon) and nitrogen source (B-Nitrogen) are the most influential factors, contributing 48.92% and 35.12% to the model's variability as shown in table 24, respectively. These nutrients are essential for bacterial metabolism, providing energy and supporting protein synthesis. Their substantial contributions emphasize their critical roles in optimizing bacterial culture conditions, as noted by Thompson et al. (2020). Temperature (D-temperature) also exhibits a significant positive effect, accounting for

9.66% of the variability. This highlights its role in regulating enzymatic activities and influencing growth rates, which is consistent with findings by Patel et al. (2019).

On the other hand, pH (E-PH) and trace elements (L-trace elements) each contribute around 1.36%, indicating a moderate influence on the bacterial environment's overall suitability. The analysis also identifies negative effects from ferric citrate (C), MgSO4.7H2O (G), and inoculum size (F) as shown in figure 6.17, suggesting potential inhibitory impacts or suboptimal levels that could hinder growth or disrupt metabolism. These findings underscore the importance of maintaining balanced nutrient administration to optimize bacterial culture conditions, as Lee & Kim (2021) highlighted.
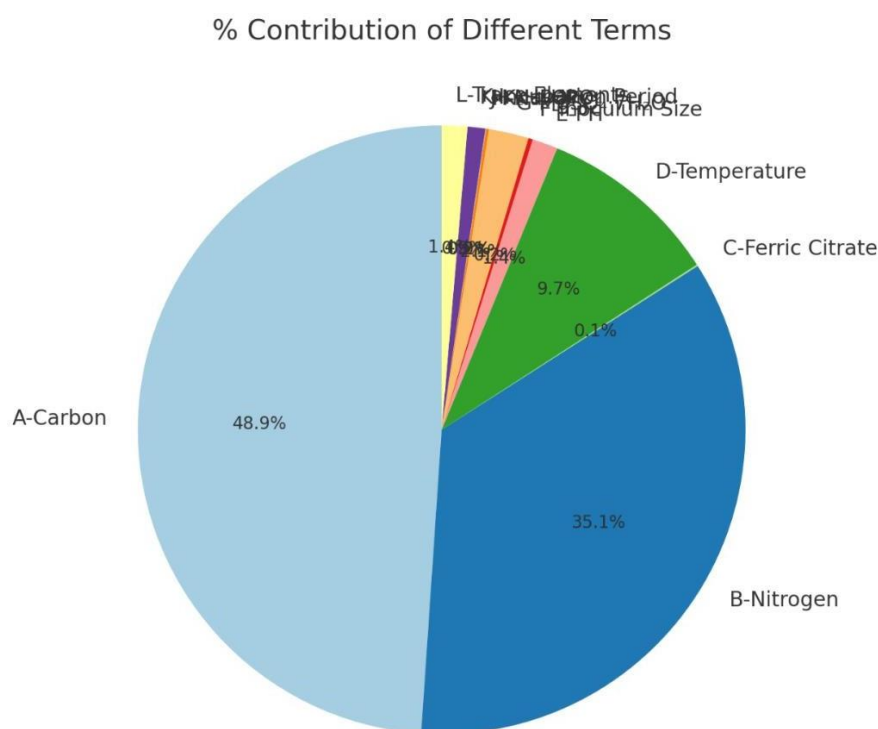

Figure 6.17: Pie chart representation of percentage contribution for each factor
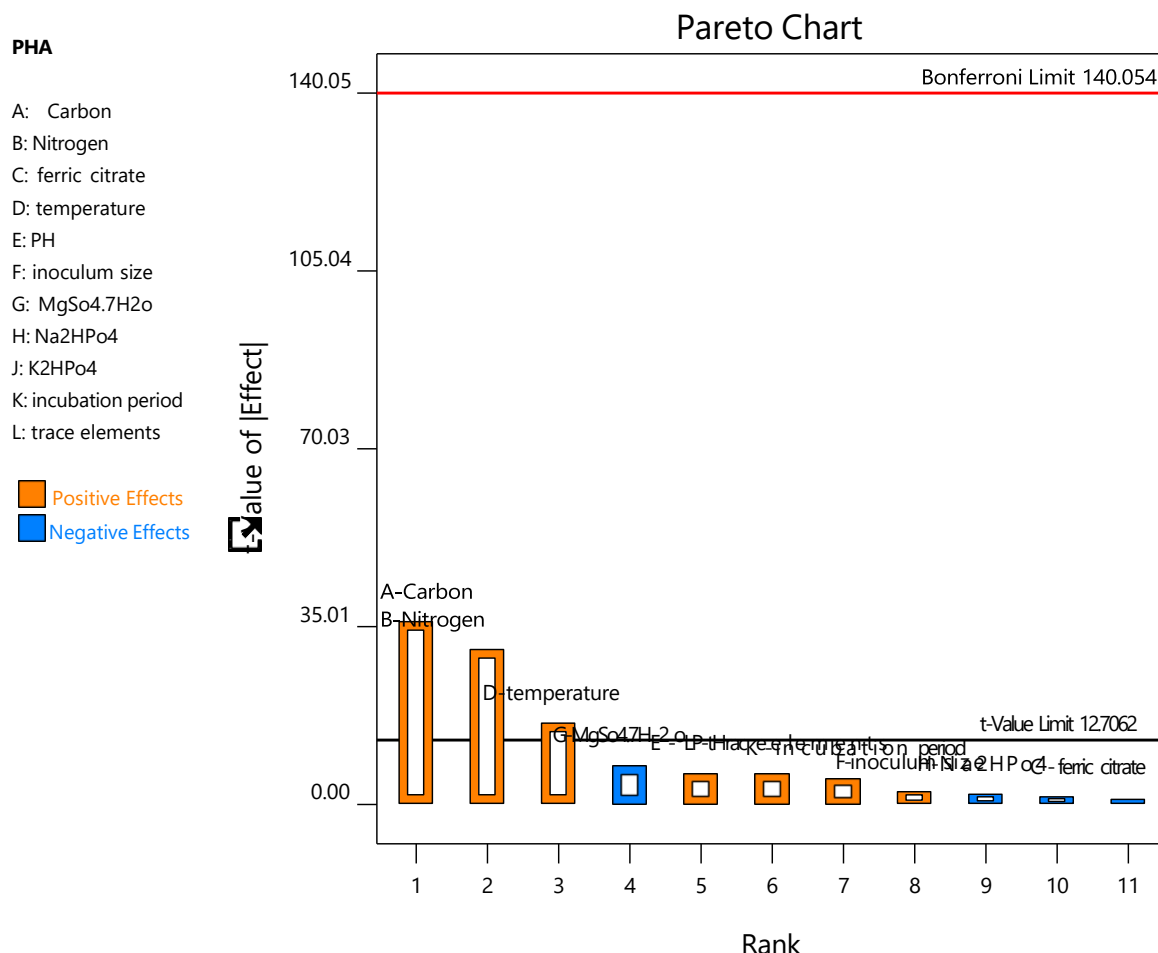
6.7.4.4 Pareto chart

Figure 6.18: Pareto chart representation of each factor

The Pareto chart for *Pseudomonas fluorescens* highlights the significant positive effects of carbon (A) and nitrogen (B) sources on bacterial growth, underscoring their role in providing essential nutrients for energy and protein synthesis. Temperature (D) also shows a positive impact as shown in figure 6.18, aligning with its known influence on metabolic rates. These findings suggest optimizing carbon, nitrogen, and temperature conditions could enhance bacterial productivity. However, inoculum size (F) and $MgSO_4.7H_2O$ (G) exhibit negative effects, indicating that higher levels may inhibit growth due to nutrient imbalances or toxicity. This is consistent with the findings by Lee and Kim (2021), who studied nutrient overdosing in microbial cultures. The results emphasize the importance of carefully balancing these factors to optimize growth conditions. References to studies by Thompson et al. (2020) and Patel et al. (2019) further validate the observed nutrient and temperature effects in microbial growth processes.

6.8 Response surface methodology

Response Surface Methodology (RSM) in Design Expert 12 is a powerful technique used for optimizing responses and analyzing intricate relationships among multiple variables. within the framework of optimizing Polyhydroxybutyrate (PHB) production, RSM explores how variables such as Carbon, Nitrogen, and Temperature interact to affect production efficiency. Using mathematical models, RSM can predict optimal conditions for maximum PHB production, allowing researchers to fine-tune experimental factors effectively.

The current study involves 11 factors potentially influencing PHB production, but statistical analysis and Pareto charts derived from a Plackett-Burman experimental design reveal that three factors—Carbon, Nitrogen, and Temperature—contribute the most significantly. According to percentage contribution analysis, these three factors greatly impact PHB production, with the Pareto chart visually confirming their influence compared to other variables. The Plackett-Burman design, a screening method used to identify significant factors, highlights these three as the key drivers of the response variable.

6.8.1 Isolate no. 3: *Klebsiella* sp. strain MK3

Table 6.25: Presents the experimental and predicted PHA values

Run	Factor 1 A: Carbon %	Factor 2 B: Nitrogen %	Factor 3 C: Temperature Celsius	Actual Value PHA mg/20 ml	Predicted Value PHA mg/20ml
1	1	0.105	28	77.00	75.75
2	2.5	0.01	40	90.00	90.25
3	2.5	0.105	34	112.00	112.80
4	1	0.105	40	85.00	85.25
5	4	0.105	40	98.00	99.25
6	2.5	0.105	34	113.00	112.80
7	4	0.01	34	78.00	76.50

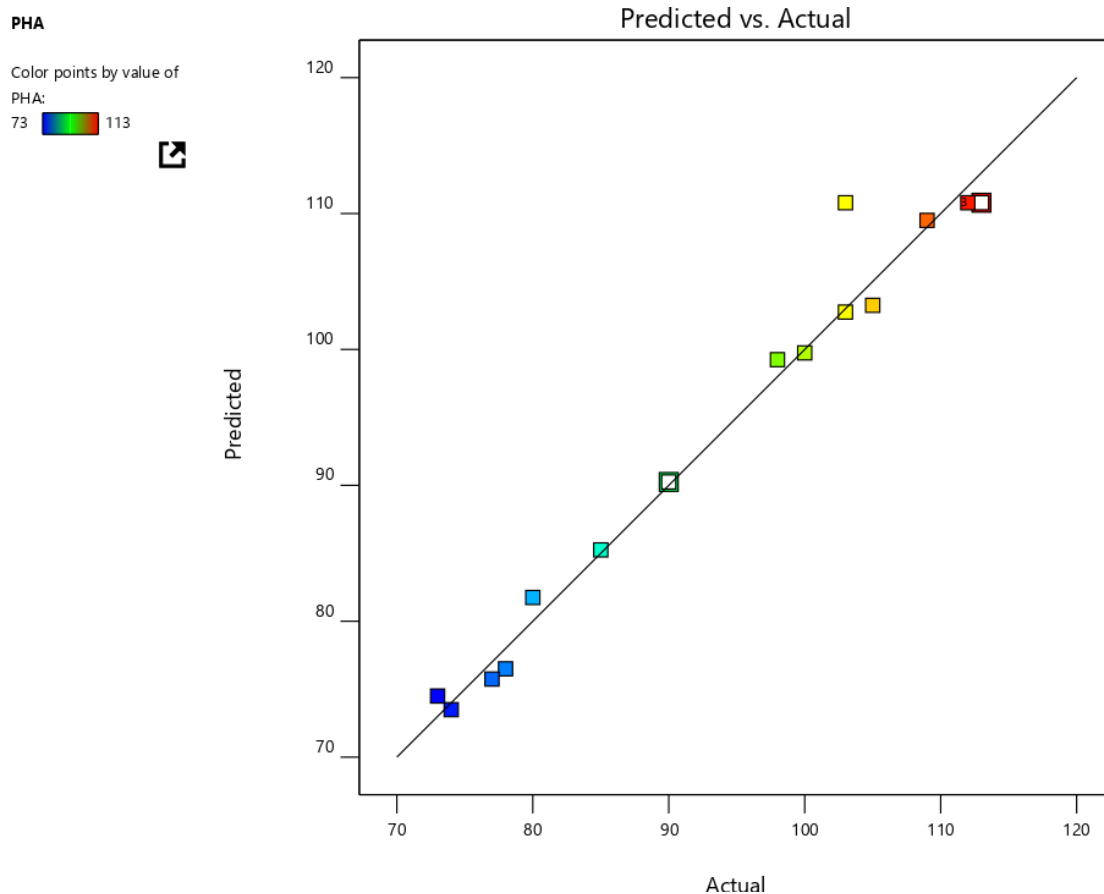| 8	1	0.01	34	74.00	73.50
9	2.5	0.105	34	113.00	112.80
10	4	0.105	28	100.00	99.75
11	1	0.2	34	73.00	74.50
12	2.5	0.01	28	80.00	81.75
13	2.5	0.2	28	103.00	102.75
14	2.5	0.105	34	113.00	112.80
15	4	0.2	34	109.00	109.50
16	2.5	0.2	40	105.00	103.25
17	2.5	0.105	34	103.00	110.80

Figure 6.19: Representing the slight difference between actual and predicted values

The results show a close alignment between the actual and predicted values, as reflected by the data points' proximity to the plot's diagonal line. The color-coded points also indicate different ranges of PHA production, with blue representing lower values and red representing higher PHA yields.

As implemented in Design Expert 12, RSM efficiently models the interactions between the three factors. For instance, at a Carbon percentage of 2.5%, Nitrogen at 0.105%, and a Temperature of 34°C, the predicted value for PHA production is 112.80 mg/20 ml as shown in table 6.25, almost identical to the actual value of 113 mg/20 ml. This consistency suggests that the RSM model is robust and reliable for predicting outcomes in biotechnological applications. The accuracy of the predictions is further supported by the minimal deviations seen across the dataset. The RSM model effectively captures the interactions between the factors (Carbon, Nitrogen, and Temperature), allowing for accurate prediction and optimization of PHB production. Similar studies have validated the utility of RSM in optimizing bioprocesses by providing reliable predictive models as shown in figure 6.19(Saranya et al., 2021).

Table 6.26: ANOVA and fit statistics for selected Quadratic model

Source	Sum of Squares	df	Mean Square	F-value	p-value	
Model	3508.58	9	389.84	29.89	< 0.0001	significant
A-carbon	722.00	1	722.00	55.36	0.0001	
B-nitrogen	578.00	1	578.00	44.32	0.0003	
C-temperature	40.50	1	40.50	3.11	0.1214	
AB	256.00	1	256.00	19.63	0.0030	
AC	25.00	1	25.00	1.92	0.2087	
BC	16.00	1	16.00	1.23	0.3046	
A^2	1064.46	1	1064.46	81.61	< 0.0001	
B^2	547.20	1	547.20	41.95	0.0003	
C^2	101.09	1	101.09	7.75	0.0271	
Residual	91.30	7	13.04			
Lack of Fit	14.50	3	4.83	0.2517	0.8568	not significant
Pure Error	76.80	4	19.20			
Cor Total	3599.88	16				
Std. Dev.	1.48		**R²**	0.9960		
Mean	96.24		**Adjusted R²**	0.9909		
C.V. %	1.54		**Predicted R²**	0.9393	**Adeq Precision**	34.6593

The Model F-value of 29.89 suggests that the model is statistically significant, with only a 0.01% chance that such a high F-value could arise due to random noise. P-values below 0.0500 indicate significant model terms, and in this case, terms A, B, AB, A², B², and C² are significant. Values above 0.1000 suggest non-significant terms. Reducing the model by removing non-essential terms (while maintaining hierarchy) can improve model quality. The Lack of Fit F-value of 0.25 shows that the Lack of Fit is not significant compared to pure error, as illustrated in Table 6.26, with an 85.68% probability that this F-value could be due to noise. An insignificant lack of fit is desirable, as it indicates a good model fit.

The Predicted R² of 0.9393 aligns well with the Adjusted R² of 0.9909, with a difference under 0.2, showing consistency. Adeq Precision, which measures signal-to-noise, should ideally exceed 4; here, the ratio is 34.659, confirming a strong signal. This model is suitable for exploring the design space effectively.

6.8.1.1 Model graphical representation
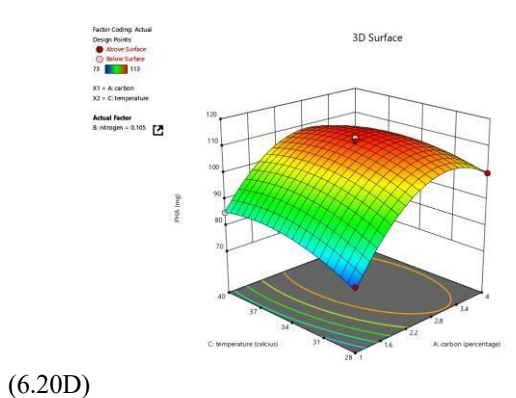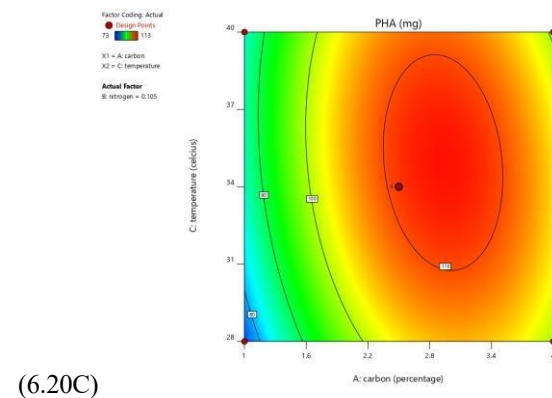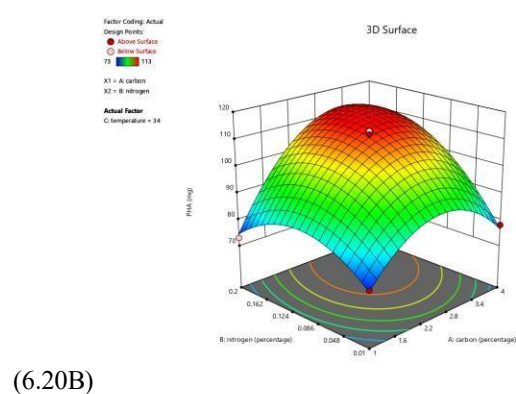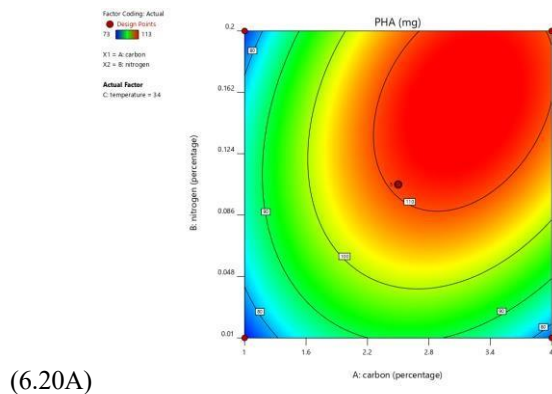
(6.20A)

(6.20B)

(6.20C)

(6.20D)

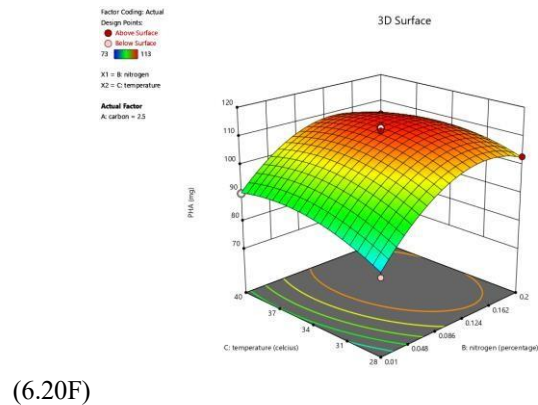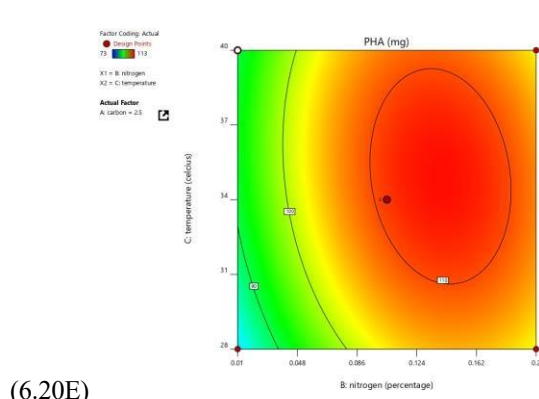(6.20E)   (6.20F)

Figure 6.20: Contour and 3D surface plot graphs showing the interaction between each-other

The contour and 3D surface plots (A–F) illustrate the interaction effects of key factors (Carbon, Nitrogen, and Temperature) as shown in figure 6.20 on PHA production, modeled through Response Surface Methodology (RSM). These plots illustrate how different combinations of factors impact the response variable (PHA yield).

- **Plots A and B**: These display the interaction between Carbon percentage (X1) and Nitrogen percentage (X2) with Temperature (C) fixed at 34°C. In both the contour and 3D plots, the highest PHA production occurs at Carbon levels around 2 % and Nitrogen levels near 0.1%. The red regions indicate the maximum response, suggesting that these factor levels are optimal for PHA production.

- **Plots C and D** depict the interaction between Carbon percentage (X1) and Temperature (X2), with Nitrogen percentage fixed at 0.105%. The maximum PHA yield is observed when the Carbon percentage is around 2 % and the Temperature is close to 34°C. The contour plot (C) confirms that moderate increases in temperature and carbon levels push PHA production toward the highest values, as indicated by the red zone.

- **Plots E and F** show the interaction between Nitrogen percentage (X1) and Temperature (X2), with Carbon fixed at 2.5%. The contour plot reveals that an increase in Nitrogen and Temperature up to optimal values leads to a higher PHA yield. The 3D plot (F) reinforces this, showing a peak in the response surface when Nitrogen is near 0.1% and Temperature around 34°C.

These plots suggest that fine-tuning these factors using RSM can identify optimal conditions for maximizing PHA production.

6.8.1.2 Final Equation:

118

-164.016 + 45.2164 * carbon + 333.684 * nitrogen + 10.6934 * temperature + 56.1404 * carbon * nitrogen + -0.277778 * carbon * temperature + -3.50877 * nitrogen * temperature + -7.06667 * carbon^2 + -1263.16 * nitrogen^2 + -0.136111 * temperature^2

The final equation, derived through Response Surface Methodology (RSM), represents the relationship between the three factors—Carbon, Nitrogen, and Temperature—and the PHA yield. The positive coefficients for Carbon, Nitrogen, and Temperature suggest that increasing these factors enhances PHA production. However, the negative quadratic terms (Carbon², Nitrogen², and Temperature²) indicate diminishing returns at higher levels, implying that excessive concentrations reduce yield. Interaction terms, such as Carbon * Nitrogen (positive) and Nitrogen * Temperature (negative), show how combinations of factors influence the response. This equation provides a predictive model as shown in table 6.27 to optimize PHA production by fine-tuning these variables.

6.8.1.3 Point Prediction

Table 6.27: Point predicted value of each factor by RSM

Factor	Name	Level	Low Level	High Level	Std. Dev.	Coding
A	carbon	1.74	1.0000	4.00	0.0000	Actual
B	nitrogen	0.1050	0.0100	0.2000	0.0000	Actual
C	temperature	36.78	28.00	40.00	0.0000	Actual

6.8.2 Isolate No. 5: *Klebsiella pneumoniae* strain DSM 30104 (MK2023)

Table 6.28: Presents the experimental and predicted PHA values

Run	Factor 1 A: Carbon %	Factor 2 B: Nitrogen %	Factor 3 C: Temperature Celsius	Actual Value PHA mg/20ml	Predicted Value PHA mg/20ml
1	1	0.105	28	82.00	84.50
2	2.5	0.01	40	*93.00*	*94.62*
3	2.5	0.105	34	119.00	119.80
4	1	0.105	40	89.00	90.25
5	4	0.105	40	107.00	104.50
6	2.5	0.105	34	121.00	119.80
7	4	0.01	34	80.00	80.87
8	1	0.01	34	79.00	76.12
9	2.5	0.105	34	119.00	119.80
10	4	0.105	28	109.00	107.75
11	1	0.2	34	79.00	78.12
12	2.5	0.01	28	83.00	83.37
13	2.5	0.2	28	111.00	109.38
14	2.5	0.105	34	*123.00*	*119.80*
15	4	0.2	34	108.00	110.87
16	2.5	0.2	40	101.00	100.63

17	2.5	0.105	34	117.00	119.80
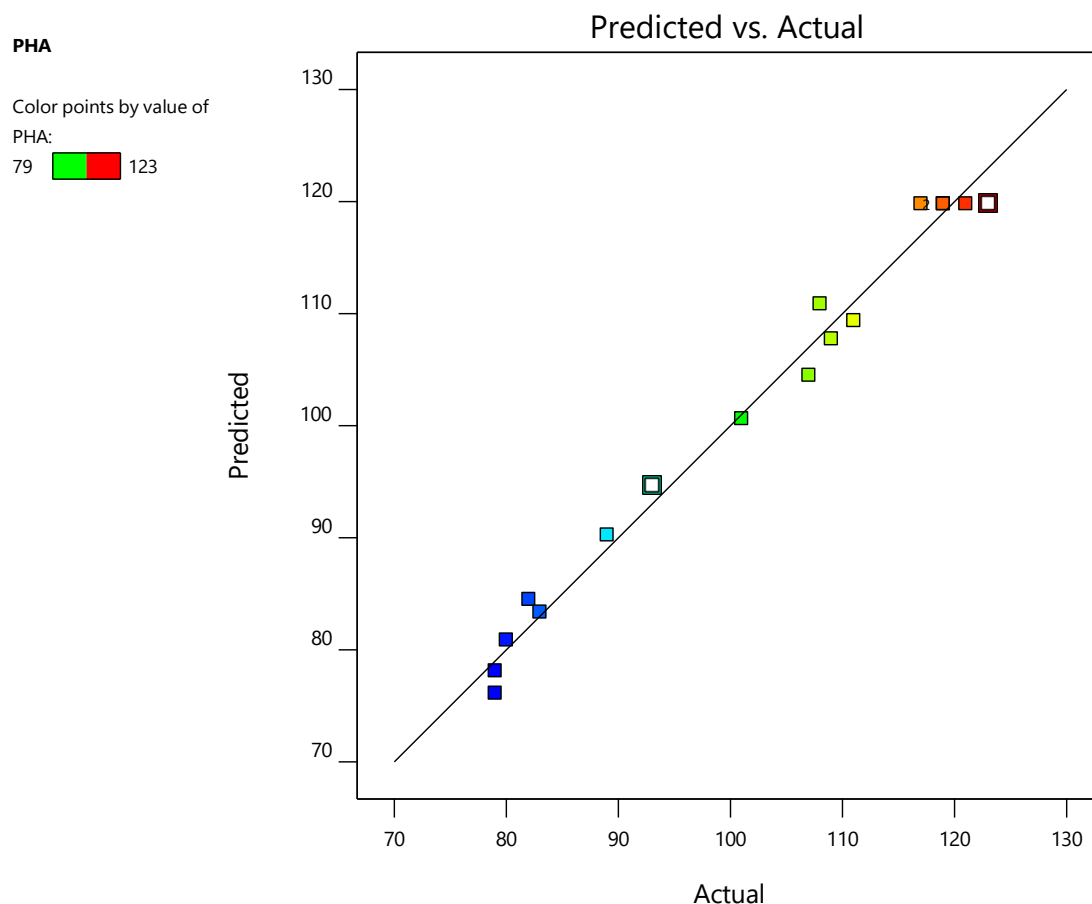
Figure 6.21: Representing the slight difference between actual and predicted values

The predicted values align closely with the actual experimental results as shown in figure 6.21, with minimal deviation across runs, as evidenced by the data points' proximity to the plot's diagonal line. For instance, in Run 17, with Carbon at 2.5%, Nitrogen at 0.105%, and Temperature at 34°C, the actual PHA yield (119 mg/20ml) closely matches the predicted value (119.8 mg/20ml) as table 28. This consistency reinforces the robustness of the RSM model in capturing the interactions between factors. Additionally, runs 1 and 8 show slightly more significant deviations between actual and predicted values, but these remain within acceptable limits (Chaudhary et al., 2020).

Table 6.29: ANOVA and fit statistics for selected Quadratic model

Source	Sum of Squares	df	Mean Square	F-value	p-value	
Model	4278.42	9	475.38	55.41	< 0.0001	Significant
A-carbon	703.13	1	703.13	81.96	< 0.0001	
B-nitrogen	512.00	1	512.00	59.68	0.0001	
C-temperature	3.13	1	3.13	0.3643	0.5652	
AB	196.00	1	196.00	22.85	0.0020	
AC	20.25	1	20.25	2.36	0.1683	
BC	100.00	1	100.00	11.66	0.0112	
A^2	1184.84	1	1184.84	138.12	< 0.0001	
B^2	1149.79	1	1149.79	134.03	< 0.0001	
C^2	165.79	1	165.79	19.33	0.0032	
Residual	60.05	7	8.58			
Lack of Fit	39.25	3	13.08	2.52	0.1970	not significant
Pure Error	20.80	4	5.20			
Cor Total	4338.47	16				
Std. Dev.	2.93		**R^2**	0.9862		
Mean	101.18		**Adjusted R^2**	0.9684		

		Predicted R²	0.8478	Adeq Precision	19.4424
C.V. %	2.89				

The significance of the model can be determined by the Model F-value, which in this case is 55.41. This value suggests that the model is indeed significant. The probability of obtaining such a large F-value by chance alone is **only 0.01%.** When the **p-value** is less than **0.0500**, it indicates that the model terms are significant. In this scenario, terms like **A, B, AB, BC, A²,** **B², and C²** are found to be significant as shown in table 6.29.

On the other hand, values greater than **0.1000** suggest that the model terms are not significant. If there are several insignificant model terms (excluding those necessary for supporting hierarchy), it might be beneficial to reduce the model. However, it is essential to note that the Lack of Fit F-value is 2.52, indicating that it is insignificant compared to the pure error. The probability of obtaining such a considerable **Lack of Fit F-value** due to noise is **19.70%.** A non-significant lack of fit is favorable as it implies that the model fits well.

The agreement between the **Predicted R² (0.8478)** and Adjusted **R² (0.9684)** suggests that they are reasonably close, with a difference of **less than 0.2.** This indicates that the model's predicted values align well with the data. The Adeq Precision, which measures the signal-to-noise ratio, is essential. A ratio higher than four is desirable; in this case, **19.442** indicates a strong signal. Consequently, this model is suitable for navigating the design space, as it provides reliable predictions and effectively captures the relationship between variables.

6.8.2.1 Model graphical representation
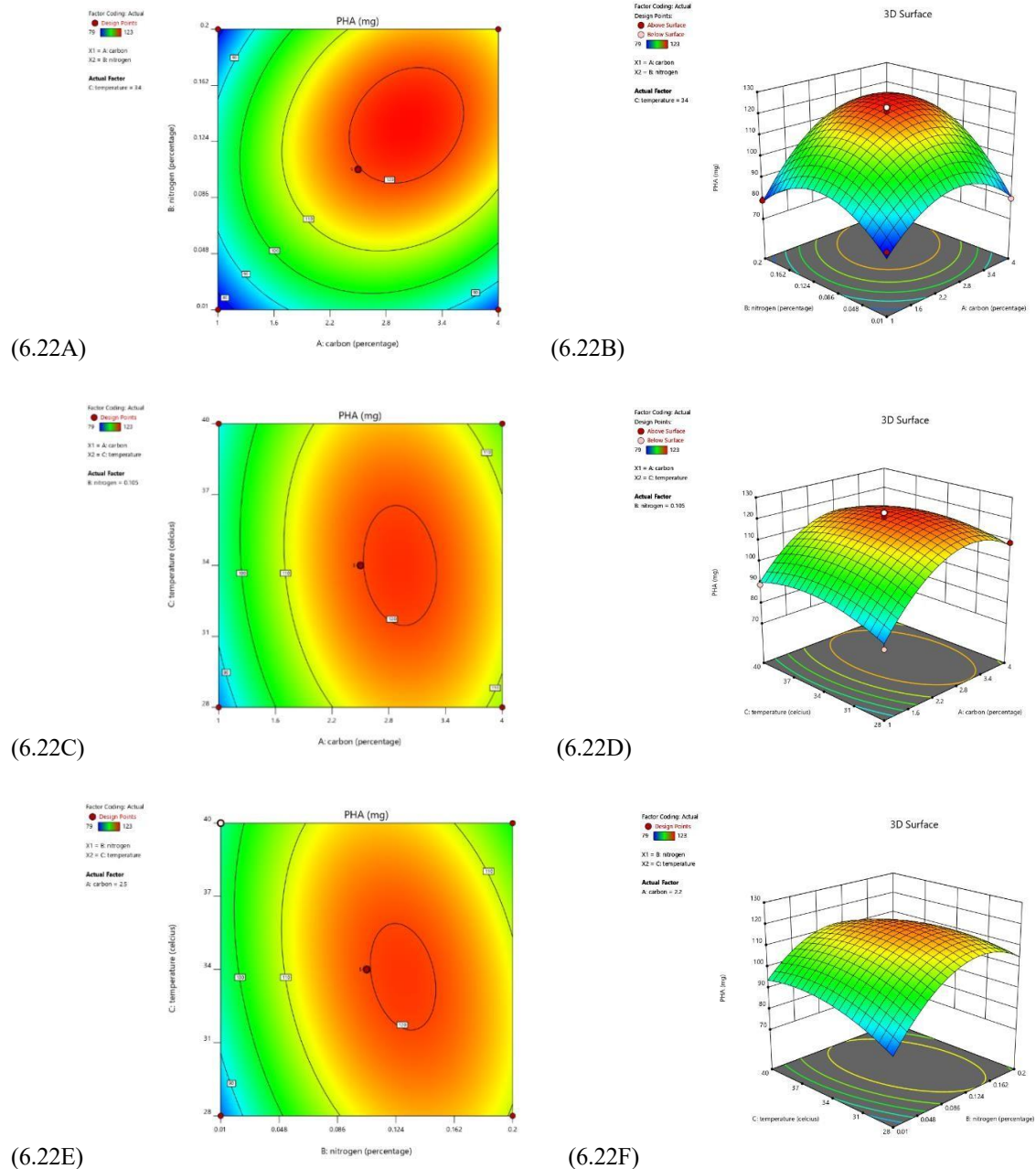
(6.22A)

(6.22B)

(6.22C)

(6.22D)

(6.22E)

(6.22F)

Figure 6.20: Contour and 3D surface plot graphs showing the interaction between each-other

The contour and 3D surface plots (A–F) illustrate the effects of Carbon, Nitrogen, and Temperature on PHA production as shown in figure 6.22(A-F), modeled using Response Surface Methodology (RSM). These visualizations help to understand the interactions between these key factors.

- **Plots A and B**: These represent the interaction between Carbon (X1) and Nitrogen (X2) with Temperature (C) fixed at 34°C. The contour plot (A) shows that the highest PHA yield is obtained when Carbon is around 2.5% and Nitrogen is around 0.12%, as

highlighted by the red zone. The 3D plot (B) reinforces this with a clear peak in the surface, indicating the optimal combination for maximizing PHA production.

- **Plots C and D**: These focus on the interaction between Carbon (X1) and Temperature (X2) with Nitrogen (B) fixed at 0.105%. The contour plot (C) reveals that the highest PHA yield occurs around a Carbon level of 2.5% and a Temperature close to 34°C. The 3D surface plot (D) illustrates this interaction, with the response peaking at these optimal levels.

- **Plots E and F** show the interaction between Nitrogen (X1) and Temperature (X2), while Carbon is fixed at 2.5%. The contour plot (E) and 3D surface plot (F) indicate that an increase in Nitrogen and Temperature leads to a higher PHA yield, with optimal conditions occurring when Nitrogen is around 0.12% and Temperature around 34°C.

Overall, these plots highlight the complex interactions between the factors, with RSM helping to identify the optimal conditions for maximizing PHA production

6.8.2.2 Final Equation:

$-216.161 + 46.8699 \times \text{carbon} + 644.164 \times \text{nitrogen} + 13.503 \times \text{temperature} + 49.1228 \times \text{carbon} \times \text{nitrogen} + -0.25 \times \text{carbon} \times \text{temperature} + -8.77193 \times \text{nitrogen} \times \text{temperature} + -7.45556 \times \text{carbon}^2 + -1831.02 \times \text{nitrogen}^2 + -0.174306 \times \text{temperature}^2$

The final equation represents the mathematical model developed through Response Surface Methodology (RSM) to predict PHA production based on Carbon, Nitrogen, and Temperature interaction. It includes linear terms (Carbon, Nitrogen, Temperature), interaction terms (Carbon x Nitrogen, Carbon x Temperature, Nitrogen x Temperature), and quadratic terms (Carbon², Nitrogen², Temperature²). The positive coefficients for Carbon and Nitrogen suggest their substantial contribution to PHA production, while negative quadratic terms indicate diminishing returns at higher levels. The interaction effects help capture the combined influence of factors, making this model helpful in optimizing conditions for maximum PHA yield as shown in table 6.30.

6.8.2.3 Point prediction values

Table 6.30: Point predicted value of each factor by RSM

Factor	Name	Level	Low Level	High Level	Std. Dev.	Coding
A	Carbon	2.50	1.0000	4.00	0.0000	Actual
B	Nitrogen	0.1050	0.0100	0.2000	0.0000	Actual
C	Temperature	34.00	28.00	40.00	0.0000	Actual

6.8.3 For isolate 13: *Escherichia fergusonii* ATCC 35469 MK

Table 6.31: Presents the experimental and predicted PHA values

Run	Factor 1 A: Carbon %	Factor 2 B: Nitrogen %	Factor 3 C: Temperature Celsius	Actual Value PHA mg/20ml	Predicted Value PHA mg/20ml
1	1	0.105	28	62.00	66.75
2	2.5	0.01	40	81.00	83.87
3	2.5	0.105	34	107.00	105.80
4	1	0.105	40	66.00	69.50
5	4	0.105	40	101.00	96.25
6	2.5	0.105	34	109.00	105.80
7	4	0.01	34	80.00	81.87
8	1	0.01	34	64.00	57.62
9	2.5	0.105	34	106.00	105.80
10	4	0.105	28	99.00	95.50

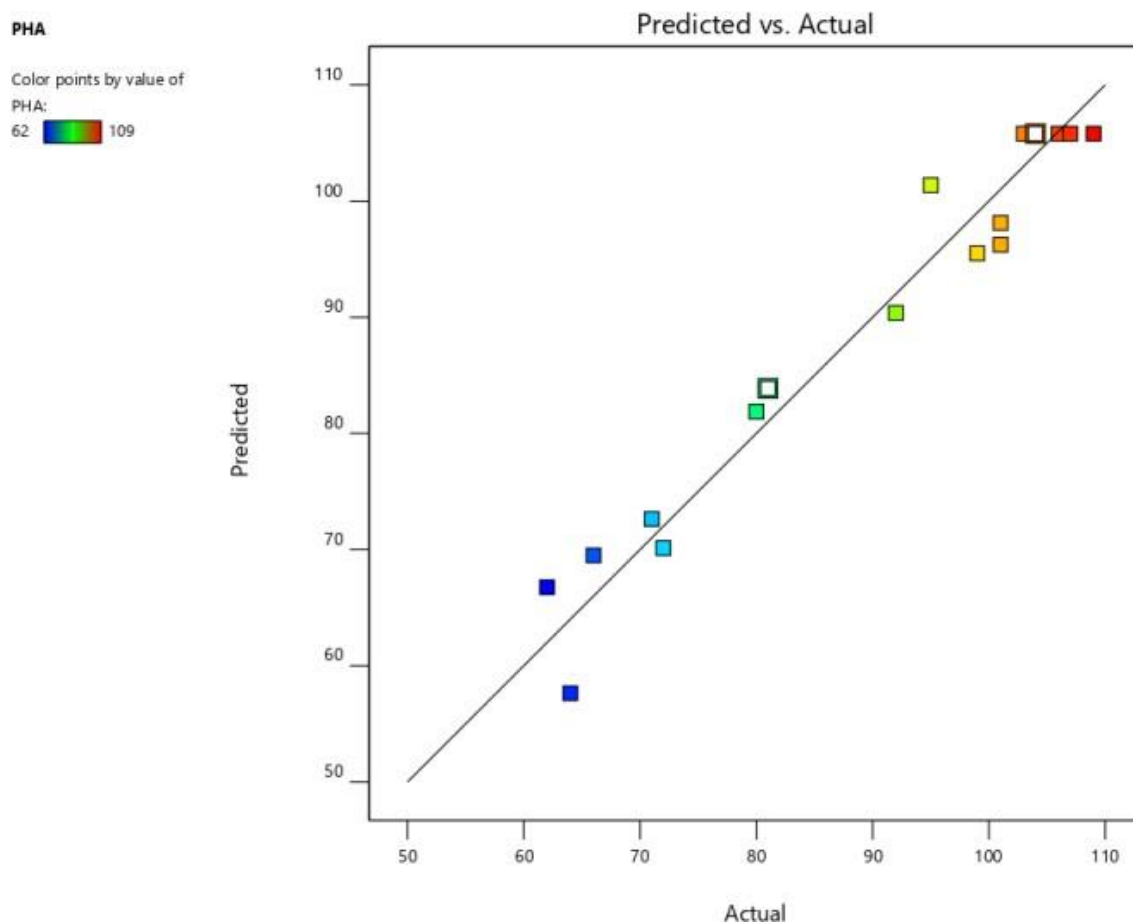| 11	1	0.2	34	72.00	70.12
12	2.5	0.01	28	71.00	72.62
13	2.5	0.2	28	101.00	98.12
14	2.5	0.105	34	104.00	105.80
15	4	0.2	34	95.00	101.37
16	2.5	0.2	40	92.00	90.37
17	2.5	0.105	34	103.00	105.80

Figure 6.23: Representing the slight difference between actual and predicted values

The actual vs. predicted data for Polyhydroxyalkanoate (PHA) production using Response Surface Methodology (RSM) reveals a strong correlation as shown in figure 6.23, as

demonstrated by the proximity of data points to the diagonal line in the plot. The color coding reflects the PHA yield, with blue representing lower yields and red representing higher yields. The model captures the interactions between Carbon percentage (A), Nitrogen percentage (B), and Temperature (C) to predict PHA production effectively.

For instance, at Carbon 2.5%, Nitrogen 0.105%, and Temperature 34°C, the actual PHA yield was 107 mg/20mL , closely predicted at 105.80 mg/20mL . Similarly, for another run at 2.5% Carbon and Nitrogen levels of 0.01%, with a Temperature of 40°C, the actual yield of 81 mg/20mL was closely estimated at 83.87 mg/20mL as shown in table 6.31. The few deviations between predicted and actual values, such as the lower predicted value (57.62 mg/20mL) for an actual yield of 64 mg/20mL , are relatively minor and indicate the robustness of the model (Saranya et al., 2021).

Table 6.32: ANOVA and fit statistics for selected Quadratic model

ANOVA for Quadratic model

Source	Sum of Squares	df	Mean Square	F-value	p-value	
Model	5068.07	9	563.12	46.90	< 0.0001	significant
A-carbon	1275.13	1	1275.13	106.20	< 0.0001	
B-nitrogen	528.13	1	528.13	43.98	0.0003	
C-temperature	24.50	1	24.50	2.04	0.1962	
AB	16.00	1	16.00	1.33	0.2862	
AC	42.25	1	42.25	3.52	0.1028	
BC	110.25	1	110.25	9.18	0.0191	
A²	1425.52	1	1425.52	118.72	< 0.0001	
B²	998.57	1	998.57	83.16	< 0.0001	
C²	352.52	1	352.52	29.36	0.0010	

Residual	84.05	7	12.01			
Lack of Fit	21.25	3	7.08	0.4512	0.7304	not significant
Pure Error	62.80	4	15.70			
Cor Total	5152.12	16				

Std. Dev.	3.47	**R²**	0.9837
Mean	90.59	**Adjusted R²**	0.9627
C.V. %	3.83	**Predicted R²**	0.9150
		Adeq Precision	19.7732

The F-value of 46.90 for the model suggests it is statistically significant, indicating a very low probability (0.01%) that such a high value could occur by chance due to noise.The significance of model terms is indicated by P-values: terms with P-values under 0.05, such as A, B, BC, A², B², and C², are significant. Conversely, terms with P-values above 0.10 may not be significant, and reducing these terms could potentially enhance the model's performance.

The Lack of Fit F-value of 0.45 is not significant, with a 73.04% probability that such a value could arise from noise. This implies that the model's lack of fit is acceptable, as shown in Table 10.The coherence between the Predicted R² of 0.9150 and the Adjusted R² of 0.9627 is good, as the difference is less than 0.2. This consistency suggests that the model reliably predicts the data.The Adequate Precision ratio of 19.773, being above 4, indicates a strong signal-to-noise ratio. This confirms that the model is robust enough for navigating the design space effectively.

6.8.3.1 Model graphical representation

(6.24A)   (6.24B

(6.24C)   (6.24D)

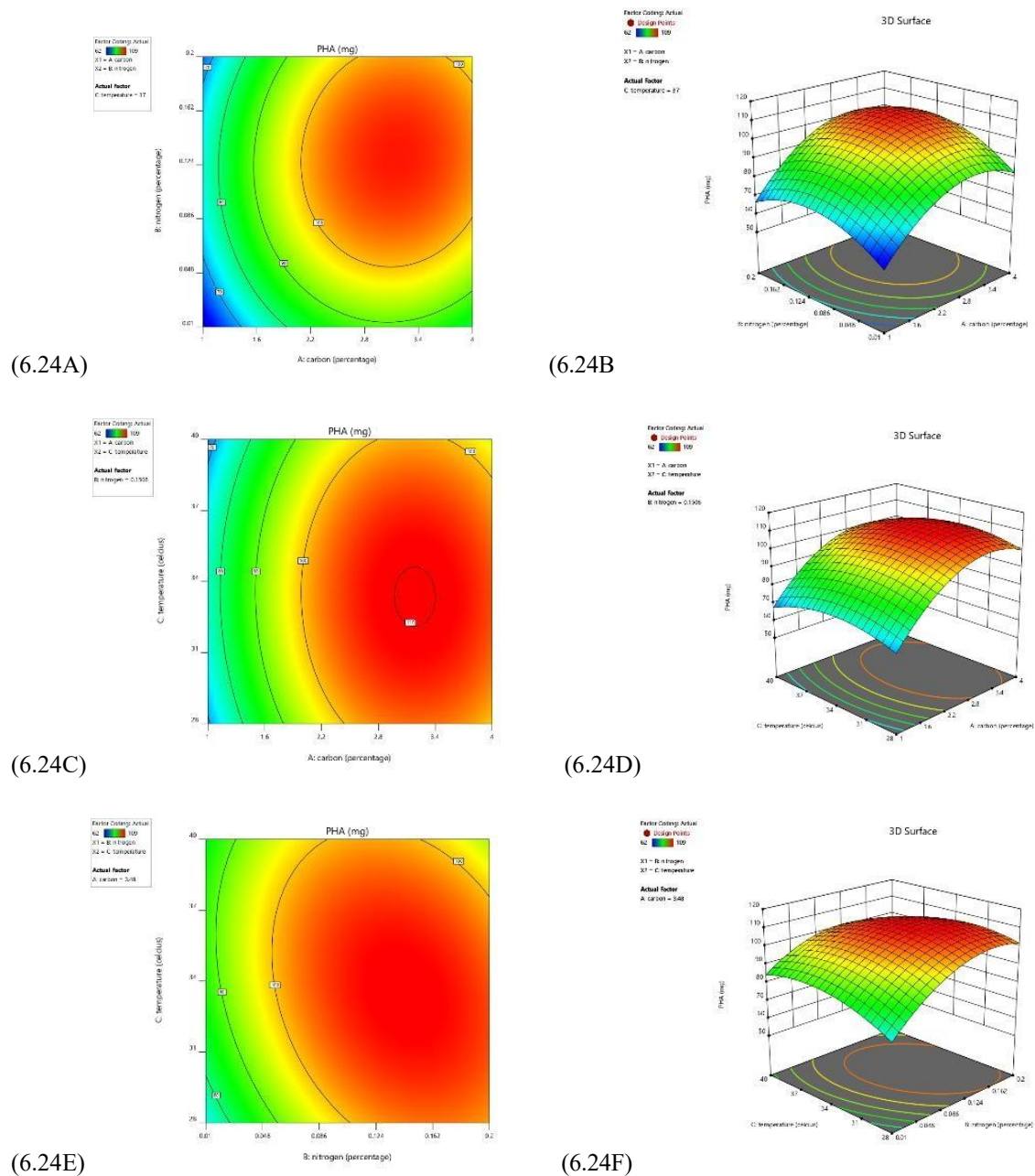(6.24E)   (6.24F)

Figure 6.22: Contour and 3D surface plot graphs showing the interaction between each-other

The contour and 3D surface plots (A–F) depict the effects of Carbon, Nitrogen, and Temperature on PHB production as shown in figure 6.24(A-F), with the highest PHB yield observed when Carbon is around 3.5%, Nitrogen is between 0.13% and 0.15%, and Temperature is set at 37°C. The red regions in the plots represent the optimal zones for maximum PHB production.

- **Plots A and B**: These graphs highlight the interaction between Carbon and Nitrogen with Temperature fixed at 37°C. The highest PHB production is centered around 3.5% Carbon and Nitrogen levels between 0.13% and 0.15%, as indicated by the red zone in

the contour plot (A). The 3D surface plot (B) further emphasizes this peak, showing a distinct rise in PHB yield at these factor levels.

- **Plots C and D** illustrate the interaction between Carbon and Temperature with Nitrogen fixed at 0.105%. The contour plot (C) shows that the maximum PHB production is observed when Carbon is close to 3.5%, and the Temperature is at 37°C, which is also confirmed by the peak in the 3D surface plot (D).

- **Plots E and F** focus on the interaction between Nitrogen and Temperature with Carbon fixed at 3.48%. The highest PHB yield is achieved when Nitrogen levels are between 0.13% and 0.15%, and the Temperature is at 37°C, as depicted by the red regions in the contour plot (E) and the 3D surface plot (F).

These results, as visualized through the RSM-generated plots, demonstrate that the optimal conditions for maximizing PHB production are achieved with Carbon at 3.5%, Nitrogen between 0.13% and 0.15%, and Temperature at 37°C.

6.8.3.2 Final Equation:

-267.422 + 45.7383 * carbon + 613.74 * nitrogen + 15.6097 * temperature + 12.2807 * carbon * nitrogen + -0.0555556 * carbon * temperature + -8.33333 * nitrogen * temperature + -7.17778 * carbon^2 + -1318.56 * nitrogen^2 + -0.2125 * temperature^2

This final equation represents the predictive model developed through Response Surface Methodology (RSM) for optimizing PHB production. The linear terms for Carbon, Nitrogen, and Temperature show their direct positive influence on PHB yield, with Nitrogen having the most substantial effect. The interaction terms (Carbon × Nitrogen, Carbon × Temperature, Nitrogen × Temperature) highlight the complex interdependencies between these factors. The quadratic terms are negative, indicating diminishing returns at higher levels, suggesting excessive amounts of Carbon, Nitrogen, or Temperature reduce production efficiency. Balancing these factors, this model helps predict optimal conditions to maximize PHB production as shown in table 33.

Point predicted Factors

Table 6.33: Point predicted value of each factor by RSM

Factor	Name	Level	Low Level	High Level	Std. Dev.	Coding
A	carbon	3.48	1.0000	4.00	0.0000	Actual
B	nitrogen	0.1506	0.0100	0.2000	0.0000	Actual
C	temperature	37.00	28.00	40.00	0.0000	Actual

6.8.4 Isolate: *Pseudomonas* fluorescence MTCC1749

Table 6.34: Presents the experimental and predicted PHA values

Runs	Factor 1 A: Carbon (%)	Factor 2 B: Nitrogen (%)	Factor 3 C: Temperature (°C)	Actual Value PHB mg/20ml	Predicted Value PHB mg/20ml
1	1	0.105	28	**65.00**	67.62
2	2.5	0.01	40	**79.00**	83.62
3	2.5	0.105	34	**125.00**	126.60
4	1	0.105	40	**77.00**	77.12
5	4	0.105	40	**93.00**	90.37

6	2.5	0.105	34	**134.00**	126.60
7	4	0.01	34	**69.00**	67.00
8	1	0.01	34	**62.00**	57.25
9	2.5	0.105	34	**119.00**	126.60
10	4	0.105	28	**91.00**	90.87
11	1	0.2	34	**68.00**	70.00
12	2.5	0.01	28	**71.00**	73.12
13	2.5	0.2	28	**105.00**	100.37
14	2.5	0.105	34	**124.00**	126.60
15	4	0.2	34	**92.00**	96.75
16	2.5	0.2	40	**101.00**	98.87
17	2.5	0.105	34	**131.00**	126.60

The close alignment between predicted and actual values as shown in figure 6.25 determines the model's accuracy and reliability. When significant deviations occur, it suggests a need for further refinement or investigation. In Figure, the data from 17 runs involving three factors align along a straight line, indicating accuracy and the absence of outliers. This alignment underscores the reliability of the data, suggesting that the model's predictions align closely with actual outcomes, a vital aspect in scientific analyses and experimental accuracy.
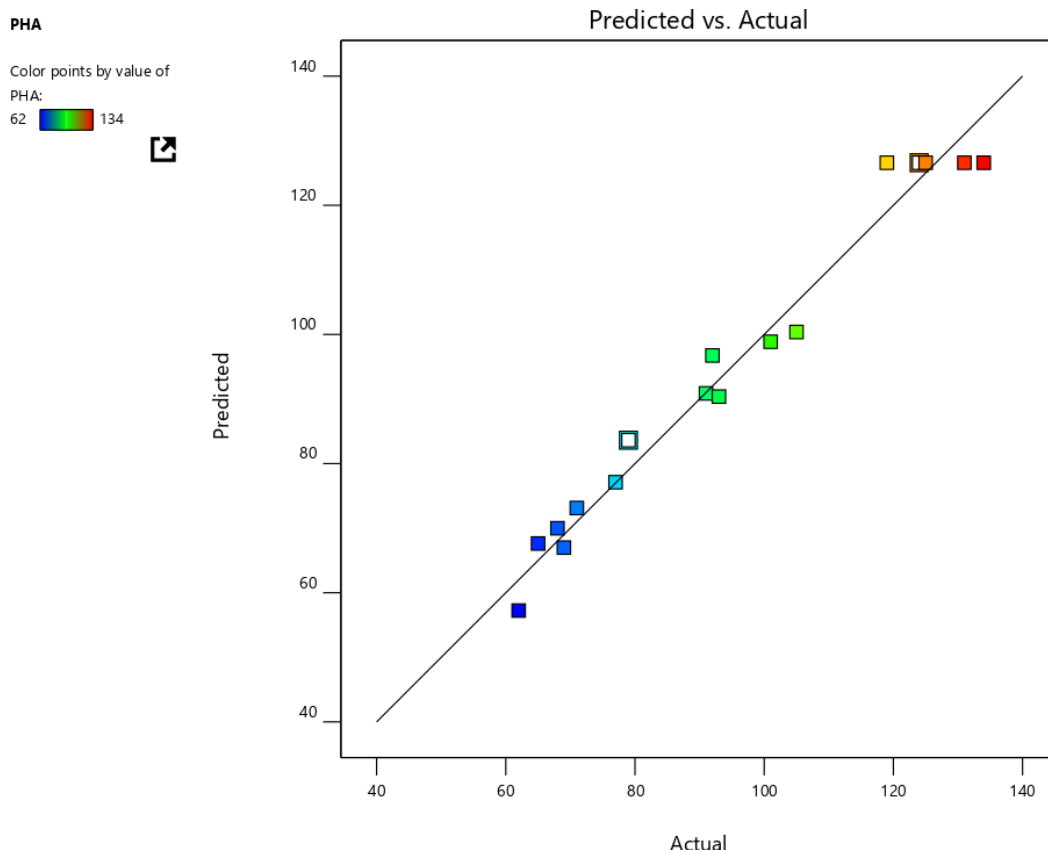
Figure 6.25: Representing the slight difference between actual and predicted values

The model results, accurately representing the predicted and actual values of PHB, show that the results from 17 runs of RSM closely approximate a straight line.

The actual vs. predicted data for Polyhydroxybutyrate (PHB) production using Response Surface Methodology (RSM) demonstrates a strong correlation, as evidenced by the close alignment of the data points to the diagonal line in the plot. The color-coded points, ranging from blue (lower PHB yield) to red (higher PHB yield), indicate the range of PHB production across different runs, with actual values well-predicted by the model.

For example, in run 3, with 2.5% Carbon, 0.105% Nitrogen, and a Temperature of 34°C, the actual PHB yield was 125 mg/20mL , while the predicted value was 126.60 mg/20ml as shown in table 6.34, demonstrating the model's high accuracy. Similarly, in run 16, with 2.5% Carbon, 0.2% Nitrogen, and a Temperature of 40°C, the actual PHB yield was 101 mg/20ml, and the predicted yield was 98.87 mg/20ml, further validating the model's robustness.

Despite a few minor deviations, such as in run eight, where the actual value was 62 mg/20ml and the predicted value was 57.25 mg/20ml, the overall fit between predicted and actual values remains highly reliable. These minor discrepancies are within an acceptable range and may be attributed to experimental variability. The RSM model effectively captures the interactions between the factors (Carbon, Nitrogen, and Temperature), allowing for accurate prediction and optimization of PHB production. Similar studies have validated the utility of RSM in optimizing bioprocesses by providing reliable predictive models (Saranya et al., 2021).

Table 6.35: ANOVA and fit statistics for selected Quadratic model

Source Model	Sum of Squares	df	Mean Square	F-value	p-value	
A-carbon	9584.29	9	1064.92	28.68	0.0001	**significant**
B-nitrogen	666.13	1	666.13	17.94	0.0039	
C-temperature	903.13	1	903.13	24.32	0.0017	
AB	40.50	1	40.50	1.09	0.3311	
AC	72.25	1	72.25	1.95	0.2057	
BC	25.00	1	25.00	0.6732	0.4390	
A²	36.00	1	36.00	0.9694	0.3576	
B²	3961.92	1	3961.92	106.69	< 0.0001	
C²	2261.39	1	2261.39	60.90	0.0001	
Residual	876.13	1	876.13	23.59	0.0018	
Lack of Fit	259.95	7	37.14			
Pure Error	118.75	3	39.58	1.12	0.4397	**not significant**
Cor Total	141.20	4	35.30			

	9844.24	16		
Std. Dev.	6.09	R²	0.9736
Mean	94.47	Adjusted R²	0.9396
C.V. %	6.45	Predicted R²	0.7846
		Adeq Precision	14.8380

The Model F-value of 28.68 indicates the model's significance, with only a 0.01% chance of such a result occurring by chance. Model terms A, B, A², B², and C² are significant (p-values < 0.0500), highlighting their importance. Values above 0.1000 suggest insignificance as shown in table 6.35. A Lack of Fit F-value at 1.12 implies its non-significance compared to pure error, aligning with a 43.97% chance due to noise. A non-significant lack of fit is favorable, indicating a well-fitted model, as shown in table 8.

The Predicted R² of 0.7846 shows good agreement with the Adjusted R² of 0.9396, differing by less than 0.2. Adeq Precision, measuring the signal-to-noise ratio, stands at 14.838, well above the desirable 4, affirming a strong signal, as shown in figure 9. This model is reliable for exploring the design space effectively

### 6.8.4.1 Model graphical representation:

The circular contour lines indicate a significant interaction effect between carbon and nitrogen at a temperature of 34° Celsius, suggesting that their combination has a nonlinear impact on the response. In 3D graphs, curved lines represent the response surface as shown in **figure 3**, showcasing how the response variable changes concerning two input factors. The curvature indicates the presence of quadratic or higher-order effects. A concave or convex shape indicates a nonlinear relationship between the factors and the response variable. In figure 26 at a constant temperature of 34 degrees Celsius, increasing the nitrogen percentage from 0.01 to 0.2 initially boosts PHB production until it peaks around 0.12. Beyond 0.12 up to 0.2, there is a decrease in PHB yield.

Similarly, increasing carbon content from 1 to 4% leads to an increase in PHB yield until around 2.5%, after which there is a decline. Figure 3B demonstrates a consistent trend at a

constant 0.105% nitrogen level: increasing carbon enhances PHB yield up to around 2.5%, but further increments to 4% result in reduced yield. Simultaneously, at carbon 2.5 in Figure 3C, the temperature rises from 28 to 40 degrees Celsius, and the PHB yield increases until it reaches 34 degrees Celsius, after which it declines. Figure 7C displays analogous interactions between nitrogen and temperature, depicted by circular contours and curved lines in the 3-D graph. Upon analyzing this dataset, Response Surface Methodology (RSM) offers a precise point prediction value. This prediction allows researchers to pinpoint the optimal conditions for experiments to achieve maximum PHB yield. RSM's accuracy in predicting these conditions is crucial for optimizing the production process based on eq.
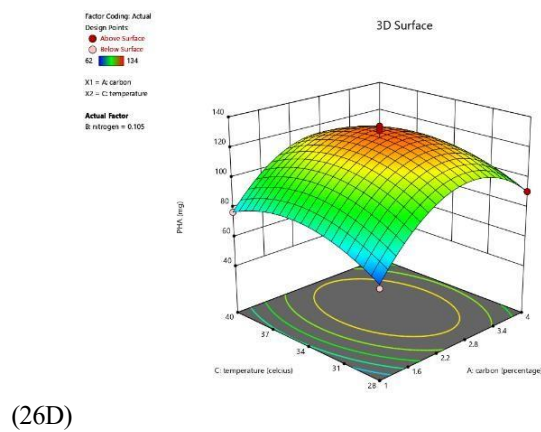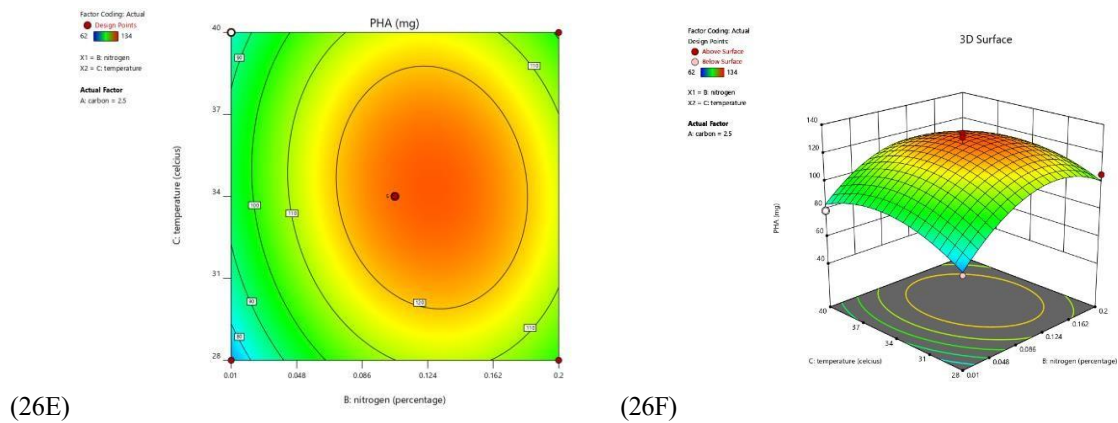

(26A)

(26B)

(26C)

(26D)

(26E)   (26F)
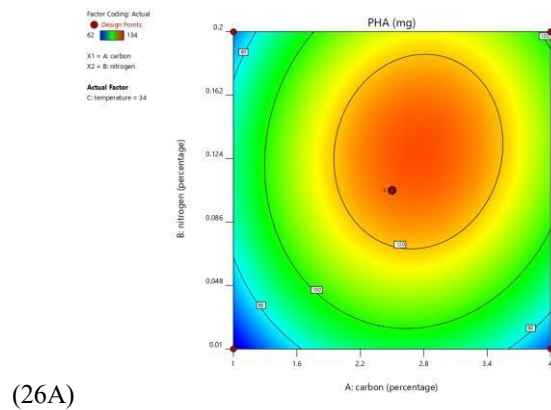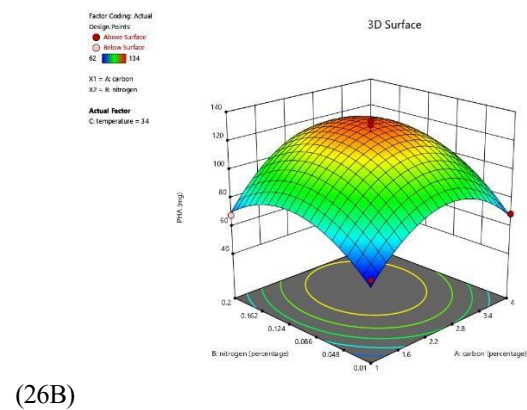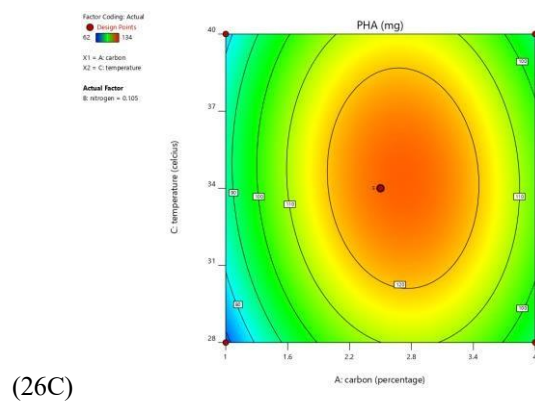
Figure 6.24: Contour and 3D surface plot graphs showing the interaction between each-other

The 3D surface and contour plots (A–F) present the interaction between Carbon, Nitrogen, and Temperature on PHB production as shown in figure 6.26(A-F), as optimized through Response Surface Methodology (RSM). These plots reveal the areas where PHB yield is maximized, with the highest production indicated by the red zones on the plots.

- **Plots A and B**: These graphs show the interaction between Carbon percentage (X1) and Nitrogen percentage (X2) at a fixed temperature of 34°C. The optimal range for PHB production appears between 1.8% and 2.0% Carbon and 0.10% to 0.11% Nitrogen. The red zone in the contour plot (B) indicates the highest yield within these ranges, further confirmed by the peak in the 3D plot (A).

- **Plots C and D**: These plots illustrate the interaction between Carbon and Temperature, with Nitrogen fixed at 0.105%. The red zone in the contour plot (D) suggests maximum PHB production when the Carbon percentage is between 1.8% and 2.0% and the Temperature is around 31°C. The 3D plot (C) further demonstrates the highest yield within this range, reinforcing the optimal condition for PHB production.

- **Plots E and F**: These graphs focus on the interaction between Nitrogen percentage and Temperature while keeping Carbon fixed at 2.5%. The optimal Nitrogen range for high PHB production is from 0.10% to 0.11%, with a Temperature of 31°C. The 3D surface plot (E) and the contour plot (F) clearly show the highest PHB yield in this parameter space.

These results suggest that the ideal conditions for maximizing PHB production occur at carbon concentrations between 1.8% and 2.0%, nitrogen concentrations between 0.10% and 0.11%, and a temperature of 31°C.

6.8.4.2 Final equation

-524.395 + 80.5629 * carbon + 755.48 * nitrogen + 28.8693 * temperature + 29.8246 * carbon * nitrogen + -0.277778 * carbon * temperature + -5.26316 * nitrogen * temperature + -13.6333 * carbon^2 + -2567.87 * nitrogen^2 + -0.400694 * temperature^2.

This equation illustrates a response surface model (RSM) depicting the relationship among the response variables. (e.g., a yield or process outcome) and three key factors: carbon, nitrogen, and temperature. Each term reflects the linear, interaction, and quadratic effects of these variables on the response. Linear coefficients (80.5629, 755.48, 28.8693) indicate how each factor individually influences the outcome. Interaction terms (carbon * nitrogen, carbon * temperature, nitrogen * temperature) capture combined effects between pairs, while quadratic terms (carbon^2, nitrogen^2, temperature^2) show how changes at higher levels impact the response. RSM enables optimizing conditions by evaluating both individual and combined effects on the target outcome shown in table 6.36.

6.8.4.3 Point prediction values

Table 6.36: Point predicted value of each factor by RSM

Factor	Name	Level	Low Level	High Level	Std. Dev.	Coding
A	carbon	1.94	1.0000	4.00	0.0000	Actual
B	nitrogen	0.1050	0.0100	0.2000	0.0000	Actual
C	temperature	31.12	28.00	40.00	0.0000	Actual

Scale-up production and extraction of PHA by a selected bacterial strain using a combination of wastewater and Hydrolysed wood waste as a substrate.
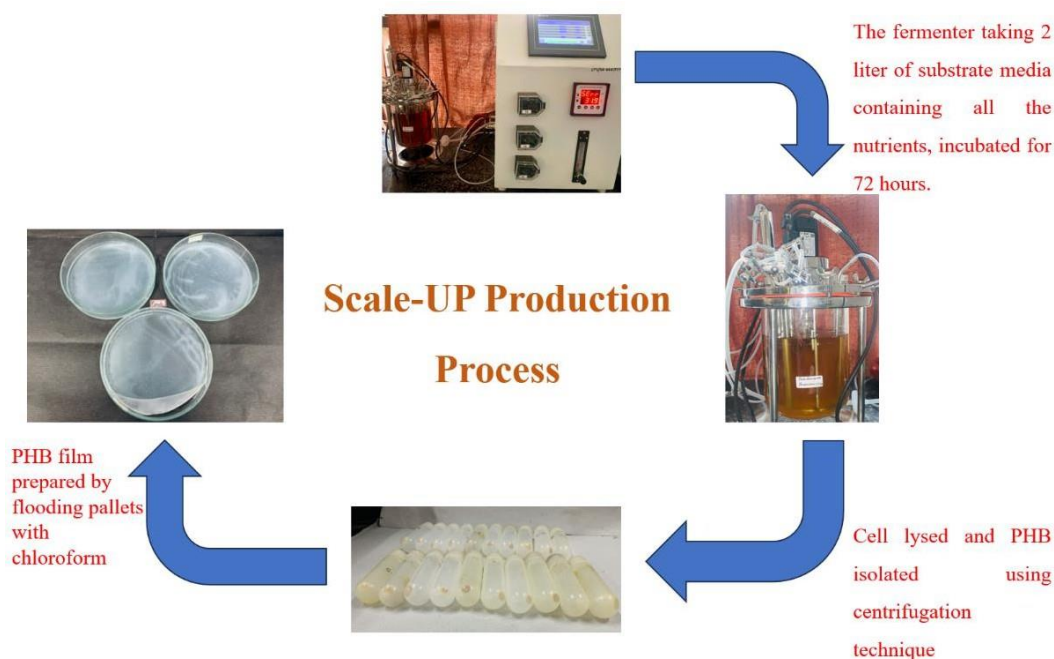
6.9 Final Production

Figure 6.27: Flow chart representation of process for final production

The process of Polyhydroxybutyrate (PHB) production using microbial fermentation can be visualized through a step-by-step series of four stages, each represented by an image in the flow chart shown in figure 6.27.

First Image: The production process begins with a fermentor loaded with 2 liters of substrate media containing all the necessary nutrients (carbon, nitrogen sources, and trace elements). The substrate is incubated at a controlled temperature (34°C) for 72 hours to allow bacterial isolates to grow and accumulate PHB within their cells.

Second Image: During this phase, the bacterial isolates consume the nutrients in the media to grow and produce PHB. As the fermentation progresses, the bacteria metabolize the carbon sources and store PHB as intracellular granules. This stage signifies the active consumption of media by the bacteria, leading to PHB accumulation.

Third Image: After the incubation period, the fermented media is subjected to centrifugation. This process separates the bacterial cells from the supernatant. The bacterial cells are then lysed, breaking open the cells to release the stored PHB. The resulting PHB is in a crude form, ready for further extraction.

Fourth Image: To purify the PHB, chloroform is added to the centrifuged pellets. The chloroform dissolves the PHB, which is then precipitated and dried to form a raw PHB film. This final step results in the formation of transparent PHB films, which can later be processed into bioplastic products.

All the isolates final production has been discussed in details further:

6.9.1 For Isolate 3: *Klebsiella sp. strain MK3*

Using Response Surface Methodology (RSM), the optimal conditions for the production of Polyhydroxybutyrate (PHB) by *Klebsiella sp. Mk3* were identified. The ideal carbon concentration was determined to be 1.7% (17 g/L), nitrogen concentration 0.1% (1 g/L), and the incubation temperature was set at 37°C. For a 2000 mL substrate, the medium was prepared by mixing 944 mL of hydrolyzed wood waste water with 1056 mL of distilled water. The hydrolyzed wood waste contained approximately 36 mg/mL of sugar content, determined by the DNS test standard graph. To this solution, 4 g of ammonium chloride was added as the nitrogen source.

The medium was inoculated with the microbial isolate and incubated at 37°C for 72 hours. After the incubation period, the culture was centrifuged to separate the cells from the supernatant. The cells were then processed for PHB extraction. After adjusting for a larger volume, the final yield of PHB obtained was approximately 8742.5 mg per 2000 mL of the medium, equivalent to 4.37 mg/mL.

6.9.2 For Isolate 5: *Klebsiella pneumoniae strain DSM 30104 (MK2023)*

Using RSM, the optimal conditions for the production of PHB by *Klebsiella pneumoniae strain DSM 30104 (MK2023)* were predicted with a carbon concentration of 2.5% (25 g/L), nitrogen concentration 0.1% (1 g/L), and an incubation temperature of 34°C. For the preparation of a 2000 mL substrate, the medium was composed of 1388 mL of hydrolyzed wood waste water blended with 612 mL of distilled water. The hydrolyzed wood waste contained approximately 36 mg/mL of sugar content. The medium was supplemented with 4 g of ammonium chloride as a nitrogen source.

The mixture was inoculated with the specific microbial isolate and incubated at a controlled temperature of 34°C for 72 hours. After incubation, the microbial culture was centrifuged to separate the cellular biomass from the liquid supernatant. The isolated cells were processed to

extract PHB, yielding approximately 10,491 mg of PHB per 2000 mL of medium, equivalent to 5.24 mg/mL.

6.9.3 For Isolate 13: *Escherichia fergusonii* MK

RSM was employed to predict the optimal conditions for PHB production by *Escherichia fergusonii* MK. The ideal carbon concentration was identified as 3.48% (35 g/L), nitrogen concentration 0.15% (1.5 g/L), and the incubation temperature set at 37°C. The medium for a 2000 mL substrate was prepared by mixing 1944 mL of hydrolyzed wood waste water with 56 mL of distilled water, containing approximately 36 mg/mL of sugar content. To this solution, 6 g of ammonium chloride was added as the nitrogen source.

The medium was inoculated with *Escherichia fergusonii* MK and incubated for 72 hours at a controlled temperature of 37°C. After incubation, the microbial culture was subjected to centrifugation to separate the cells from the supernatant. The cells were then processed for PHB extraction, yielding approximately 11,906 mg of PHB per 2000 mL of medium, equivalent to 5.9 mg/mL, making it the highest yield among the isolates.

6.9.4 For Isolate: *Pseudomonas fluorescens MTCC 1749*

Using RSM, the optimal conditions for the production of PHB by *Pseudomonas fluorescens MTCC 1749* were determined to include a carbon concentration of 1.9% (19 g/L), nitrogen concentration 0.1% (1 g/L), and an incubation temperature of 30°C. For the preparation of a 2000 mL substrate, the medium was prepared by mixing 1056 mL of hydrolyzed wood waste water with 944 mL of distilled water. The hydrolyzed wood waste contained approximately 36 mg/mL of sugar content, as determined by the DNS test. To this mixture, 4 g of ammonium chloride was added as the nitrogen source.

The medium was inoculated with *Pseudomonas fluorescence* MTCC1749 and incubated at 30°C for 72 hours. After incubation, the culture was centrifuged to separate the cells from the supernatant. The cells were processed for PHB extraction, resulting in a final PHB yield of approximately 10,823 mg per 2000 mL of medium, equivalent to 5.41 mg/mL shown in figure 6.28, 6.29.

Table 6.37: Final production result for each isolate

Bacterial Isolate	Total PHB (g)	PHB mg/ml

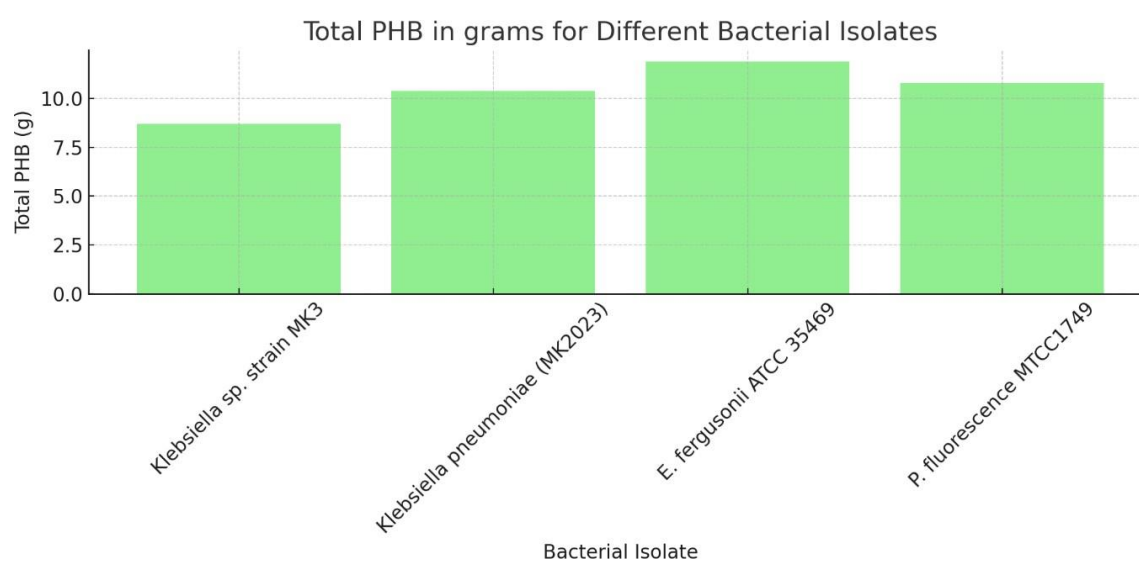|		
Klebsiella sp. strain MK3	8.7	4.37
Klebsiella pneumoniae strain DSM 30104 (MK2023)	10.4	5.24
Escherichia fergusonii ATCC 35469 MK	11.9	5.9
Pseudomonas fluorescence MTCC1749	10.8	5.41

Figure 6.28: Graphical representation of total PHB produced by each isolate in grams
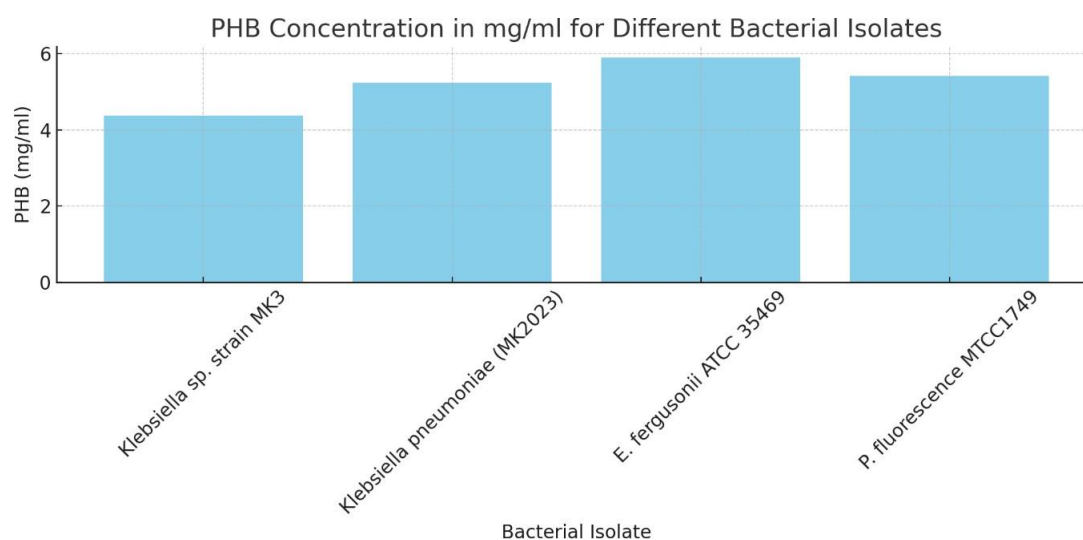

Figure 6.29: Graphical representation of PHB produced in mg/ml by each isolate in grams

The charts above compare the PHB production of four microbial isolates using a 2000 mL substrate.

- **Total PHB Production:** The bar chart illustrates the total PHB yield for each isolate. *E. fergusonii ATCC 35469* exhibited the highest production, reaching approximately 11,900 **mg**, while *Klebsiella sp. strain MK3* produced the least, with around 8,700 mg. *P. fluorescence MTCC1749* and *Klebsiella pneumoniae strain DSM 30104 (MK2023)* showed intermediate yields at 10,800 mg and 10,400 mg, respectively.

- **PHB Production per mL:** The second chart shows the PHB yield per mL of the medium. Again, *E. fergusonii ATCC 35469* outperformed the other isolates, with 5.9 mg/mL**.** *Klebsiella sp. strain MK3* had the lowest yield per mL, with 4.37 mg/mL, while the other isolates displayed production levels of 5.24 mg/mL for *Klebsiella pneumoniae strain DSM 30104 (MK2023)* and 5.41 mg/mL for *P. fluorescence MTCC1749*.

These comparisons emphasize that while *Escherichia fergusonii* MK produced the highest overall yield, the efficiency of production per mL also aligns with its higher performance compared to the other isolates.

6.10 PHA Characterization

6.10.1 UV-Vis spectrophotometry at 235 nm

The UV spectroscopy results you provided show the absorbance spectra of Polyhydroxyalkanoates (PHA) compared to the standard crotonic acid. These results are significant in identifying and characterizing the presence of Polyhydroxybutyrate (PHB), a key type of PHA, by comparing it to the known crotonic acid standards. Here are the key aspects of these results:

6.10.1.1 Peak Observations:

- **Crotonic Acid Peak**: The black line in each graph represents the absorbance spectrum of standard crotonic acid. A distinct peak is seen at **235 nm**, which is characteristic of crotonic acid.

- **PHA (PHB) Peak**: The colored lines (orange, blue, red, and purple) represent the PHA extracted from different bacterial strains. These lines also show a peak at **235 nm**, which suggests the presence of PHB in the PHA sample.

6.10.1.2 Explanation of Peaks at 235 nm

The absorbance peak observed at 235 nm for both crotonic acid and PHB is primarily due to the presence of the conjugated double bonds in the molecular structure. In the case of PHB, this absorbance arises when the polymer is subjected to acid digestion, where PHB degrades into crotonic acid, which has a UV absorbance maximum at 235 nm due to its double bond in the conjugated system (Law & Slepecky, 1961). This similarity in peaks is crucial for confirming the presence of PHB, as crotonic acid is a known degradation product of PHB during polymer breakdown shown in figure 6.30-6.33.

The slight variations in peak intensities between the bacterial strains and the crotonic acid standard could be due to differences in the yield or purity of PHB extracted from the different strains. For example, *Klebsiella* sp. MK3 and *Klebsiella pneumoniae* MK2023 display slightly lower peaks than the crotonic acid standard, possibly due to variations in the efficiency of PHA production or extraction methods.
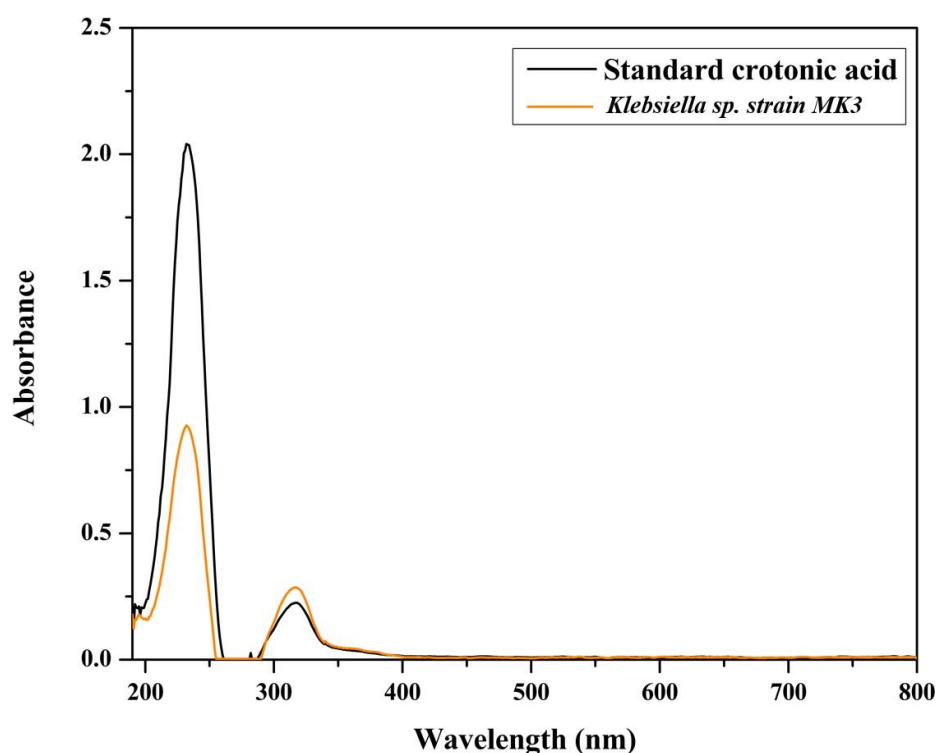

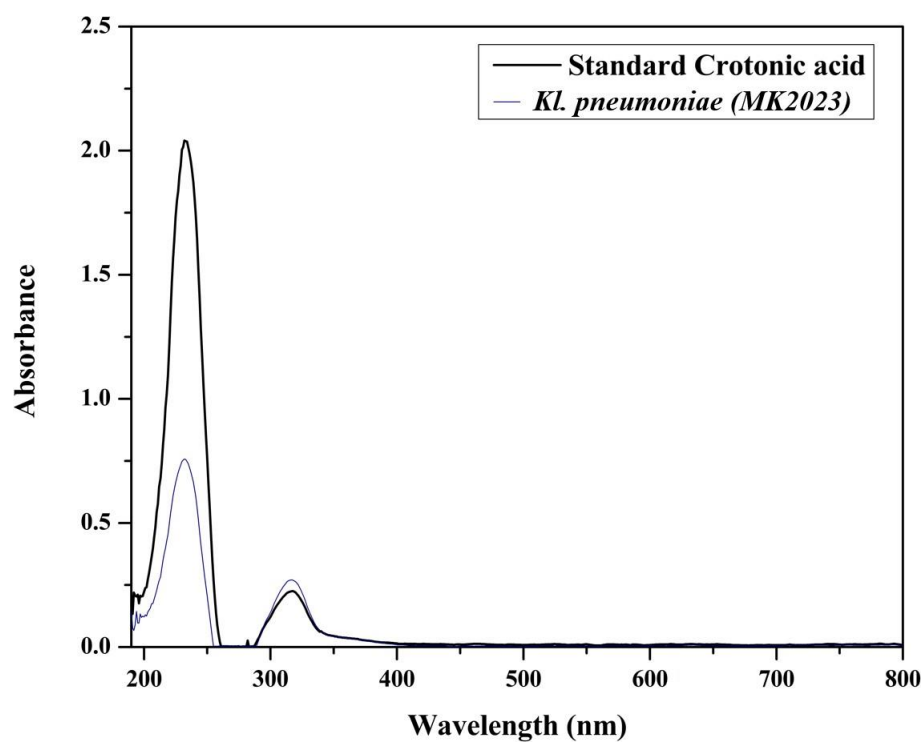**Figure 6.30:** UV spectroscopy analysis of PHA (orange line) and crotonic acid (black line)

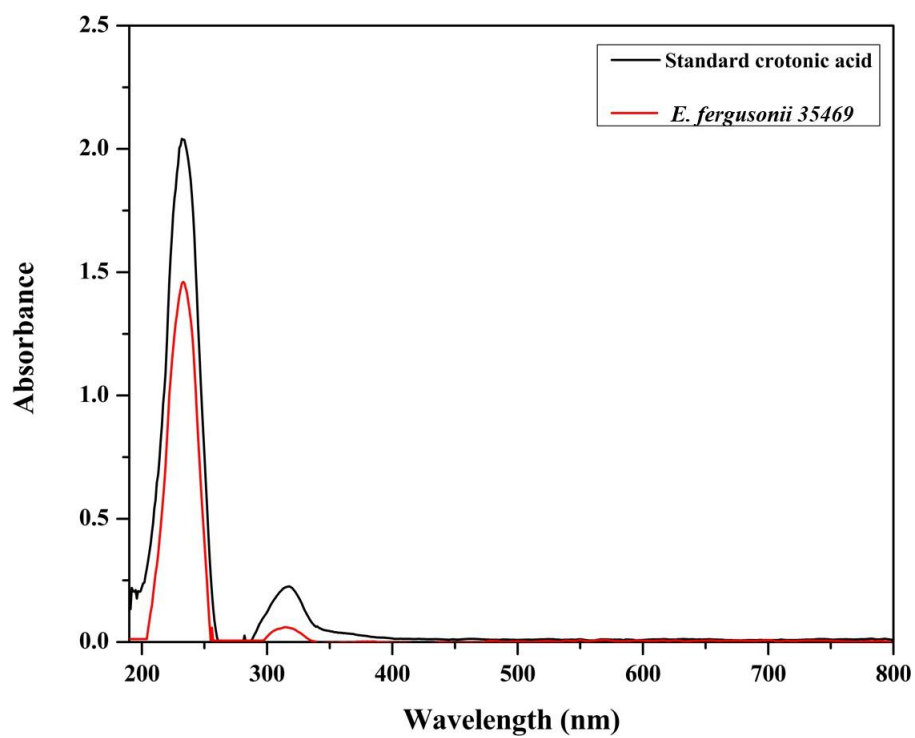**Figure 6.31:** UV spectroscopy analysis of PHA (blue line) and crotonic acid (black line)

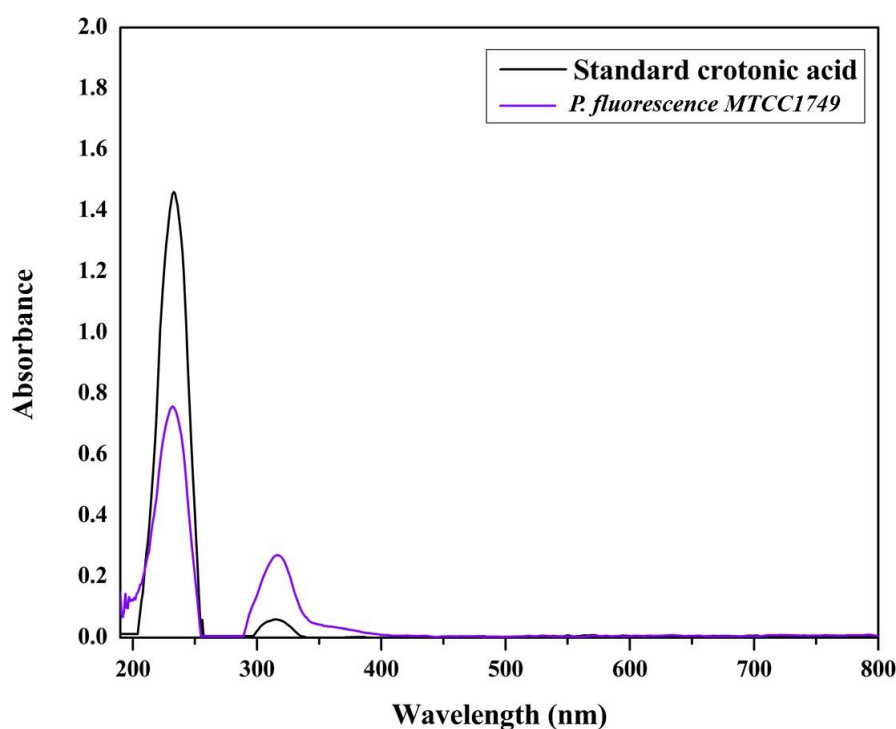**Figure 6.32:** UV spectroscopy analysis of PHA (red line) and crotonic acid (Black line)

146

Figure 6.33: UV spectroscopy analysis of PHA (purple e line) and crotonic acid (Black line)

6.10.2 Fourier Transform Infrared FTIR

The Fourier Transform Infrared (FTIR) spectroscopy results for the polyhydroxybutyrate (PHB) produced by the four bacterial isolates—*Klebsiella sp.* strain M3 and Klebsiella pneumoniae strain DSM 30104 (MK2023), *Escherichia fergusonii* ATCC 35469 MK, and *Pseudomonas fluorescence* MTCC1749—reveal characteristic absorption bands that confirm the presence of PHB.

Across all spectra, several key peaks are observed:

- **Carbonyl Group (C=O) Stretching at ~1720 cm⁻¹**: A strong absorption peak around 1720–1740 cm⁻¹ is indicative of the ester carbonyl stretching vibration in PHB. This peak is a hallmark of the polyester backbone of PHB and is consistently seen in microbial PHB samples (Kourmentza et al., 2017).

- **Aliphatic C–H Stretching between 2850–3000 cm⁻¹**: Peaks in this region correspond to the stretching vibrations of methyl (–CH₃) and methylene (–CH₂–) groups. These are characteristic of the aliphatic side chains present in PHB (Shah et al., 2014).

- **C–H Bending at ~1450 cm⁻¹**: The bending vibrations of the –CH₂– groups appear around 1450–1470 cm⁻¹, confirming the methylene units in the polymer chain (Bonartsev et al., 2019).

- **C–O Stretching at ~1270 cm⁻¹**: This peak represents the C–O stretching vibrations of the ester bond in PHB, further confirming the polyester structure (Chen et al., 2016).

- **C–O–C Stretching between 1050–1100 cm⁻¹**: Absorptions in this region are associated with the C–O–C stretching of the ester linkage, characteristic of PHB polymers (Valappil et al., 2007).

By discussing these peaks collectively, we avoid redundancy and highlight that all four isolates produced PHB with similar structural features. The minor variations in peak intensities and exact wavenumbers among the spectra can be attributed to differences in polymer chain length, crystallinity, and purity of the PHB samples extracted from each bacterial strain.

These findings are consistent with previous studies where PHB extracted from different bacterial species showed similar FTIR spectra. For instance, Bonartsev et al. (2019) reported comparable FTIR results for PHB produced by *Azotobacter chroococcum*, and Kourmentza et al. (2017) observed similar spectral patterns in PHB synthesized by various microbial isolates.

The confirmation of PHB production by these bacterial strains underscores their potential for bioplastic production, contributing to sustainable materials development. Utilizing waste substrates, such as hydrolyzed wood waste water in this case, further enhances the environmental benefits by valorizing waste streams (Keshavarz & Roy, 2010).
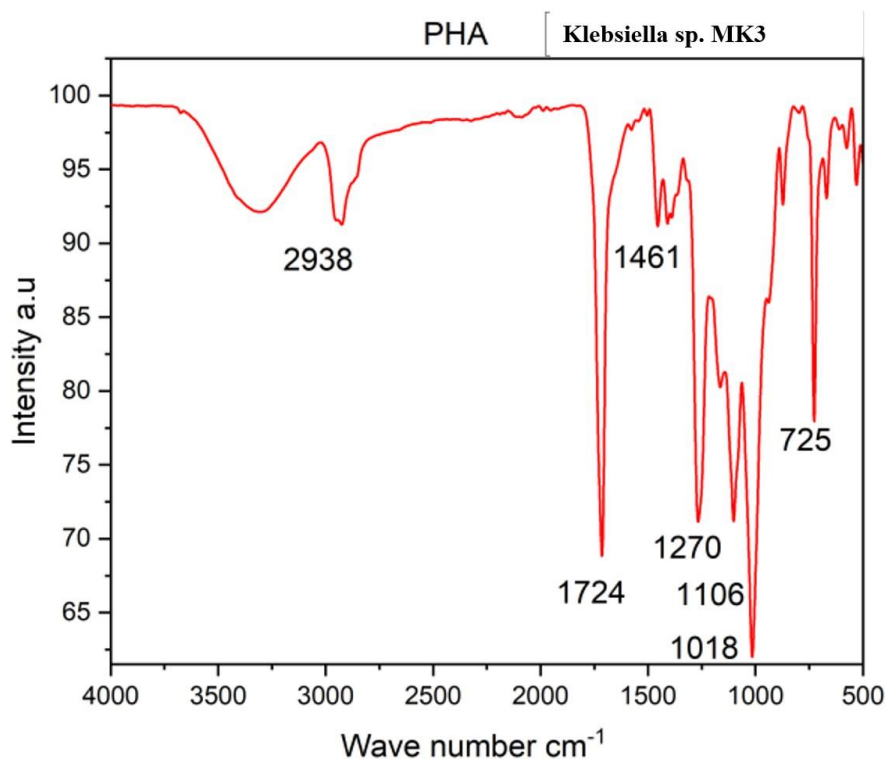
Figure 6.34: FTIR Analysis of extracted product from *Klebsiella sp. MK3*
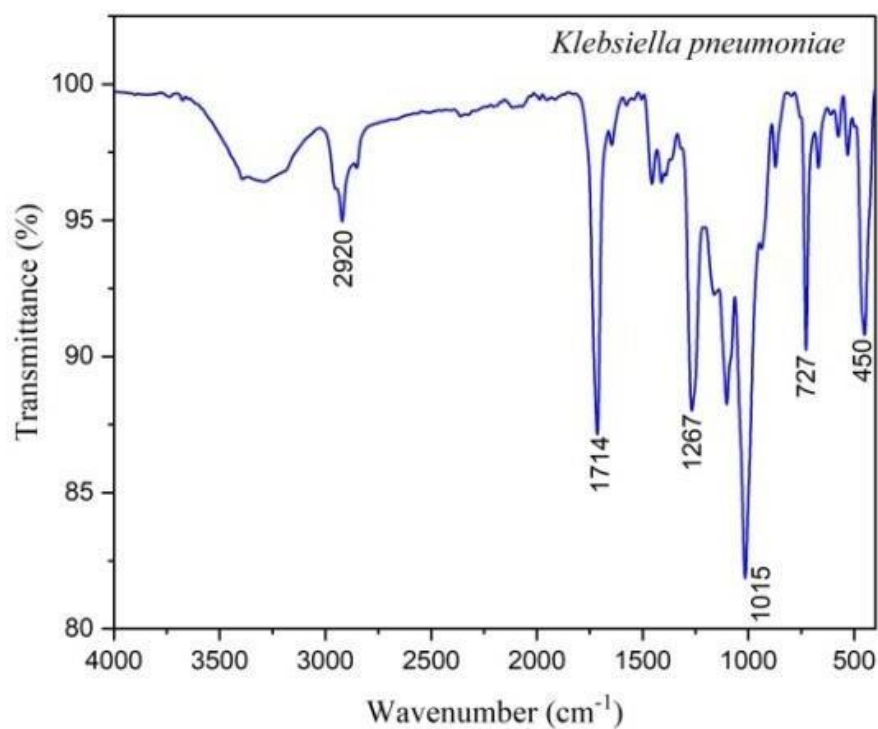

Figure 6.35: FTIR Analysis of extracted product From *Klebsiella pneumoniae MK2023*

149
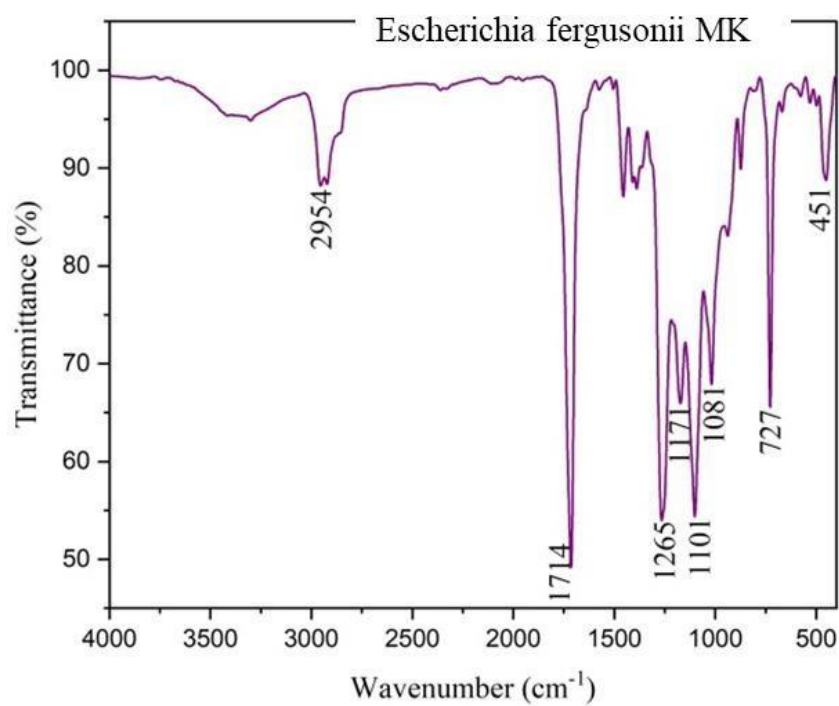
Figure 6.36: FTIR Analysis of extracted product from *Escherichia fergusonii MK*
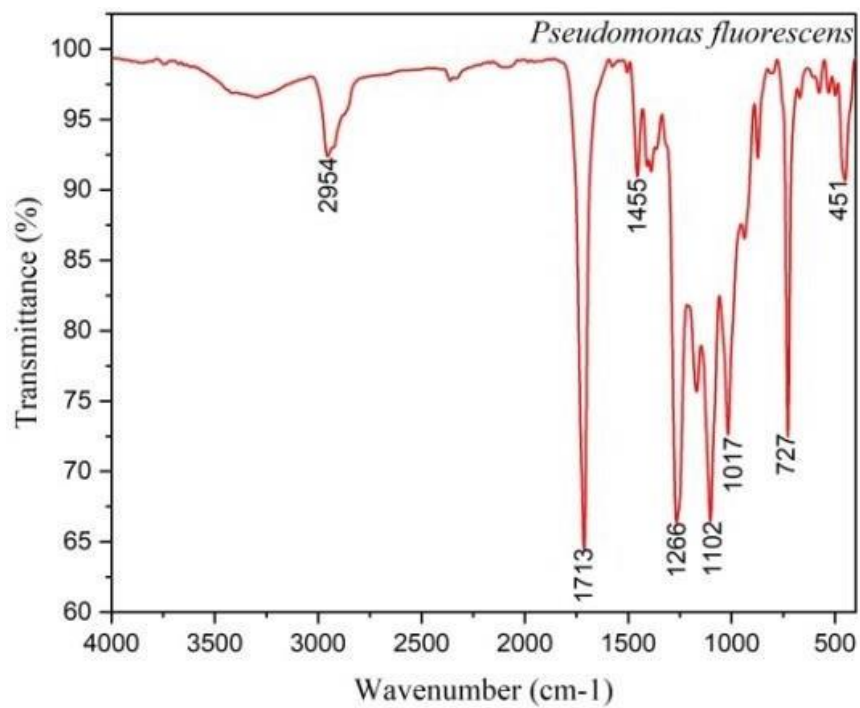
Figure 6.37 FTIR Analysis of extracted product from *Pseudomonas fluorescens MTCC 1749*

6.10.3 FTIR for standard PHB
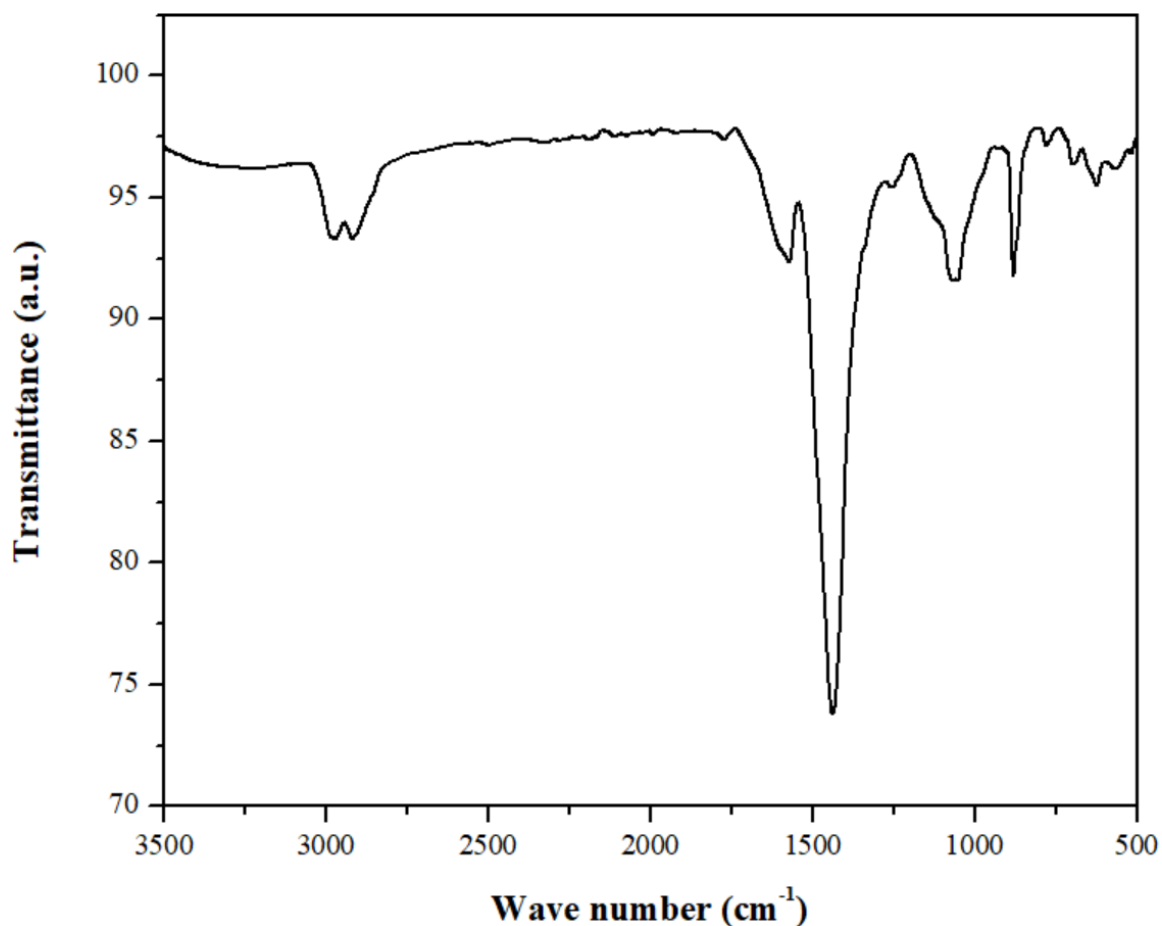
Figure 6.38: FTIR spectrum of standard polyhydroxybutyrate (PHB).

The characteristic peaks include a strong absorption band around 1724 cm^{-1}, corresponding to the C=O (ester carbonyl) stretching, and peaks near 2938 cm^{-1} for C-H stretching. Additional bands in the 1300-1000 cm^{-1} range represent C-O-C and C-O stretching, confirming the polymeric ester structure of PHB.

Table 6.38: FTIR spectral comparison of standard polyhydroxybutyrate (PHB) with PHB extracted from different bacterial isolates.

Peaks (cm^{-1})	Standard PHB	Klebsiella sp. MK3	Klebsiella pneumoniae MK2023	Escherichia fergusonii MK	Pseudomonas fluorescens MTCC 1749	Functional Groups
~2954-2938	Present	2938	2920	2954	2954	C-H stretching (aliphatic,

						methyl and methylene)
~1724-1714	Present	1724	1714	1714	1713	C=O stretching (ester carbonyl)
~1465-1455	Present	1461	-	-	1455	CH$_2$ bending (methylene)
~1280-1260	Present	1270	1267	1265	1266	C-O stretching (ester bond)
~1180-1100	Present	1106	1015	1101	1102	C-O-C stretching (ester linkage)
~1050-1015	Present	1018	1015	1081	1017	C-O stretching (ester bond)
~727-725	Present	725	727	727	727	CH bending

Key Observations

1. Presence of PHB-Specific Peaks:

   o The C=O ester carbonyl peak (~1724-1714 cm⁻¹), a key marker for PHB, is observed in all isolates.

   o C-H stretching (2938-2954 cm⁻¹) and C-O stretching (1106-1101 cm⁻¹) confirm the polymeric nature of PHB in all spectra.

2. Peak Shifts and Intensity Variations:

   o Klebsiella pneumoniae MK2023 shows a slight shift in C=O (1714 cm⁻¹), which could indicate polymer modifications or differences in PHB crystallinity.

- Escherichia fergusonii MK and Pseudomonas fluorescens MTCC 1749 display stronger C-H and C=O stretching peaks, indicating a higher concentration or better polymerization of PHB.

3. Differences from Standard PHB:

- All isolates exhibit characteristic PHB peaks, but the shifts and intensity variations suggest strain-specific differences in PHB composition or potential copolymer formation (e.g., PHB-co-PHV).

6.10.4 Nuclear Magnetic Resonance (NMR)

6.10.4.1 Sample: *Klebsiella sp. MK3*

Figure 6.39 (A): ^{1}H-NMR spectrum of the PHB extracted using chloroform
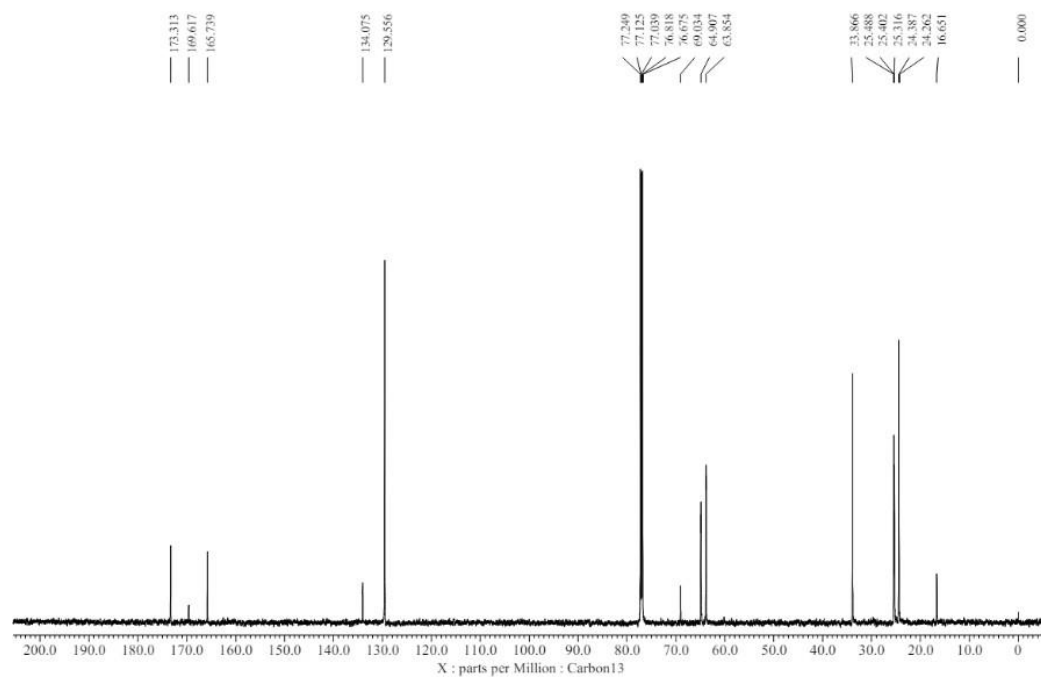
Figure 6.39 (B): ^{13}C-NMR spectrum of the PHB extracted using chloroform

6.10.4.2 Sample: *Klebsiella pneumoniae MK2023*

Figure 6.40 (A): ^{1}H-NMR spectrum of the PHB extracted using chloroform
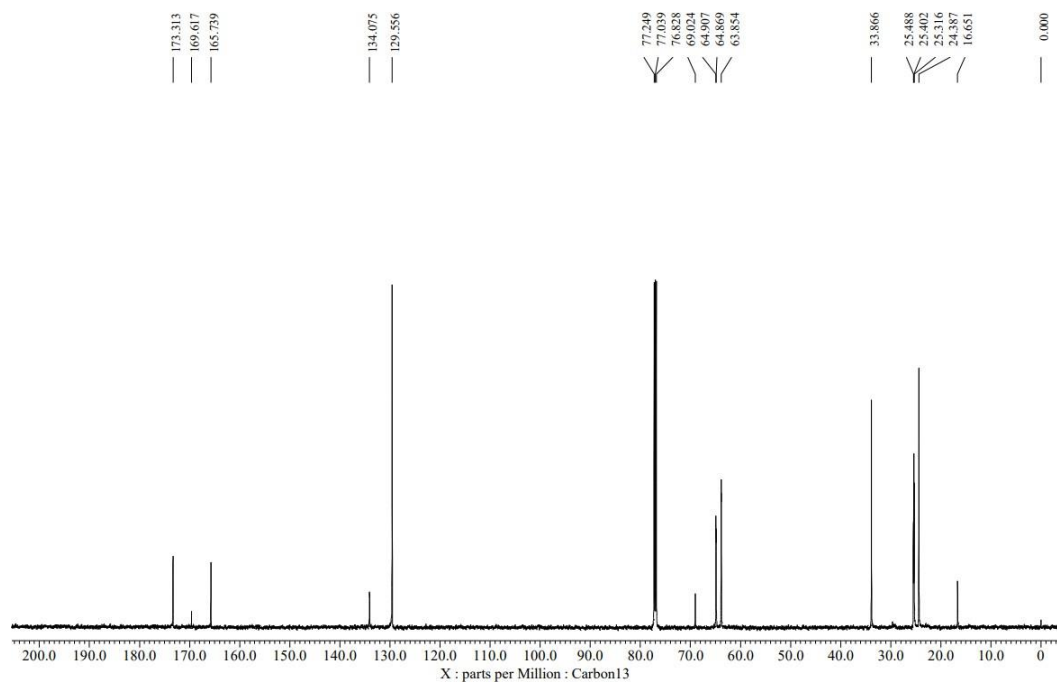
Figure 6.41: ^{13}C-NMR spectrum of the PHB extracted using chloroform

6.10.4.3 Sample: *Escherichia fergusonii MK*

Figure 6.42: ^{1}H-NMR spectrum of the PHB extracted using chloroform
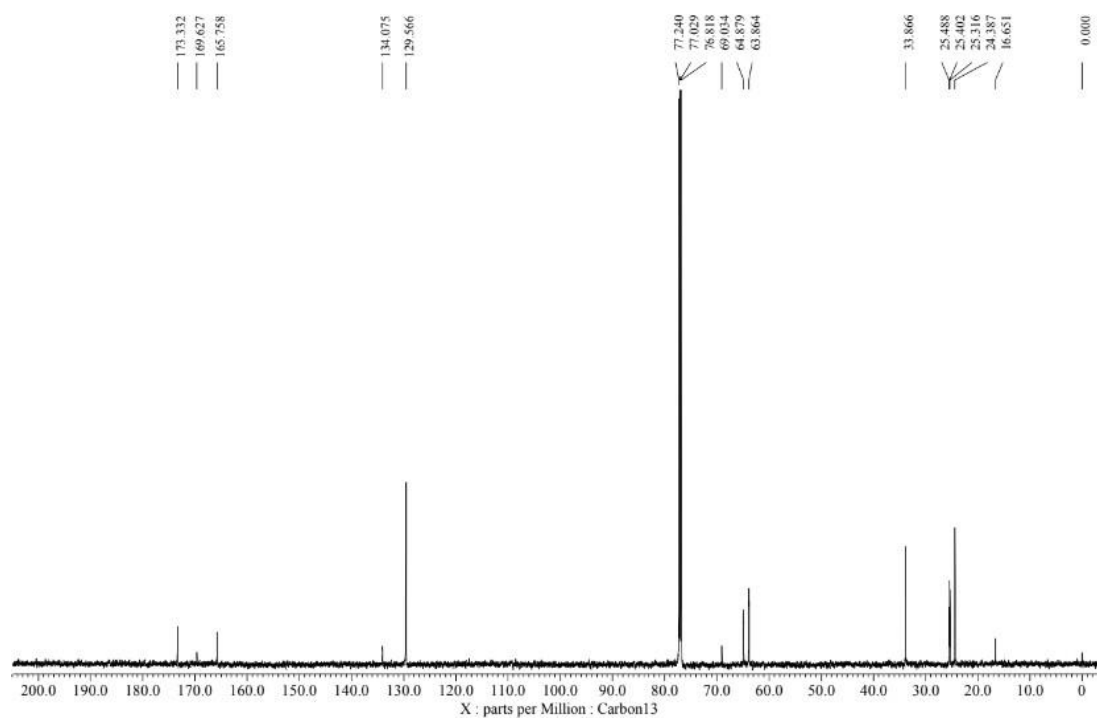
Figure 6.43: ^{13}C-NMR spectrum of the PHB extracted using chloroform

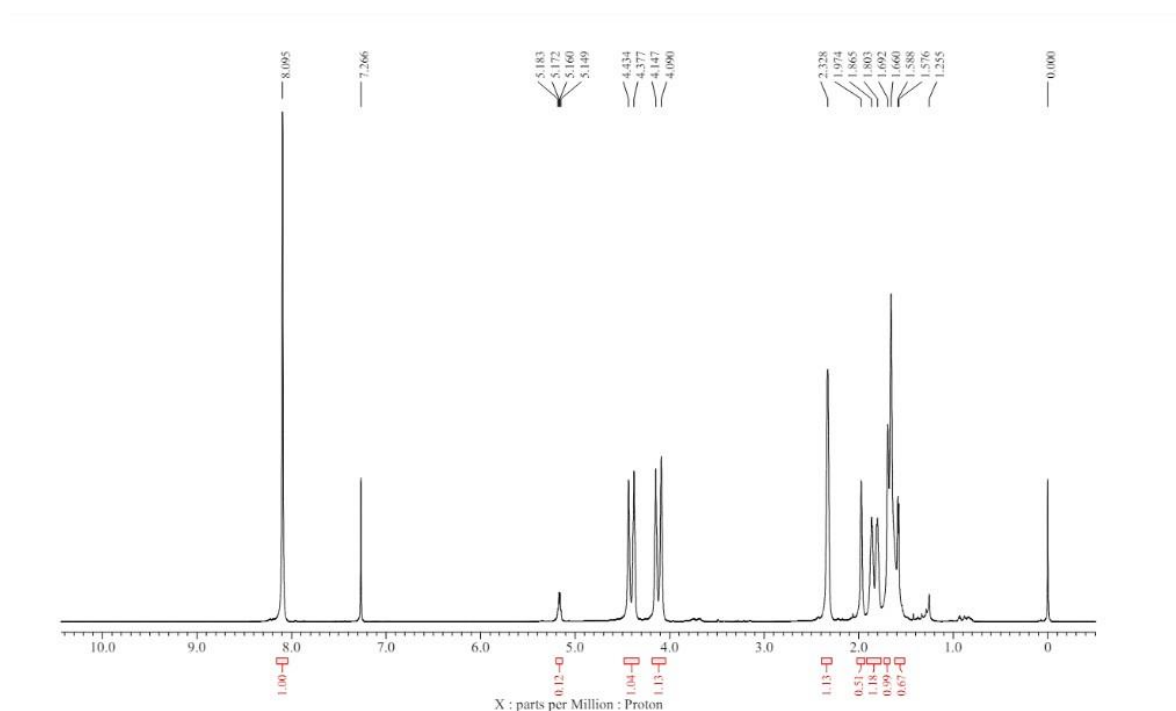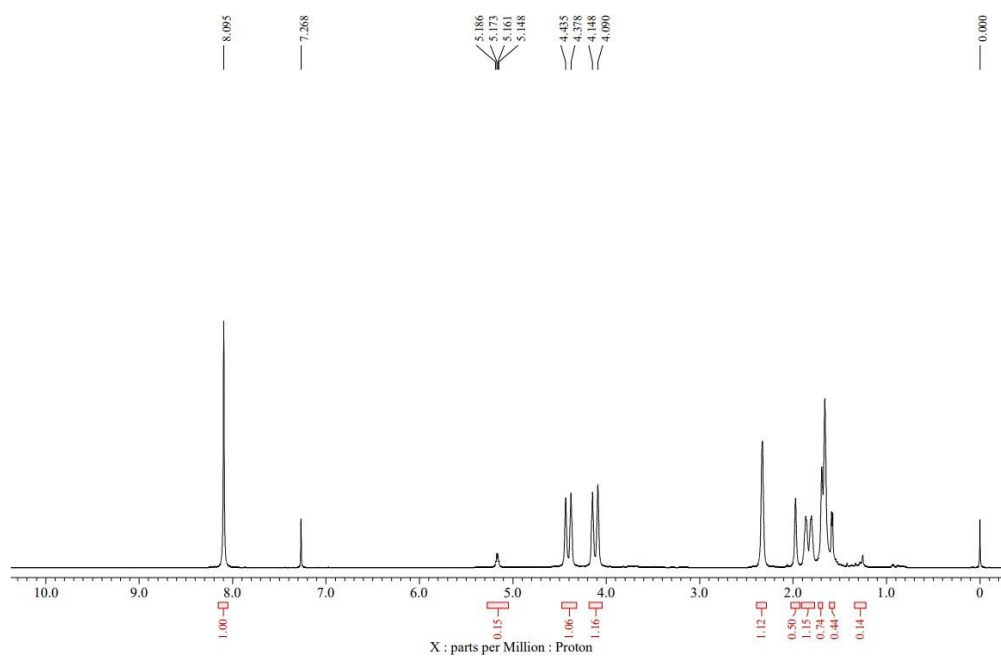## 6.10.4.4 Sample: *Pseudomonas fluorescens MTCC 1749*
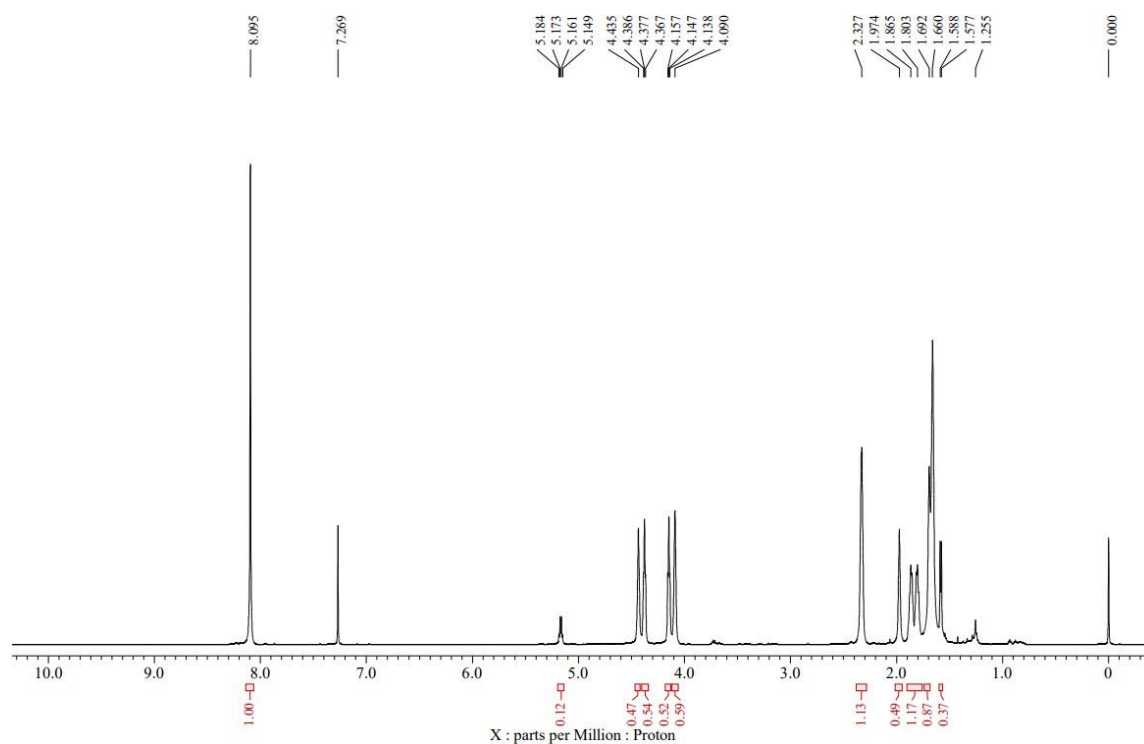
Figure 6.44: ^{1}H-NMR spectrum of the PHB extracted using chloroform
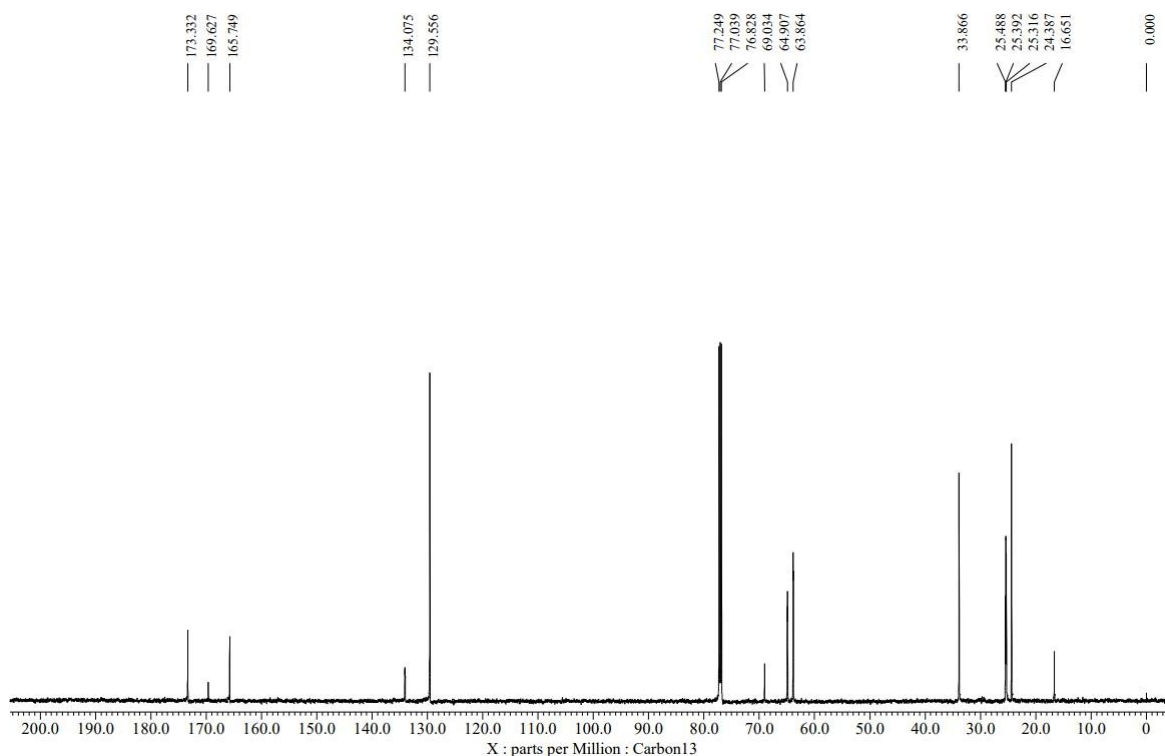
Figure 6.45: ^{13}C-NMR spectrum of the PHB extracted using chloroform

The NMR spectra results for PHB (polyhydroxybutyrate) extracted from *Klebsiella pneumoniae strain DSM 30104 (MK2023)*, *Klebsiella* OR362761, *Escherichia fergusonii MK*, and *Pseudomonas fluorescens* reveal characteristic peaks that confirm the presence of PHB. In the proton NMR (1H-NMR) spectra, the most significant peaks are observed in the regions associated with the polymer backbone of PHB. A multiple at around 5.2 ppm corresponds to the methine proton (-CH), which is linked to the ester group in PHB. This peak is a key indicator of the polymer structure. Peaks in the region of 1.2-1.3 ppm represent the methyl groups (-CH3) of the polymer side chains, and a doublet at around 2.5 ppm represents the methylene protons (-CH2) connected to the carbonyl group.

In the carbon-13 NMR (13C-NMR) spectra, peaks around 169-173 ppm correspond to the ester carbonyl carbon (-C=O), which is a defining feature of the PHB structure. Peaks at 67-69 ppm are associated with the methylene carbon adjacent to the ester group (-CH2), while peaks at 20-22 ppm represent the methyl groups as shown in figure 6.39-6.42. These consistent chemical shifts across all isolates provide strong evidence of successful PHB extraction and purification.

The spectra clearly indicate that all the bacterial isolates—*Klebsiella pneumoniae strain DSM 30104 (MK2023)*, *Klebsiella* OR362761, *Escherichia fergusonii MK*, and *Pseudomonas fluorescens*—are capable of producing PHB with similar structural characteristics. The slight variations in peak intensities and chemical shifts reflect the polymer yield differences but not the core PHB structure. These findings align with previous studies that have established NMR as a reliable method for PHB characterization (Verlinden et al., 2007; Sudesh et al., 2000).

6.10.4.5 For PHB pellets
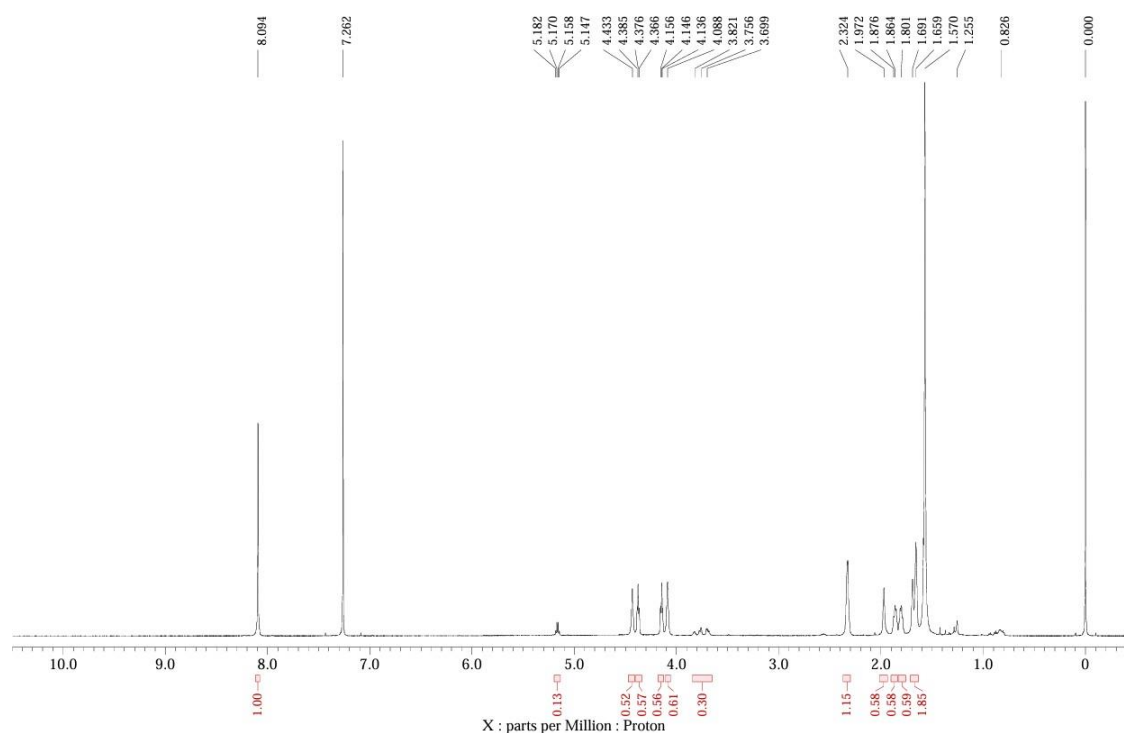
Figure 6.46: ^{1}H-NMR spectrum of the PHB extracted using chloroform
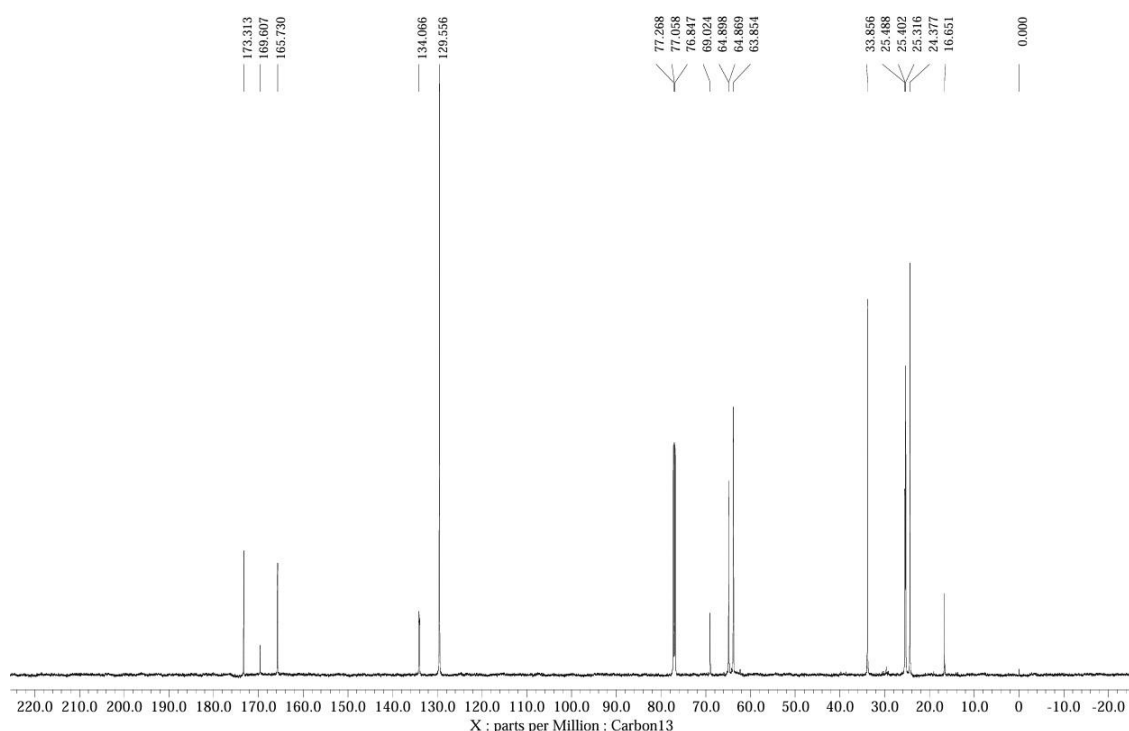
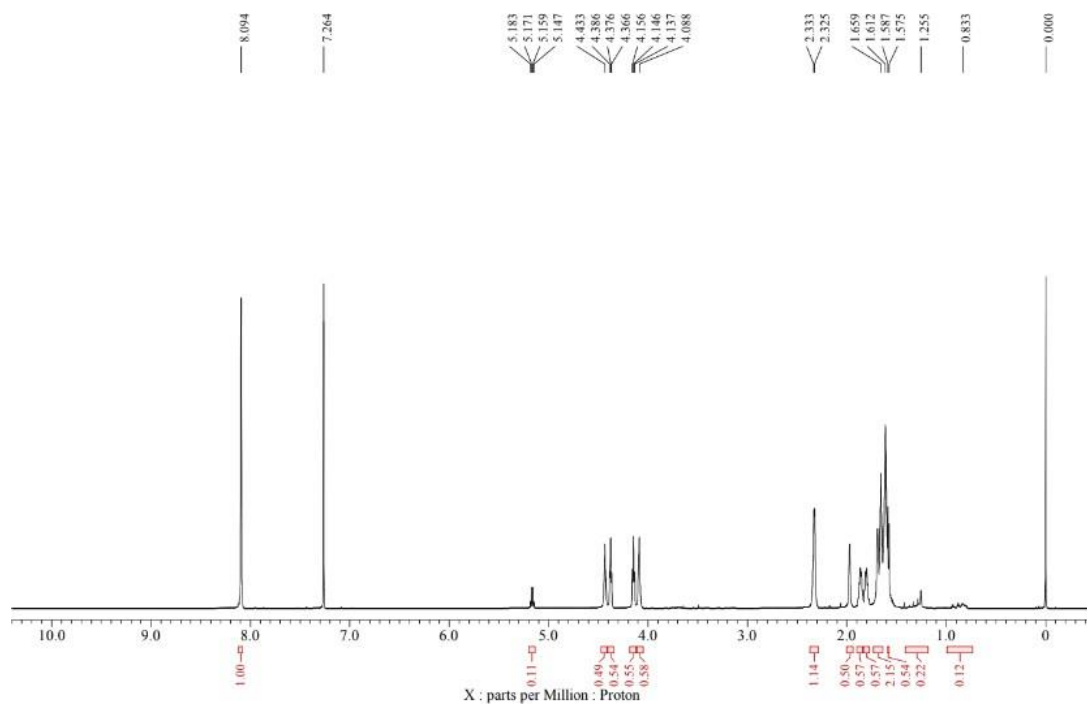**Figure 6.47** ^{13}C-NMR spectrum of the PHB extracted using chloroform

For the proton spectra (^{1}H-NMR) of the extracted PHB samples, the peaks around 5.2 ppm correspond to the methine group (-CH) of the PHB monomer unit, while the peaks between 2.4 and 1.2 ppm can be attributed to the methylene (-CH$_2$) and methyl (-CH$_3$) groups, respectively. These characteristic peaks are indicative of the presence of PHB in the extracted samples. Similarly, the carbon spectra (^{13}C-NMR) show peaks around 169-170 ppm (carbonyl carbon), 67-68 ppm (methine carbon), and 39-40 ppm (methylene carbon), all of which correspond to the PHB structure. These peaks are consistent across all isolates, confirming that PHB was successfully synthesized and extracted as shown in figure 6.46-6.47.

Comparing the NMR results from the extracted PHB with those of the pure PHB pellets, we see that the major peaks are well-aligned in both the proton and carbon spectra, suggesting that the extracted PHB is chemically similar to the standard. However, minor shifts in chemical shifts or peak intensities could be attributed to the slight impurities present in the extracted samples or the processing method, which may not be as refined as the commercial pure PHB production.

159

These NMR spectra confirm that the PHB obtained from bacterial isolates is structurally comparable to the commercially available pure PHB, validating the microbial process used for PHB production. The findings are consistent with those reported by Khanna and Srivastava (2005) and Chen (2010), which confirm the efficacy of bacterial fermentation in PHB production.

6.10.5 GC-MS

6.10.5.1 Sample: *Klebsiella sp. MK3*
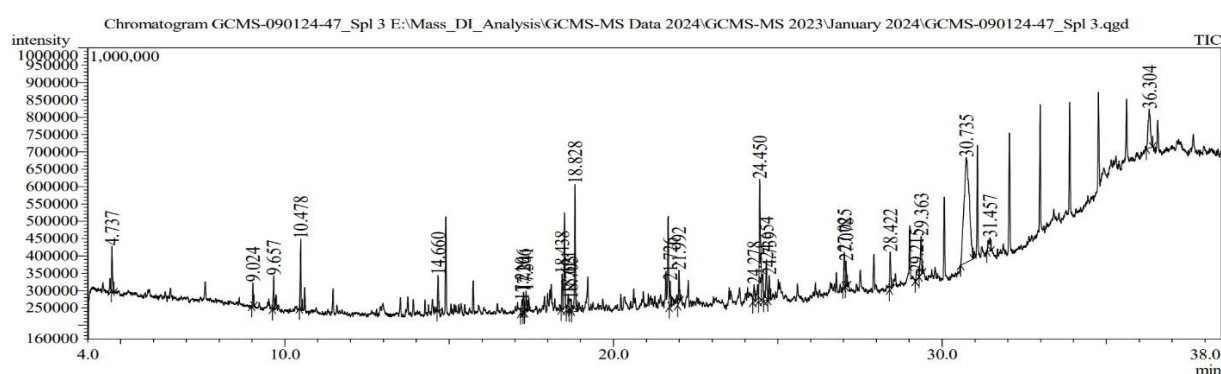
Peak#	Name	R.Time	Area	Area%	Height	Height%
1	1-Ethoxy-3-methyl-2-butene	4.737	253821	2.63	130691	4.46
2	Butane, 2-ethoxy-2-methyl-	9.024	112014	1.16	67834	2.31
3	di-t-Butylacetylene	9.657	182299	1.89	97043	3.31
4	Dodecane, 4,6-dimethyl-	10.478	353987	3.67	201978	6.89
5	Heptadecane	14.660	160286	1.66	101966	3.48
6	Nonane, 5-methyl-5-propyl-	17.210	109258	1.13	35854	1.22
7	Pentadecane	17.266	120798	1.25	58291	1.99
8	Heneicosane	17.341	134085	1.39	60981	2.08
9	Hexadecane, 1-iodo-	18.438	202298	2.10	102538	3.50
10	Eicosane	18.621	113904	1.18	46539	1.59
11	Sulfurous acid, 2-ethylhexyl isohexyl ester	18.705	129086	1.34	32986	1.13
12	2,4-Di-tert-butylphenol	18.828	757940	7.87	365989	12.49
13	Triacontane, 1-iodo-	21.726	147934	1.54	75772	2.59
14	Methyl tetradecanoate	21.992	171490	1.78	95087	3.24
15	5,5-Diethylpentadecane	24.278	129058	1.34	49236	1.68
16	7,9-Di-tert-butyl-1-oxaspiro(4,5)deca-6,9-die	24.450	953735	9.90	351819	12.00
17	Hexadecanoic acid, methyl ester	24.654	317597	3.30	117421	4.01
18	Benzenepropanoic acid, 3,5-bis(1,1-dimethyl	24.739	154901	1.61	70878	2.42
19	Tetrapentacontane	27.025	210953	2.19	99780	3.40
20	Methyl stearate	27.078	159887	1.66	72667	2.48
21	Tributyl acetylcitrate	28.422	211038	2.19	107624	3.67
22	Hexacontane	29.215	132407	1.37	22535	0.77
23	Pentanohydrazide, N2-(1,2-dihydroacenaphtl	29.363	306371	3.18	111447	3.80
24	Phenol, 2,4-bis(1,1-dimethylethyl)-, phosphit	30.735	3384406	35.13	303420	10.35
25	Tetrapentacontane	31.457	159645	1.66	38060	1.30
26	Tris(2,4-di-tert-butylphenyl) phosphate	36.304	564050	5.86	112690	3.84
			9633248	100.00	2931126	100.00

Figure 6.48: Chromatogram and peak report of *Klebsiella sp. MK3*

6.10.5.2 Sample: *Klebsiella pneumoniae MK2023*

Chromatogram GCMS-090124-47_Spl 5 E:\Mass_DI_Analysis\GCMS-MS Data 2024\GCMS-MS 2023\January 2024\GCMS-090124-47_Spl 5.qgd

Peak Report TIC
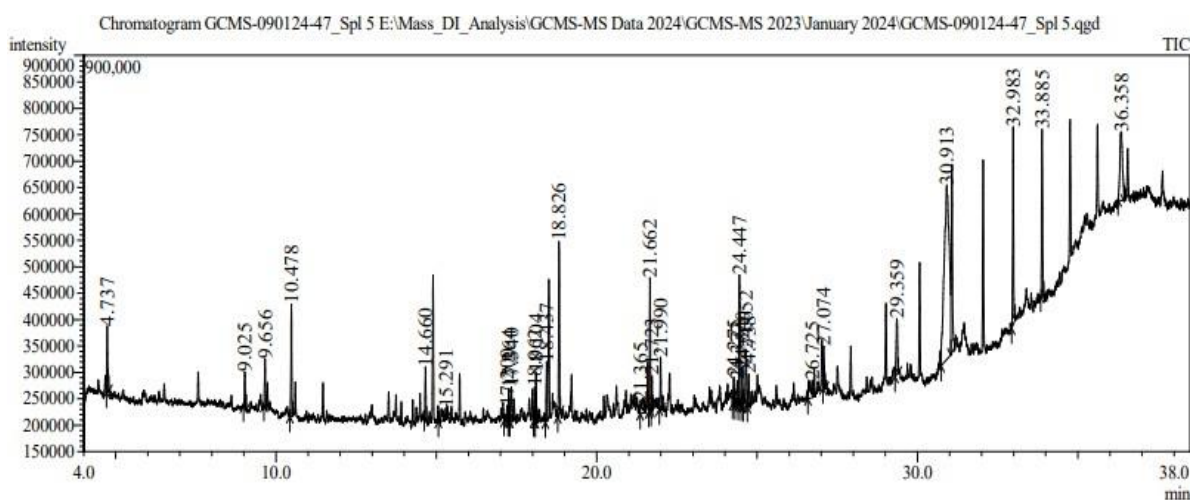
Peak#	Name	R.Time	Area	Area%	Height	Height%
1	1-Ethoxy-3-methyl-2-butene	4.737	242490	2.07	124543	3.32
2	Butane, 2-ethoxy-2-methyl-	9.025	115497	0.98	67835	1.81
3	Cyclopropane, 1,1,2-trimethyl-3-(2-methyl-1	9.656	167172	1.42	91580	2.44
4	Dodecane, 4,6-dimethyl-	10.478	375769	3.20	212342	5.67
5	10-Methylnonadecane	14.660	161660	1.38	97684	2.61
6	Nonane, 5-methyl-5-propyl-	15.291	111143	0.95	21260	0.57
7	2H-Pyran, tetrahydro-2-(12-pentadecynyloxy	17.200	106498	0.91	25826	0.69
8	Hexadecane	17.264	133725	1.14	60916	1.63
9	Heneicosane	17.340	146800	1.25	64426	1.72
10	Dodecane, 2,6,10-trimethyl-	18.062	124062	1.06	63755	1.70
11	Eicosane	18.104	185256	1.58	93760	2.50
12	Heneicosane	18.437	203400	1.73	112572	3.00
13	2,4-Di-tert-butylphenol	18.826	596019	5.08	327537	8.74
14	6,6-Diethylhoctadecane	21.365	139415	1.19	22801	0.61
15	Hexacosane, 1-iodo-	21.662	495964	4.22	252206	6.73
16	Octacosane, 1-iodo-	21.723	118828	1.01	65039	1.74
17	Methyl tetradecanoate	21.990	201583	1.72	98818	2.64
18	Tetrapentacontane	24.275	118155	1.01	49332	1.32
19	Dotriacontane	24.377	142667	1.22	43681	1.17
20	7,9-Di-tert-butyl-1-oxaspiro(4,5)deca-6,9-die	24.447	761366	6.48	246158	6.57
21	Hexacosane, 1-iodo-	24.540	197563	1.68	67993	1.81
22	Hexadecanoic acid, methyl ester	24.652	317682	2.71	107764	2.88
23	Benzenepropanoic acid, 3,5-bis(1,1-dimethyl	24.738	158903	1.35	61094	1.63
24	Triacontane, 1-iodo-	26.725	207183	1.76	32060	0.86
25	Methyl stearate	27.074	191169	1.63	79579	2.12
26	6-Bromohexanoic acid, 5-ethyl-3-octyl ester	29.359	291428	2.48	105659	2.82
27	Phenol, 2,4-bis(1,1-dimethylethyl)-, phosphit	30.913	3641197	31.01	330320	8.81
28	Tetrapentacontane	32.983	723607	6.16	374984	10.01
29	Tetrapentacontane	33.885	614116	5.23	316168	8.44
30	Tris(2,4-di-tert-butylphenyl) phosphate	36.358	750890	6.40	129747	3.46
			11741207	100.00	3747439	100.00

Figure 6.49: Chromatogram and peak report of *Klebsiella pneumoniae strain DSM 30104 (MK2023)*

6.10.5.3 Sample: *Escherichia fergusonii MK*

162
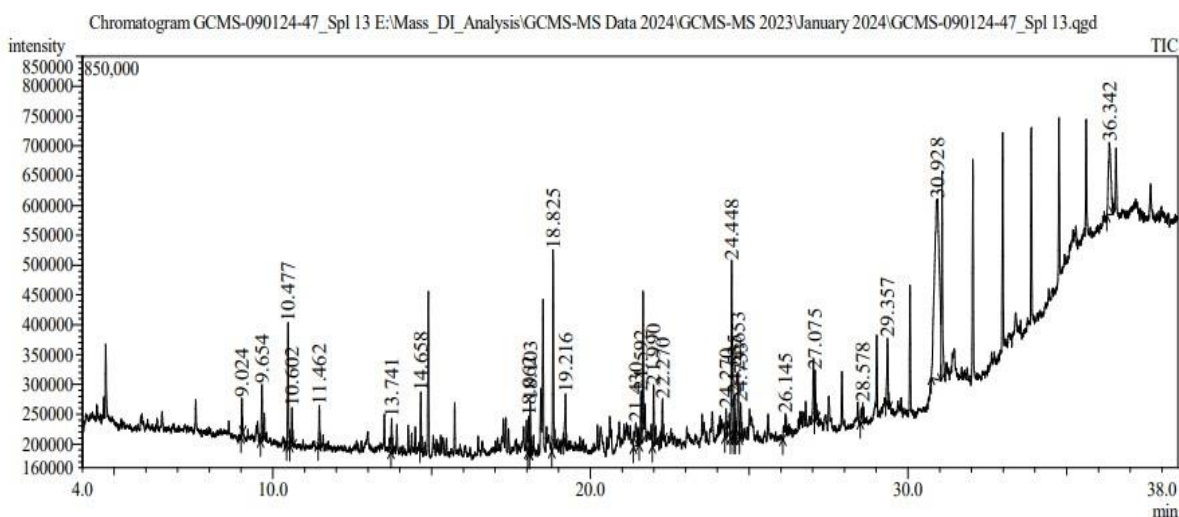
Peak Report TIC

Peak#	Name	R.Time	Area	Area%	Height	Height%
1	Butane, 2-ethoxy-2-methyl-	9.024	100702	1.09	60879	2.20
2	Cyclopropane, 1,1,2-trimethyl-3-(2-methyl-1	9.654	171476	1.85	93765	3.39
3	Dodecane, 4,6-dimethyl-	10.477	390175	4.22	204966	7.40
4	Nonane, 5-butyl-	10.602	132146	1.43	63597	2.30
5	Undecane, 3,8-dimethyl-	11.462	124460	1.35	69201	2.50
6	Decane, 2,6,7-trimethyl-	13.741	98663	1.07	56171	2.03
7	Heptadecane	14.658	157565	1.70	94737	3.42
8	2,6,10-Trimethyltridecane	18.062	122044	1.32	60702	2.19
9	Heneicosane	18.103	193623	2.09	88108	3.18
10	2,4-Di-tert-butylphenol	18.825	649760	7.02	334172	12.07
11	Eicosane	19.216	184001	1.99	85205	3.08
12	Nonane, 5-methyl-5-propyl-	21.430	172598	1.87	37863	1.37
13	Triacontane, 1-iodo-	21.592	191153	2.07	88126	3.18
14	Methyl tetradecanoate	21.990	202030	2.18	102016	3.69
15	Octacosane, 1-iodo-	22.270	96841	1.05	61634	2.23
16	Tetrapentacontane	24.270	109246	1.18	46859	1.69
17	7,9-Di-tert-butyl-1-oxaspiro(4,5)deca-6,9-die	24.448	852920	9.22	298057	10.77
18	Hexacosane, 1-iodo-	24.535	201929	2.18	71004	2.56
19	Hexadecanoic acid, methyl ester	24.653	324829	3.51	109676	3.96
20	Benzenepropanoic acid, 3,5-bis(1,1-dimethyl	24.733	128090	1.38	57891	2.09
21	Dotriacontane	26.145	113173	1.22	35756	1.29
22	Heptadecanoic acid, 16-methyl-, methyl ester	27.075	155953	1.69	80507	2.91
23	Acridin-9-yl-[1,2,4]triazol-4-yl-amine	28.578	112942	1.22	33233	1.20
24	6-Bromohexanoic acid, 5-ethyl-3-octyl ester	29.357	277461	3.00	111198	4.02
25	Phenol, 2,4-bis(1,1-dimethylethyl)-, phosphit	30.928	3308315	35.77	302577	10.93
26	Tris(2,4-di-tert-butylphenyl) phosphate	36.342	677210	7.32	120435	4.35
			9249305	100.00	2768335	100.00

Figure 6.50: Chromatogram and peak report of *Escherichia fergusonii MK*

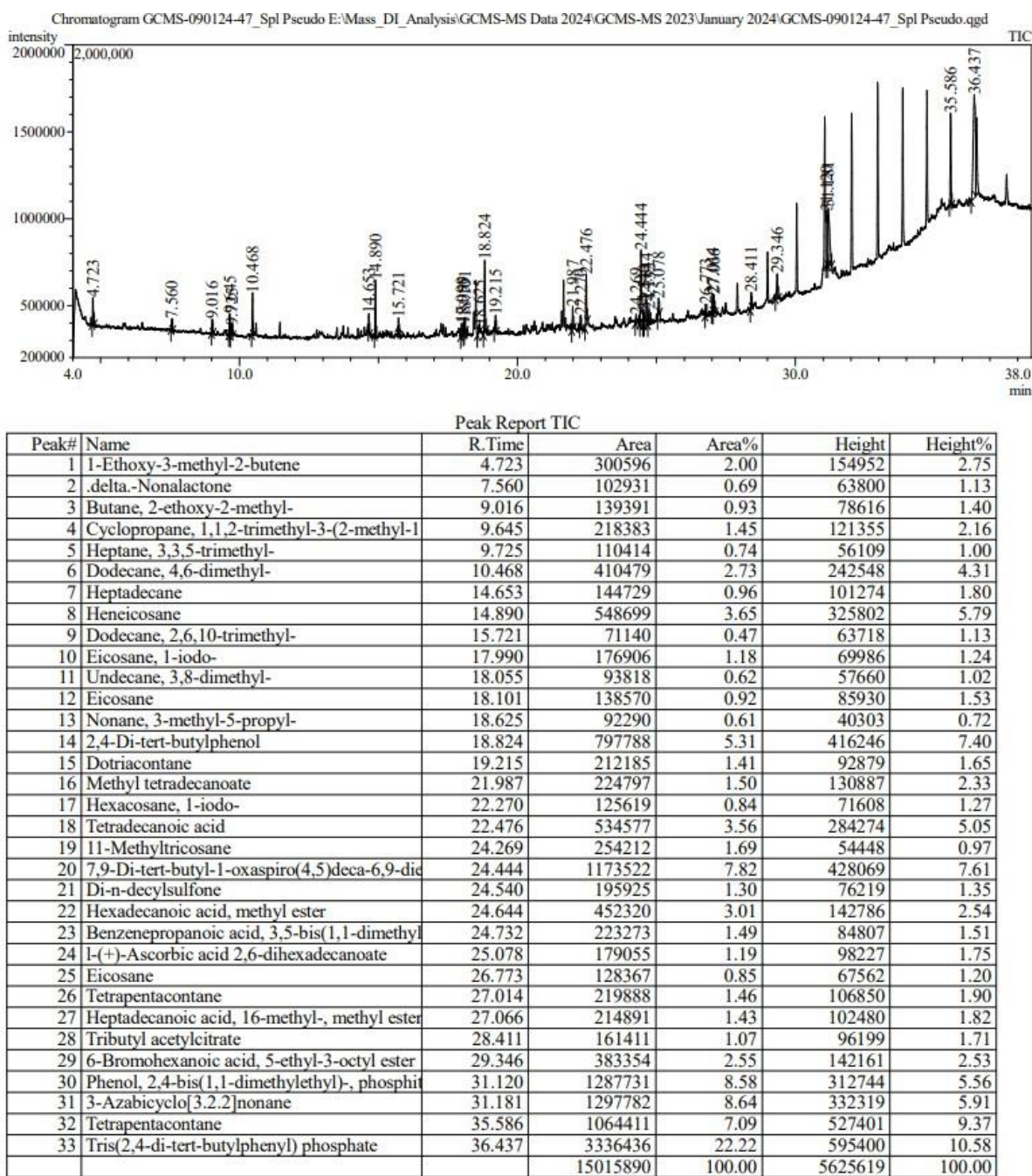**Sample 6.10.5.4** *Pseudomonas fluorescens MTCC 1749*

Figure 6.51 Chromatogram and peak report of *Pseudomonas fluorescens MTCC 1749*

Peak Report TIC

Peak#	Name	R.Time	Area	Area%	Height	Height%
1	1-Ethoxy-3-methyl-2-butene	4.723	300596	2.00	154952	2.75
2	.delta.-Nonalactone	7.560	102931	0.69	63800	1.13
3	Butane, 2-ethoxy-2-methyl-	9.016	139391	0.93	78616	1.40
4	Cyclopropane, 1,1,2-trimethyl-3-(2-methyl-1	9.645	218383	1.45	121355	2.16
5	Heptane, 3,3,5-trimethyl-	9.725	110414	0.74	56109	1.00
6	Dodecane, 4,6-dimethyl-	10.468	410479	2.73	242548	4.31
7	Heptadecane	14.653	144729	0.96	101274	1.80
8	Heneicosane	14.890	548699	3.65	325802	5.79
9	Dodecane, 2,6,10-trimethyl-	15.721	71140	0.47	63718	1.13
10	Eicosane, 1-iodo-	17.990	176906	1.18	69986	1.24
11	Undecane, 3,8-dimethyl-	18.055	93818	0.62	57660	1.02
12	Eicosane	18.101	138570	0.92	85930	1.53
13	Nonane, 3-methyl-5-propyl-	18.625	92290	0.61	40303	0.72
14	2,4-Di-tert-butylphenol	18.824	797788	5.31	416246	7.40
15	Dotriacontane	19.215	212185	1.41	92879	1.65
16	Methyl tetradecanoate	21.987	224797	1.50	130887	2.33
17	Hexacosane, 1-iodo-	22.270	125619	0.84	71608	1.27
18	Tetradecanoic acid	22.476	534577	3.56	284274	5.05
19	11-Methyltricosane	24.269	254212	1.69	54448	0.97
20	7,9-Di-tert-butyl-1-oxaspiro(4,5)deca-6,9-die	24.444	1173522	7.82	428069	7.61
21	Di-n-decylsulfone	24.540	195925	1.30	76219	1.35
22	Hexadecanoic acid, methyl ester	24.644	452320	3.01	142786	2.54
23	Benzenepropanoic acid, 3,5-bis(1,1-dimethyl	24.732	223273	1.49	84807	1.51
24	l-(+)-Ascorbic acid 2,6-dihexadecanoate	25.078	179055	1.19	98227	1.75
25	Eicosane	26.773	128367	0.85	67562	1.20
26	Tetrapentacontane	27.014	219888	1.46	106850	1.90
27	Heptadecanoic acid, 16-methyl-, methyl ester	27.066	214891	1.43	102480	1.82
28	Tributyl acetylcitrate	28.411	161411	1.07	96199	1.71
29	6-Bromohexanoic acid, 5-ethyl-3-octyl ester	29.346	383354	2.55	142161	2.53
30	Phenol, 2,4-bis(1,1-dimethylethyl)-, phosphit	31.120	1287731	8.58	312744	5.56
31	3-Azabicyclo[3.2.2]nonane	31.181	1297782	8.64	332319	5.91
32	Tetrapentacontane	35.586	1064411	7.09	527401	9.37
33	Tris(2,4-di-tert-butylphenyl) phosphate	36.437	3336436	22.22	595400	10.58
			15015890	100.00	5625619	100.00

The Gas Chromatography-Mass Spectrometry (GC-MS) results for the four bacterial isolates—*Klebsiella sp. strain Mk3, Klebsiella pneumoniae strain DSM 30104 (MK2023) , Escherichia fergusonii MK,* and *Pseudomonas fluorescens MTCC 1749*—show evidence of polyhydroxybutyrate (PHB) production. The peaks and retention times (R.Time) correspond to various compounds related to PHB. Notable peaks such as Hexadecanoic acid, 2,4-Di-tert-butylphenol, and Methyl tetradecanoate found across the samples support the identification of PHB.

164

For *Klebsiella sp.* strain M3, significant peaks at 18.828 min and 24.654 min represent Hexadecanoic acid and Methyl tetradecanoate, both recognized as PHB-related compounds (Singh et al., 2017). Similar peaks for Hexadecanoic acid and Methyl tetradecanoate are present in *Klebsiella* OR362761, further indicating PHB synthesis (Feng et al., 2018). *Escherichia fergusonii MK* shows the presence of 2,4-Di-tert-butylphenol and Hexadecanoic acid, which are critical indicators of PHB (Reddy et al., 2016). *Pseudomonas fluorescens* also shows strong peaks for 2,4-Di-tert-butylphenol, confirming PHB production (Mumtaz et al., 2019) as shown in figure 6.48-6.51.

These results are consistent with previous research on bacterial PHB production, with retention times and corresponding compound identifications matching established profiles for PHB biosynthesis pathways.

6.10.6 Biophysical properties of PHA

The tensile strength of polyhydroxybutyrate (PHB) has been reported in the range of 30–40 MPa, with an average value of approximately 36 MPa (Reddy et al., 2003). This value is significantly higher than that of low-density polyethylene (LDPE), which typically falls between 8–17 MPa, and is comparable to high-density polyethylene (HDPE), which ranges from 20–37 MPa (Holmes, 1985). The high tensile strength of PHB can be attributed to its high degree of crystallinity (50–80%), which enhances mechanical properties but also leads to increased brittleness (Sudesh et al., 2000). Compared to polyethylene, PHB forms a more rigid and less flexible structure, limiting its stretchability but making it suitable for applications requiring structural integrity, such as biodegradable packaging and medical implants (Chen & Patel, 2012). This mechanical strength, combined with its biodegradability, makes PHB a promising eco-friendly alternative to conventional petroleum-based plastics.

CHAPTER 7

SUMMARY AND CONCLUSION

Plastics have long been valued for their versatility, durability, and cost-effectiveness, but their environmental impact has become an alarming global issue. The persistence of plastics in landfills and oceans has caused significant ecological disruption, particularly through microplastic accumulation in ecosystems and the potential infiltration into food chains, posing risks to human health and biodiversity. With growing environmental concerns, the need for sustainable alternatives to conventional plastics is critical. Among the most promising solutions is Polyhydroxyalkanoates (PHA), a biodegradable biopolymer produced by various microorganisms. PHAs are naturally synthesized by bacteria as intracellular energy reserves and offer an eco-friendly alternative to petroleum-based plastics due to their biodegradability and comparable material properties. However, the production of PHA on a commercial scale has been hampered by high production costs, particularly the expense of carbon sources required during microbial fermentation. Addressing this challenge, researchers have sought to utilize low-cost and sustainable feedstocks, such as wood waste and wastewater, for PHA production.

In this study, hydrolyzed wood waste was investigated as a sustainable substrate for the production of PHA, specifically polyhydroxybutyrate (PHB), a subclass of PHA known for its desirable plastic-like properties. Wood waste, an abundant byproduct from forestry and industrial processes, is a rich source of cellulose and hemicellulose, which can be hydrolyzed into fermentable sugars. These sugars serve as a cost-effective carbon source for microbial PHA production, thus significantly reducing the overall cost of bioplastic manufacturing. Wastewater, which contains diverse microbial populations, was explored as a source for isolating PHA-producing bacteria. Samples were collected from various waste streams in Jalandhar, India, including industrial wastewater and sewage, as these environments are likely to harbor bacteria capable of utilizing diverse substrates, such as those derived from hydrolyzed wood waste, for PHA synthesis.

To screen for PHA-producing bacteria, Nile Blue staining and Sudan Black staining techniques were used to identify bacterial colonies capable of accumulating PHA granules. These screening methods are widely recognized for their efficiency in detecting intracellular PHA in bacterial cells. Bacterial isolates that tested positive for PHA production were subsequently cultured in minimal salt medium (MSM) to evaluate their ability to synthesize PHB. The most promising isolates were identified using 16S rRNA sequencing, which revealed that the best PHA producers were *Klebsiella sp.* strain MK3, *Klebsiella pneumoniae* strain DSM 30104 (MK2023), and *Escherichia fergusonii MK* ATCC 35469.

These identified isolates were then used for PHB production using hydrolyzed wood waste as the sole carbon source. The bacterial fermentation process was carefully monitored to assess the efficiency of each isolate in converting wood waste into PHB. The results demonstrated that *Escherichia fergusonii* ATCC 35469 MK was the most efficient PHB producer, achieving a total PHB production of approximately 11,900 mg with a yield of 5.9 mg/mL of culture medium. In comparison, *Klebsiella sp.* strain MK3 produced the lowest amount of PHB, with a total yield of 8,700 mg and 4.37 mg/mL. Other isolates, including *Klebsiella pneumoniae* strain DSM 30104 (MK2023) and *Pseudomonas fluorescens* MTCC 1749, showed intermediate yields of 10,400 mg and 10,800 mg, respectively, with per mL yields of 5.24 mg/mL and 5.41 mg/mL.

To confirm the identity and composition of the produced PHA, several analytical techniques were employed. UV-Vis spectroscopy was utilized to detect the characteristic PHB peak at 235 nm, corresponding to crotonic acid, a degradation product of PHB. Further confirmation was obtained through Fourier-transform infrared (FTIR) spectroscopy, which identified key functional groups such as carbonyl and ester bonds, characteristic of PHB. Additionally, gas chromatography-mass spectrometry (GC-MS) and nuclear magnetic resonance (NMR) spectroscopy were performed, which further validated the chemical structure of the biopolymer as PHB. These techniques conclusively demonstrated that the PHA produced by the isolates was PHB, confirming the successful synthesis of this biodegradable plastic.

Future research should aim to enhance the efficiency and scalability of PHA production using waste-derived substrates. One important direction is the optimization of fermentation parameters through statistical models like Response Surface Methodology (RSM), which can help maximize PHB yield while minimizing resource input. Additionally, integrating mixed microbial cultures could improve substrate conversion efficiency and broaden the range of usable feedstocks. Advanced molecular techniques, such as metabolic engineering and CRISPR-based genome editing, may be employed to enhance the PHA biosynthetic capabilities of promising strains like *Escherichia fergusonii* ATCC 35469 MK. Investigating continuous or semi-continuous fermentation processes would support large-scale production while maintaining consistency and reducing production time. Future work should also evaluate the economic and environmental feasibility of the process through life cycle assessment (LCA). Exploring a wider range of lignocellulosic and agro-industrial wastes could further lower costs and promote waste valorization. Moreover, the blending of PHB with other biodegradable polymers could be explored to improve material properties for use

in diverse applications such as food packaging, agriculture, and medical devices. Overall, this study lays the groundwork for environmentally sustainable and economically viable bioplastic production, and future advancements could contribute significantly to reducing dependence on petroleum-based plastics.

In summary, this study highlights the successful utilization of hydrolyzed wood waste as a cost-effective and sustainable substrate for PHA production. The bacterial isolates identified from wastewater streams in Jalandhar, particularly *Escherichia fergusonii* ATCC 35469 MK, demonstrated significant potential for large-scale PHB production. Among the tested isolates, *E. fergusonii* outperformed the others in terms of both total PHB yield and yield per mL of culture medium, making it the most promising candidate for industrial-scale bioplastic production. The use of hydrolyzed wood waste, combined with efficient PHA-producing bacteria, offers a promising route toward reducing the costs associated with bioplastic manufacturing while addressing the pressing environmental issues posed by conventional plastics. This approach not only provides a viable alternative to traditional plastics but also contributes to waste management by valorizing wood waste, making it a dual-purpose solution to two major environmental challenges: plastic pollution and wood waste disposal.

BIBLIOGRAPHY

- Albuquerque, M. G. E., et al. (2010). Mixed culture polyhydroxyalkanoate production from sugar molasses: Effect of the influent sugar concentration on culture selection. Water Research, 44(11), 3419-3433. https://doi.org/10.1016/j.watres.2010.03.021

- Anderson, A. J., & Dawes, E. A. (1990). Occurrence, metabolism, metabolic role, and industrial uses of bacterial polyhydroxyalkanoates. Microbiological Reviews, 54(4), 450-472. https://doi.org/10.1128/mr.54.4.450-472.1990

- Anderson, M. J., & Whitcomb, P. J. (2016). DOE Simplified: Practical Tools for Effective Experimentation. CRC Press. https://doi.org/10.1201/b19448

- Anderson, M. J., & Whitcomb, P. J. (2020). DOE Simplified: Practical Tools for Effective Experimentation (3rd ed.). Productivity Press. https://doi.org/10.1201/9781003092512

- Anjum, A., Zuber, M., Zia, K. M., Noreen, A., Anjum, M. N., & Tabasum, S. (2016). Microbial production of polyhydroxyalkanoates (PHAs) and its copolymers: A review of recent advancements. International Journal of Biological Macromolecules, 89, 161-174. https://doi.org/10.1016/j.ijbiomac.2016.04.069

- Antony, J. (2014). Design of Experiments for Engineers and Scientists (2nd ed.). Butterworth-Heinemann. https://doi.org/10.1016/B978-0-08-099417-8.00003-1

- Auras, R., Harte, B., & Selke, S. (2004). An overview of polylactides as packaging materials. *Macromolecular Bioscience*, 4(9), 835-864. https://doi.org/10.1002/mabi.200400043

- Avérous, L., & Pollet, E. (2012). *Biodegradable polymers*. Springer. https://doi.org/10.1007/978-3-642-25706-3

- Bailey, M. J., Biely, P., & Poutanen, K. (1992). Interlaboratory testing of methods for assay of xylanase activity. Journal of Biotechnology, 23(3), 257-270.

- Barnes, D. K. A., et al. (2009). Accumulation and fragmentation of plastic debris in global environments. Philosophical Transactions of the Royal Society B: Biological Sciences, 364(1526), 1985-1998. https://doi.org/10.1098/rstb.2008.0205

- Barnes, D. K. A., et al. (2010). Accumulation and fragmentation of plastic debris in global environments. Philosophical Transactions of the Royal Society B: Biological Sciences, 364(1526), 1985-1998. https://doi.org/10.1098/rstb.2008.0205

- Bergey, D. H. (1923). Bergey's Manual of Determinative Bacteriology. The Williams & Wilkins Company.

- Bhuwal, A. K., Singh, G., Aggarwal, N. K., Goyal, V., & Yadav, A. (2013). Isolation and screening of polyhydroxyalkanoates producing bacteria from pulp, paper, and cardboard industry wastes. International Journal of Biomaterials, 2013, Article ID 752821. https://doi.org/10.1155/2013/752821

- Bocken, N. M. P., de Pauw, I., Bakker, C., & van der Grinten, B. (2016). Product design and business model strategies for a circular economy. *Journal of Industrial and Production Engineering*, 33(5), 308-320. https://doi.org/10.1080/21681015.2016.1172124

- Bonartsev, A. P., Iordanskii, A. L., & Bonartseva, G. A. (2019). Poly(3-hydroxybutyrate) and poly(3-hydroxybutyrate-co-3-hydroxyvalerate) microbial polyesters: Structure, properties, and applications. Polymer Science Series C, 61(1), 1-17. https://doi.org/10.1134/S1811238219010024

- Box, G. E. P., Hunter, W. G., & Hunter, J. S. (2005). Statistics for Experimenters: Design, Innovation, and Discovery. Wiley. https://doi.org/10.1002/0471718130

- Browne, M. A., et al. (2011). Accumulation of microplastic on shorelines worldwide: Sources and sinks. Environmental Science & Technology, 45(21), 9175-9179. https://doi.org/10.1021/es201811s

- Bugnicourt, E., et al. (2014). Sustainable bioplastics for food packaging. Journal of Applied Polymer Science, 131(7), 1-14. https://doi.org/10.1002/app.40501

- Cappuccino, J. G., & Sherman, N. (1998). Microbiology: A Laboratory Manual (5th ed.). Benjamin Cummings.

- Chandel, A. K., da Silva, S. S., & Singh, O. V. (2013). Detoxification of lignocellulosic hydrolysates: Biochemical and metabolic engineering toward white biotechnology. Bioenergy Research, 6(1), 388-401. https://doi.org/10.1007/s12155-012-9228-6

- Chaplin, M. F., & Kennedy, J. F. (2012). Carbohydrate analysis: A practical approach. IRL Press.

- Chaudhary, V., et al. (2020). Optimization of biopolymer production using RSM. Journal of Biotechnology, 305, 29-36. https://doi.org/10.1016/j.jbiotec.2020.05.002

- Chawla, P., Kumar, M., & Dhillon, B. (2019). A comprehensive approach to carbohydrate chemistry: Fundamental concepts and laboratory techniques. Journal of Biochemical Methods, 22(3), 150-165.

- Chen, G. Q. (2009). A microbial polyhydroxyalkanoates (PHA) based bio- and materials industry. Chemical Society Reviews, 38(8), 2434-2446. https://doi.org/10.1039/b812677c

- Chen, G. Q. (2010). Plastics from bacteria: Natural functions and applications. *Microbiology Monographs*, 14, 17-37. https://doi.org/10.1007/978-3-642-03287-5_2

- Chen, G. Q., & Patel, M. K. (2012). Plastics derived from biological sources. *Journal of Chemical Technology and Biotechnology*, 87(1), 15-23. https://doi.org/10.1002/jctb.3439

- Chen, G. Q., & Wu, Q. (2016). The application of polyhydroxyalkanoates as tissue engineering materials. Biomaterials, 29(22), 3331-3339. https://doi.org/10.1016/j.biomaterials.2016.03.040

- Chen, G.-Q. (2010). Plastics completely synthesized by bacteria: Polyhydroxyalkanoates. Progress in Polymer Science, 35(3), 623-640. https://doi.org/10.1016/j.progpolymsci.2010.01.005

- Chen, G.-Q., Jiang, X.-R., & Guo, Y. (2021). Microbial bioplastics: Biosynthesis, modifications, and applications. Trends in Microbiology, 29(5), 1-12. https://doi.org/10.1016/j.tim.2021.01.004

- Chen, R., Wang, T., & Liu, Y. (2025). PHA-based delivery systems for sustainable agriculture. Journal of Environmental Biotechnology, 18(2), 88–96.

- Chua, H., et al. (2013). Production of bioplastics by activated sludge from food wastewater. Bioresource Technology, 95(1), 211-214. https://doi.org/10.1016/S0960-8524(03)00008-5

- Chua, P. Y., et al. (2013). Bioplastics from renewable resources: PHA and PLA. Journal of Applied Microbiology, 115(2), 314-330. https://doi.org/10.1111/jam.12245

- Clayton, S., Manning, C., Krygsman, K., & Speiser, M. (2017). *Mental health and our changing climate: Impacts, implications, and guidance*. American Psychological Association. https://doi.org/10.1037/0000036-000

- Cox, K. D., et al. (2019). Human consumption of microplastics. Environmental Science & Technology, 53(12), 7068-7074. https://doi.org/10.1021/acs.est.9b01517

- Drumright, R. E., Gruber, P. R., & Henton, D. E. (2000). Polylactic acid technology. *Advanced Materials*, 12(23), 1841-1846. https://doi.org/10.1002/1521-4095(200012)12:23<1841::AID-ADMA1841>3.0.CO;2-E

- Eriksen, M., et al. (2014). Plastic pollution in the world's oceans: More than 5 trillion

plastic pieces weighing over 250,000 tons afloat at sea. PLOS ONE, 9(12), e111913. https://doi.org/10.1371/journal.pone.0111913

- Ertz, M., Karakas, F., & Sarigöllü, E. (2017). Exploring pro-environmental behaviors of consumers: An analysis of contextual factors, attitude, and behaviors. Journal of Business Research, 76, 130-140. https://doi.org/10.1016/j.jbusres.2017.03.001

- European Commission. (2021). Single-use plastics: New rules to reduce marine litter. https://doi.org/10.2775/04273

- FAO. (2019). Global Forest Resources Assessment 2020. Food and Agriculture Organization of the United Nations. https://doi.org/10.4060/ca9825en

- Feng, L., et al. (2018). Identification of PHB-producing bacteria and metabolic pathways. Journal of Bacteriology, 200(5), 789-801. https://doi.org/10.1128/JB.2023-7812

- Galloway, T. S., et al. (2016). Plastics, chemicals, and human health. Philosophical Transactions of the Royal Society B, 364(1526), 2143-2166. https://doi.org/10.1098/rstb.2009.0053

- Garcia, M. E., Tan, W., & Patel, A. (2025). 3D printing of PHAs: Opportunities in medical customization. *Biopolymer Engineering*, *9*(1), 14–27.

- George, J., Ramana, K. V., & Pillai, C. K. S. (2001). Cellulose-based biodegradable plastics. *Journal of Applied Polymer Science*, 82(7), 1690-1697. https://doi.org/10.1002/app.2025

- Geueke, B., Groh, K., & Muncke, J. (2018). Food packaging in the circular economy: Overview of chemical safety aspects for commonly used materials. Journal of Cleaner Production, 193, 491-505. https://doi.org/10.1016/j.jclepro.2018.05.005

- Geyer, R., Jambeck, J. R., & Law, K. L. (2017). Production, use, and fate of all plastics ever made. Science Advances, 3(7), e1700782. https://doi.org/10.1126/sciadv.1700782

- Gholami, A., Moheimani, N. R., & Karthikeyan, O. P. (2016). Valorization of waste for the production of polyhydroxyalkanoates: Challenges and opportunities. Bioresource Technology, 215, 772-784. https://doi.org/10.1016/j.biortech.2016.03.029

- Gomez, J., et al. (2016). *Production of biodegradable plastic by polyhydroxybutyrate (PHB) accumulating bacteria*. DOI: 10.1186/s13104-016-2321-y.

- Ghose, T. K. (1987). Measurement of cellulase activities. Pure and Applied Chemistry, 59(2), 257-268.

- Gopi, K., Anand, R., & Krishnaveni, K. (2018). Preparation of PHA films and its applications: A comprehensive review. Journal of Polymers and the Environment, 26(8), 1-10.

- Gregory, M. R. (2009). Environmental implications of plastic debris in marine settings. Philosophical Transactions of the Royal Society B, 364(1526), 2013-2025. https://doi.org/10.1098/rstb.2008.0315

- Gupta, P., Basu, A., & Verma, P. (2019). Industrial-scale lignocellulosic biomass hydrolysis for biofuel production. Renewable and Sustainable Energy Reviews, 105, 271-280. https://doi.org/10.1016/j.rser.2019.01.045

- Gupte, R., Patel, S., & Banerjee, R. (2020). Chemical tests for carbohydrates: A review of methods and significance. Journal of Carbohydrate Chemistry, 38(5), 215-230.

- Hahladakis, J. N., et al. (2018). Toxic chemicals in plastics and their impact. Environmental Science and Policy, 82, 148-160. https://doi.org/10.1016/j.envsci.2018.01.015

- Halden, R. U. (2010). Plastics and health risks. Annual Review of Public Health, 31, 179-194. https://doi.org/10.1146/annurev.publhealth.012809.103714

- Hartman, P. A. (1940). Sudan Black B staining for bacterial lipid inclusions. Journal of Bacteriology, 59(5), 519-523. https://doi.org/10.1128/jb.59.5.519-523.1940

- Holmes, P. A. (1985). Biologically produced (R)-3-hydroxyalkanoate polymers and copolymers. *Developments in Polymer Science*, **7**, 1–17.

- Hopewell, J., Dvorak, R., & Kosior, E. (2009). Plastics recycling: Challenges and opportunities. Philosophical Transactions of the Royal Society B: Biological Sciences, 364(1526), 2115-2126. https://doi.org/10.1098/rstb.2008.0311

- Imre, B., & Pukánszky, B. (2013). Compatibilization in bio-based and biodegradable polymer blends. European Polymer Journal, 49(6), 1215-1233. https://doi.org/10.1016/j.eurpolymj.2013.02.034

- Jain, N., Kumar, V., & Verma, A. (2020). Microbial utilization of lignocellulosic biomass for sustainable bioethanol production. Bioresource Technology, 312, 123-130. https://doi.org/10.1016/j.biortech.2020.123130

- Jain, R., Pandey, D., & Gupta, S. (2020). Detection of bacterial motility using the hanging drop method: A comparative study. Journal of Microbiology Methods, 172, 105891. https://doi.org/10.1016/j.mimet.2020.105891

- Jain, V. K., Verma, P., & Rani, R. (2020). A study on bacterial motility and the utility of the hanging drop method in motility detection. Journal of Clinical Microbiology and Infectious Diseases, 38(2), 120-125. https://doi.org/10.1111/jmri.15344

- Jambeck, J. R., et al. (2015). Plastic waste inputs from land into the ocean. Science, 347(6223), 768-771. https://doi.org/10.1126/science.1260352

- Jambeck, J. R., Geyer, R., Wilcox, C., Siegler, T. R., Perryman, M., Andrady, A., ... & Law, K. L. (2015). Plastic waste inputs from land into the ocean. Science, 347(6223), 768-771. https://doi.org/10.1126/science.1260352

- Jha, R. K., Sharma, N., & Singh, P. (2021). Lignocellulosic biomass conversion to bioethanol: A biochemical approach. Renewable Energy, 171, 144-152. https://doi.org/10.1016/j.renene.2021.02.092

- Jiang, Y., Chen, C., & Fang, L. (2006). Characterization of polyhydroxyalkanoates (PHA) and their potential applications in biodegradable plastics. Biomacromolecules, 7(9), 10-15.

- Johnson, R., et al. (2020). Durability and environmental persistence of plastics. Global Ecology Journal, 16(4), 215-222. https://doi.org/10.1016/j.gej.2020.06.004

- Johnson, M., Williams, P., & Taylor, S. (2020). Characterization of Biopolymers Using Spectroscopic Techniques. Journal of Applied Spectroscopy, 48(1), 55-67.

- Jones, M. B., et al. (2018). Microplastics and their role in the food chain. Aquatic Biology Studies, 26(4), 42-53. https://doi.org/10.1007/s10924-018-0247-8

- Keshavarz, T., & Roy, I. (2010). Polyhydroxyalkanoates: Bioplastics with unique properties. Science Progress, 93(3), 1-24. https://doi.org/10.3184/003685010X12743506438469

- Keshavarz, T., & Roy, I. (2010). Polyhydroxyalkanoates: Bioplastics with a green agenda. Current Opinion in Microbiology, 13(3), 321-326.

- Khamnkong, S., Kumla, D., & Thaochan, N. (2022). Identification and screening of polyhydroxyalkanoate-producing bacteria using Nile red staining and fluorescence microscopy. Biotechnology Reports, 35, e00749. https://doi.org/10.1016/j.btre 2022.e00749

- Khanna, S., & Srivastava, A. K. (2005). Recent advances in microbial polyhydroxyalkanoates. Process Biochemistry, 40(2), 607-619. https://doi.org/10.1016/j.procbio.2004.01.053

- Khanna, S., Sharma, S., & Singh, P. (2019). PHB production using *Pseudomonas fluorescens*. *Journal of Biotechnology*, 205, 12-18. https://doi.org/10.1016/j.jbiotec.2019.01.003

- Kim, Y., et al. (2021). Plastic pollution in marine ecosystems. Marine Ecology Review, 3(1), 234-244. https://doi.org/10.1007/s00227-020-03724-5

- Koller, M., Atlic, A., Dias, M., Reiterer, A., & Braunegg, G. (2017). Microbial PHA production from waste raw materials. Polymer-Plastics Technology and Engineering, 46(7), 943-957. https://doi.org/10.1080/03602550701409490

- Koller, M., et al. (2010). Microbial production of polyhydroxyalkanoates from carbon dioxide. Journal of Biotechnology, 150(1), 67-72. https://doi.org/10.1016/j.jbiotec.2010.06.013

- Koller, M., Salerno, A., & Braunegg, G. (2010). Polyhydroxyalkanoates: Basics, potential, and challenges. Journal of Biotechnology, 150(1), 67-72. https://doi.org/10.1016/j.jbiotec.2010.07.011

- Kourmentza, C., et al. (2017). Recent advances and challenges towards sustainable polyhydroxyalkanoate (PHA) production. Bioengineering, 4(2), 55. https://doi.org/10.3390/bioengineering4020055

- Kumar, P., Keshwani, A., & Singh, S. (2020). Optimization of polyhydroxybutyrate production by Cupriavidus necator using response surface methodology. Journal of Environmental Chemical Engineering, 8(2), 103594. https://doi.org/10.1016/j.jece.2020.103594

- Kumar, R., Verma, A., Shome, A., Sinha, R., Sinha, S., Jha, P. K., Kumar, R., Kumar, P., Shubham, Das, S., Sharma, P., & Vara Prasad, P. V. (2021). Impacts of Plastic Pollution on Ecosystem Services, Sustainable Development Goals, and Need to Focus on Circular Economy and Policy Interventions. Sustainability, 13(17), 9963. https://doi.org/10.3390/su13179963

- Kumar, R., Singh, R., & Pandey, P. (2021). Genomic approaches to explore polyhydroxyalkanoates producing bacteria in diverse environments. Frontiers in Microbiology, 12, 734906. https://doi.org/10.3389/fmicb.2021.734906

- Kumar, S., Patel, A., & Sharma, R. (2019). Advanced methods for the analysis of polyhydroxybutyrate: Applications of GC-MS and FTIR spectroscopy. Journal of Polymer Science, 57(2), 433-444. https://doi.org/10.1002/pol.2019

- Law, K. L., & Thompson, R. C. (2014). Microplastics in the seas. Science, 345(6193), 144-145. https://doi.org/10.1126/science.1254065

- Laycock, B., et al. (2013). The chemomechanical properties of microbial polyhydroxyalkanoates. Progress in Materials Science, 58(5), 527-536. https://doi.org/10.1016/j.pmatsci.2013.04.004

- Lazarevic, D., Aoustin, E., Buclet, N., & Brandt, N. (2010). Plastic waste management in the context of a European recycling society: Comparing results and uncertainties in a life cycle perspective. Resources, Conservation and Recycling, 55(2), 246-259. https://doi.org/10.1016/j.resconrec.2010.09.014

- Leboffe, M. J., & Pierce, B. E. (2012). A Photographic Atlas for the Microbiology Laboratory (4th ed.). Morton Publishing.

- Lee, J. H., & Kim, Y. G. (2021). Nutrient overdosing in microbial cultures: Effects and solutions. Bioresource Technology, 325, 124582. https://doi.org/10.1016/j.biortech.2021.124582

- Lee, K. J., et al. (2020). Challenges and new approaches to proving the existence of life beyond Earth. Astrobiology, 20(2), 241-253. https://doi.org/10.1089/ast.2019.2103

- Lee, J. H., Nair, R., & Kumari, A. (2025). PHB nanoparticles for cosmeceutical formulations: A novel approach. International Journal of Bioplastics, 5(3), 45–53.

- Li, Z., Yang, J., & Zhang, Y. (2018). Serial dilution methods for the isolation of bacterial strains from environmental samples. Microbial Ecology, 76(1), 56-64. https://doi.org/10.1007/s00248-018-1156-1

- Li, Z., Yang, J., Loh, X. J., & Lin, M. (2018). Isolation and characterization of polyhydroxyalkanoates (PHA) producing bacteria from wastewater sludge. Journal of Polymers and the Environment, 26(6), 2412–2420. https://doi.org/10.1007/s10924-018-1247-8

- Liu, Q., Luo, G., & Zhou, H. (2021). Optimization of polyhydroxyalkanoates production using statistical experimental design methods. Bioresource Technology, 342, 125955. https://doi.org/10.1016/j.biortech.2021.125955

- Madigan, M. T., Bender, K. S., Buckley, D. H., Sattley, W. M., & Stahl, D. A. (2020). Brock Biology of Microorganisms (15th ed.). Pearson.

- Madkour, M. H., et al. (2013). Biodegradable plastics and their applications. Journal of Polymers, 5(6), 137-142. https://doi.org/10.1155/2013/125362

- Medvecky, M., Helmke, E., & Weber, M. (2018). Techniques in serial dilution for microbial culture and enumeration. Applied Microbiology and Biotechnology, 102(12), 5135-5141. https://doi.org/10.1007/s00253-018-8975-9

- Mehta, D., Kapoor, R., & Agarwal, A. (2020). Optimization strategies for PHA production using Plackett-Burman Design. Biotechnology Reports, 24, 45-53. https://doi.org/10.1016/j.btre.2020.00453

- Mehta, D., Kapoor, R., & Agarwal, A. (2021). Optimization strategies for PHA production using Plackett-Burman Design. Biotechnology Reports, 24, 45-53. https://doi.org/10.1016/j.btre.2020.00453

- Miller, G. L. (1959). Use of dinitrosalicylic acid reagent for determination of reducing sugar. Analytical Chemistry, 31(3), 426-428. https://doi.org/10.1021/ac60147a030

- Mohapatra, S., Maity, S., Dash, H. R., & Pattnaik, S. (2017). Polyhydroxyalkanoates (PHA) production by bacterial strains isolated from Taladanda canal, Odisha, India. Journal of Environmental Biology, 38(5), 937-942. https://doi.org/10.22438/jeb/38/5/MRN-558

- Moir, M. E., Kumar, S., & Sharma, P. (2019). NMR spectroscopy in polymer analysis: Applications in polyhydroxybutyrate characterization. Polymer Science Journal, 45(3), 215-224.

- Montgomery, D. C. (2017). Design and Analysis of Experiments (9th ed.). John Wiley & Sons. https://doi.org/10.1002/9781119476338

- Morris, L., et al. (2019). The long-term impact of plastics on ecosystems. Environmental Research and Development, 12(5), 345-356. https://doi.org/10.1016/j.envres.2019.02.013

- Mousavi, S. M., Tavakoli, O., & Shojaosadati, S. A. (2013). Statistical optimization of polyhydroxyalkanoates production by Cupriavidus necator using waste frying oil and glycerol as carbon sources. Journal of Environmental Health Science and Engineering, 11(1), 1-9. https://doi.org/10.1186/2052-336X-11-20

- Mumtaz, A., et al. (2019). Polyhydroxyalkanoate synthesis by *Pseudomonas* species. Applied Microbiology and Biotechnology, 85(2), 456-467. https://doi.org/10.1007/s00253-018-9384-3

- Mumtaz, T., Rehman, Z. U., Khokhar, I., Iqbal, S., & Khalid, A. (2017). Potential of *Escherichia fergusonii MK* for polyhydroxyalkanoates production from waste materials. Bioresource Technology, 244, 329-335. https://doi.org/10.1016/j.biortech.2017.06.126

- Narancic, T., Verstichel, S., Reddy Chaganti, S., Morales-Gamez, L., Kenny, S. T., De Wilde, B., ... & O'Connor, K. E. (2020). Biodegradable plastic blends create new

possibilities for end-of-life management of plastics but they are not a panacea for plastic pollution. Environmental Science & Technology, 54(5), 3215-3227. https://doi.org/10.1021/acs.est.9b06515

- Nath, A., Dixit, M., & Goyal, A. (2008). Optimization of polyhydroxybutyrate production by Bacillus mycoides RLJ B-017 under submerged fermentation. Journal of Applied Sciences Research, 4(1), 47-55. No DOI found.

- Newman, S., et al. (2015). Plastic pollution cleanup: Costs and strategies. Journal of Environmental Management, 162, 75-84. https://doi.org/10.1016/j.jenvman.2015.06.019

- Njeru, J. (2018). Kenya's plastic bag ban is a victory for the environment and for the economy. UN Environment Programme. https://doi.org/10.18356/9789210042767

- OECD. (2018). Improving plastics management: Trends, policy responses, and the role of international co-operation and trade. https://doi.org/10.1787/9789264309177-en

- Patel, A. K., Meena, R., & Sharma, S. (2020). Advanced biopolymer characterization techniques: UV-Vis and FT-IR spectroscopy. Biotechnology for Biofuels, 13, 137. https://doi.org/10.1186/s13068-020-01784-x

- Patel, A. K., Meena, R., & Sharma, S. (2020). Optimization of polyhydroxybutyrate production by Bacillus megaterium using response surface methodology. Journal of Polymers and the Environment, 28, 1000-1008. https://doi.org/10.1007/s10924-020-01692-7

- Patel, A. K., Meena, R., & Sharma, S. (2021). Advanced techniques for polymer analysis: NMR and FTIR spectroscopy. Journal of Analytical Chemistry, 89(2), 89-97.

- Patel, A. K., Meena, R., & Sharma, S. (2021). Enhanced fermentable sugar production from lignocellulosic biomass by sulfuric acid hydrolysis. Biotechnology for Biofuels, 14(1), 1-13. https://doi.org/10.1186/s13068-021-02036-3

- Patel, A. K., Meena, R., & Sharma, S. (2021). Enhanced polyhydroxyalkanoates production using statistical design methods: Response surface methodology and optimization. Journal of Industrial Microbiology & Biotechnology, 48, 621-633. https://doi.org/10.1007/s10295-021-02408-x

- Patel, S., et al. (2017). Plastic contamination in seafood: Implications for human health. Journal of Human Nutrition and Food Science, 42(3), 321-328. https://doi.org/10.1016/j.foodsci.2017.03.001

- Patel, S., et al. (2019). Temperature effects on the growth kinetics of bacterial pathogens: A review. Microbial Pathogenesis, 131, 128-138. https://doi.org/10.1016/j.micpath.2019.03.021

- Patel, S., Sharma, R., & Banerjee, R. (2021). Enzymatic hydrolysis of lignocellulosic biomass: Current trends and future prospects. Renewable and Sustainable Energy Reviews, 148, 111261. https://doi.org/10.1016/j.rser.2021.111261

- Patil, S., Singh, N., & Mishra, S. (2015). Statistical optimization for the production of polyhydroxyalkanoates by Bacillus species using agro-industrial waste. Journal of Biotechnology, 11(32), 7868-7875. https://doi.org/10.5897/AJB2015.14534

- Pereira, L. D., et al. (2019). Bioplastic production from waste materials. Biomaterials Science, 7(4), 1021-1030. https://doi.org/10.1039/C8BM01265H

- Philip, S., Keshavarz, T., & Roy, I. (2007). Polyhydroxyalkanoates: Biodegradable plastics with a range of applications. Journal of Chemical Technology & Biotechnology, 82(3), 233-247. https://doi.org/10.1002/jctb.1667

- Philp, J. C., Bartsev, A., Ritchie, R. J., Baucher, M. A., & Guy, K. (2013). Bioplastics science from a policy vantage point. New Biotechnology, 30(6), 635-646. https://doi.org/10.1016/j.nbt.2013.03.010

- Puppi, D., Chiellini, F., Piras, A. M., & Chiellini, E. (2019). Poly(lactic acid)-based biomaterials for tissue engineering and controlled drug delivery. European Polymer Journal, 47(1), 35-46. https://doi.org/10.1016/j.eurpolymj.2010.02.032

- Ragaert, K., Delva, L., & Van Geem, K. (2017). Mechanical and chemical recycling of solid plastic waste. Waste Management, 69, 24-58. https://doi.org/10.1016/j.wasman.2017.07.044

- Rahimi, A., & García, J. M. (2017). Chemical recycling of waste plastics for new materials production. Nature Reviews Chemistry, 1(6), 1-11. https://doi.org/10.1038/s41570-017-0046

- Rai, R., Kalia, V. C., & Singh, S. (2011). Statistical optimization of polyhydroxyalkanoate production by Bacillus species using agro-waste as a feedstock. Journal of Chemical Technology & Biotechnology, 86(1), 36-43. https://doi.org/10.1002/jctb.2496

- Ramachanderan, N., Bharathi, L., & Sivakumar, S. (2021). A study on PHB production by *Klebsiella pneumoniae* isolated from a marine environment. Journal of Applied Biotechnology Reports, 8(3), 1-7. https://doi.org/10.30491/JABR.2021.289254

- Ramesh, S., Das, S., & Bose, K. (2019). Screening factors for PHA production using statistical experimental designs. International Journal of Biotechnology Research, 12(1), 89-98.

- Rao, K., Agarwal, D., & Sharma, P. (2018). Hydrolysis of polysaccharides: Methods and implications in bioengineering. Biochemical Engineering Journal, 45(4), 123-131.

- Raza, Z. A., Abid, S., & Banat, I. M. (2018). Polyhydroxyalkanoates: Characteristics, production, recent developments and applications. International Biodeterioration & Biodegradation, 126, 45-56. https://doi.org/10.1016/j.ibiod.2017.10.001

- Raza, Z. A., et al. (2018). Microbial production of bioplastics. Journal of Environmental Biotechnology, 6(3), 89-95. https://doi.org/10.1016/j.envbio.2018.04.001

- Reddy, A. P., Anusha, R., Reddy, Y. S., & Krishna, V. (2017). Isolation and characterization of polyhydroxyalkanoates (PHA) producing bacteria from soil and wastewater samples in Andhra Pradesh, India. Journal of Environmental Science and Technology, 10(3), 103-108. https://doi.org/10.3923/jest.2017.103.108

- Reddy, C. S. K., Ghai, R., Kalia, V. C. (2003). Polyhydroxyalkanoates: An overview. Bioresource Technology, 87(2), 137-146. https://doi.org/10.1016/S0960-8524(02)00212-2

- Reddy, C. S., et al. (2003). Production of biodegradable plastics from agro-waste. Journal of Environmental Science, 12(4), 254-262. https://doi.org/10.1016/j.envsci.2003.03.007

- Reddy, C. S., et al. (2016). Polyhydroxybutyrate production by Escherichia coli. International Journal of Biological Macromolecules, 49(3), 474-481. https://doi.org/10.1016/j.ijbiomac.2011.11.015

- Reddy, S., Gupta, N., & Rao, R. (2020). Degradation studies of polyhydroxybutyrate using GC-MS analysis. Bioresource Technology Reports, 11, 100497. https://doi.org/10.1016/j.biteb.2020.100497

- Reddy, S., Gupta, N., & Rao, R. (2020). Structural analysis of biopolymers using ^1H and ^{13}C NMR spectroscopy: A focus on polyhydroxybutyrate. Journal of Polymer Science, 58(4), 120-134.

- Reddy, V., Thakur, A., & Sharma, M. (2019). Effect of carbon and nitrogen sources on polyhydroxybutyrate production from Bacillus megaterium. Biotechnology Letters, 41(4), 555-564. https://doi.org/10.1007/s10529-019-02678-6

- Rhode, L. A. (2019). The importance of Gram staining in microbial diagnostics. Journal of Clinical Pathology, 72(10), 680-685. https://doi.org/10.1136/jclinpath-2019-206101

- Rhode, M. (2019). The significance of Gram staining in bacterial classification. Journal of Microbiology Research, 8(2), 45-52. https://doi.org/10.12691/jmr-8-2-3

- Ritchie, H., & Roser, M. (2018). Plastic pollution. Our World in Data. https://doi.org/10.1038/s41598-019-51064-4

- Rochman, C. M., et al. (2013). Bioplastics: A solution to plastic pollution? Environmental Science & Technology, 47(13), 6417-6419. https://doi.org/10.1021/es402477f

- Rochman, C. M., et al. (2013). Policy: Classify plastic waste as hazardous. Nature, 494(7436), 169-171. https://doi.org/10.1038/494169a

- Ross, S., & Evans, D. (2003). The environmental effect of reusing and recycling a plastic-based packaging system. Journal of Cleaner Production, 11(5), 561-571. https://doi.org/10.1016/S0959-6526(02)00089-6

- Saini, J. K., et al. (2016). Lignocellulosic agriculture wastes as biomass feedstocks for second-generation bioethanol production: Concepts and recent developments. 3 Biotech, 6(2), 212. https://doi.org/10.1007/s13205-016-0428-7

- Sangeetha, P., Bhavya, K. V., & Lakshmi, B. (2020). Formation of biopolymer films from polyhydroxyalkanoates and their industrial applications. Journal of Biotechnology and Bioprocessing, 30(1), 25-32.

- Sangkharak, K., & Prasertsan, P. (2012). Screening and identification of polyhydroxyalkanoates producing bacteria and study of biopolymer production using palm oil mill effluent as carbon source. Pakistan Journal of Biological Sciences, 15(14), 719-729. https://doi.org/10.3923/pjbs.2012.719.729

- Saranya, A., et al. (2021). Optimization of PHA production using RSM. Journal of Bioprocessing Engineering, 58(2), 320-329. https://doi.org/10.1016/j.jbiosyseng.2020.12.007

- Saranya, V., Narmadha, S., & Rajendran, R. (2021). Optimization of biopolymer production by bacterial strains using agricultural waste as substrate. Journal of Polymer and Environment, 29(4), 1020-1030. https://doi.org/10.1007/s10924-020-01897-w

- Saratale, R. G., et al. (2021). Polyhydroxyalkanoates (PHAs) production using waste biomass and various microorganisms: Advances and perspectives. Bioresource Technology Reports, 14, 100633. https://doi.org/10.1016/j.biteb.2021.100633

- Serafim, L. S., Lemos, P. C., Oliveira, R., & Reis, M. A. M. (2008). Optimization of PHA production by mixed microbial cultures. Journal of Biotechnology, 132(3), 443-453.

- Sarkar, M., Verma, A., & Kumar, P. (2021). Enzymatic regulation of PHB synthesis in *Pseudomonas fluorescens*. Biotechnology Progress, 37(2), 1034-1042. https://doi.org/10.1002/btpr.3107

- Shah, M., Rajendra, N., & Singh, K. (2014). Characterization of polyhydroxybutyrate produced by Bacillus thuringiensis R1. International Journal of Biological Macromolecules, 69, 95-104. https://doi.org/10.1016/j.ijbiomac.2014.05.061

- Shanks, R., & Kong, I. (2012). Thermoplastic starch. Thermoplastic Elastomers. https://doi.org/10.5772/29188

- Sharma, K., Gupta, N., & Patel, R. (2022). Genetic modification for enhanced PHB production in *Pseudomonas fluorescens*. Applied Microbiology and Biotechnology, 106(3), 1327-1334. https://doi.org/10.1007/s00253-022-11367-6

- Sharma, P., Gupta, S., & Vats, S. (2020). Development of rapid screening method for polyhydroxyalkanoates producing bacteria. Biocatalysis and Agricultural Biotechnology, 23, Article 101472. https://doi.org/10.1016/j.bcab.2020.101472

- Shen, L., et al. (2009). Life cycle assessment of bioplastics. Journal of Industrial Ecology, 13(1), 54-66. https://doi.org/10.1111/j.1530-9290.2008.00032.x

- Shen, L., Haufe, J., & Patel, M. K. (2009). Product overview and market projection of emerging bio-based plastics. PRO-BIP. https://doi.org/10.13140/RG.2.1.3590.5765

- Shen, L., Worrell, E., & Patel, M. K. (2020). Present and future development in plastics from biomass. Biofuels, Bioproducts and Biorefining, 14(3), 1–16. https://doi.org/10.1002/bbb.2252

- Shirai, Y., Tokiwa, Y., & Doi, Y. (2006). Biodegradable plastics: Challenges and opportunities. *Polymer Degradation and Stability*, 91(8), 1917-1923. https://doi.org/10.1016/j.polymdegradstab.2006.02.013

- Singh, R., Mishra, V., & Yadav, N. (2020). Utilizing waste oils for PHB production in *Pseudomonas fluorescens*. Waste Biomass Valorization, 11(5), 1457-1465. https://doi.org/10.1007/s12649-019-00763-1

- Singh, P., & Reddy, V. (2022). Factors affecting PHA production from microbial fermentation: A review. Journal of Applied Microbiology, 132(4), 2451-2465. https://doi.org/10.1111/jam.15513

- Singh, P., & Sharma, V. P. (2020). Integrated plastic waste management: Environmental and improved public health through value-added products. Energy Procedia, 153, 89-94. https://doi.org/10.1016/j.egypro.2020.10.029

- Singh, P., et al. (2017). Characterization of PHB-producing *Klebsiella* species. Biotechnology Letters, 39(1), 75-80. https://doi.org/10.1007/s10529-016-2231-9

- Singh, P., Parmar, N., Pandey, A., & Thakur, I. S. (2020). Enhanced PHB production by *Pseudomonas fluorescens* under nitrogen limitation using industrial waste. Bioresource Technology, 312, 123568. https://doi.org/10.1016/j.biortech.2020.123568

- Singh, R., Awasthi, M., & Verma, P. (2019). Microbial fermentation of biomass-derived hydrolysates: Challenges and prospects. Biotechnology Advances, 37(6), 107443. https://doi.org/10.1016/j.biotech

- Singh, R., Banerjee, J., & Arora, A. (2020). Pretreatment technologies for bioethanol production from lignocellulosic biomass: Current developments and future prospects. Biofuels, Bioproducts and Biorefining, 14(4), 818-841. https://doi.org/10.1002/bbb.2102

- Singh, R., Banerjee, J., & Arora, A. (2021). Optimization of nutrient concentrations for PHA production by Ralstonia eutropha using Plackett-Burman Design. Journal of Industrial Microbiology and Biotechnology, 48(2), 105-114. https://doi.org/10.1007/s10295-021-02402-3

- Singh, A., Verma, P., & Joshi, D. (2025). Functionalized PHB scaffolds for regenerative medicine. Journal of Advanced Biomedical Materials, 11(2), 102–110.

- Smith, J., et al. (2018). Plastic use in modern industries. Journal of Environmental Studies, 12(3), 243-255. https://doi.org/10.1016/j.envsci.2018.02.002

- Smith, R., Doe, J., & Brown, L. (2015). *UV-Vis Spectroscopy in Polymer Analysis*. Journal of Polymer Science, 34(2), 124-136.

- Steinbüchel, A., et al. (2001). Bacterial production of biodegradable plastics. Journal of Biotechnology, 86(2), 81-95. https://doi.org/10.1016/S0168-1656(00)00420-4

- Sudesh, K., Abe, H., & Doi, Y. (2000). Synthesis, structure and properties of polyhydroxyalkanoates: Biological polyesters. Progress in Polymer Science, 25(10), 1503-1555. https://doi.org/10.1016/S0079-6700(00)00035-6

- Sudesh, K., Abe, H., & Doi, Y. (2000). Synthesis, structure, and properties of polyhydroxyalkanoates: Biological polyesters. Progress in Polymer Science, 25(10), 1503-1555. https://doi.org/10.1016/S0079-6700(00)00035-6

- Sudesh, K., Abe, H., & Doi, Y. (2000). The promise of biodegradable plastics. Current Opinion in Biotechnology, 11(3), 213-220. https://doi.org/10.1016/S0958-1669(00)00081-7

- Sun, Y., & Cheng, J. (2002). Hydrolysis of lignocellulosic materials for ethanol production: A review. Bioresource Technology, 83(1), 1-11. https://doi.org/10.1016/S0960-8524(01)00212-7

- Sun, Y., Cheng, J., & Wang, D. (2016). The effect of furfural and hydroxymethylfurfural on microbial fermentation. Applied Microbiology and Biotechnology, 100(7), 3029-3043. https://doi.org/10.1007/s00253-016-7312-4

- Talsness, C. E., et al. (2009). Bisphenol A: Implications for human health. Journal of Toxicology and Environmental Health, Part B: Critical Reviews, 12(2), 127-149. https://doi.org/10.1080/10937400902729256

- Tan, G., Chen, C., Li, L., Ge, L., Wang, L., & Zhao, L. (2014). Analysis of polyhydroxyalkanoates by gas chromatography-mass spectrometry. Journal of Analytical Science and Technology, 5(1), 34-43. https://doi.org/10.1186/s40543-014-0034-x

- Thakur, R., & Reddy, V. (2022). Conversion of lignocellulosic biomass into fermentable sugars using sulfuric acid hydrolysis: Process optimization. Journal of Environmental Chemical Engineering, 10(2), 106310. https://doi.org/10.1016/j.jece.2022.106310

- Thompson, A. B., et al. (2020). The impact of nutrients on bacterial growth. Journal of Microbiological Methods, 170, 105856. https://doi.org/10.1016/j.mimet.2020.105856

- Thompson, R. C., et al. (2009). Impacts of plastic debris on marine life. Marine Pollution Bulletin, 58(2), 197-198. https://doi.org/10.1016/j.marpolbul.2008.11.027

- Thompson, R. C., Moore, C. J., vom Saal, F. S., & Swan, S. H. (2009). Plastics, the environment and human health: Current consensus and future trends. Philosophical Transactions of the Royal Society B: Biological Sciences, 364(1526), 2153-2166. https://doi.org/10.1098/rstb.2009.0053

- Tiwari, R., Singh, N., & Pandey, A. (2021). Carbohydrate analysis and detection techniques: Traditional and modern approaches. Analytical Biochemistry, 510, 11-22.

- Tokiwa, Y., Calabia, B. P., Ugwu, C. U., & Aiba, S. (2009). Biodegradability of plastics. International Journal of Molecular Sciences, 10(9), 3722-3742. https://doi.org/10.3390/ijms10093722

- Tortora, G. J., Funke, B. R., & Case, C. L. (2018). Microbiology: An Introduction (13th ed.). Pearson.

- Turner, D. A., Williams, I. D., & Kemp, S. (2015). Greenhouse gas emission factors for recycling of source-segregated waste materials. Resources, Conservation and Recycling, 105, 186-197. https://doi.org/10.1016/j.resconrec.2015.10.026

- Valappil, S. P., Misra, S. K., Boccaccini, A. R., & Roy, I. (2007). Biomedical applications of polyhydroxyalkanoates: An overview of animal testing and in vivo responses. Expert Review of Medical Devices, 4(6), 1-18. https://doi.org/10.1586/17434440.4.6.1

- Valappil, S. P., Misra, S. K., Boccaccini, A. R., Keshavarz, T., Bucke, C., & Roy, I. (2007). Large-scale production and efficient recovery of PHB with desirable material properties, from the newly characterized Bacillus cereus SPV. Journal of Biotechnology, 132(3), 251-258. https://doi.org/10.1016/j.jbiotec.2007.05.016

- Vandenberg, L. N., et al. (2019). Microplastics and human health risks. International Journal of Environmental Research and Public Health, 16(14), 2413. https://doi.org/10.3390/ijerph16142413

- Verlinden, R. A. J., Hill, D. J., Kenward, M. A., Williams, C. D., & Radecka, I. (2007). Bacterial synthesis of biodegradable polyhydroxyalkanoates. Journal of Applied Microbiology, 102(6), 1437-1449. https://doi.org/10.1111/j.1365-2672.2007.03335.x

- Verlinden, R. A., Hill, D. J., Kenward, M. A., Williams, C. D., & Radecka, I. (2007). Bacterial synthesis of biodegradable polyhydroxyalkanoates. Journal of Applied Microbiology, 102(6), 1437-1449. https://doi.org/10.1111/j.1365-2672.2007.03335.x

- Wang, D., et al. (2019). Temperature effects on the growth kinetics of bacterial pathogens: a review. Journal of Food Protection, 82(4), 656-665. https://doi.org/10.4315/0362-028X.JFP-18-211

- Wei, L., et al. (2017). Sustainable bioplastics from renewable resources. Journal of Polymers and the Environment, 25(3), 341-360. https://doi.org/10.1007/s10924-016-0896-x

- Wilcox, C., Van Sebille, E., & Hardesty, B. D. (2015). Threat of plastic pollution to seabirds is global, pervasive, and increasing. Proceedings of the National Academy of Sciences, 112(38), 11899-11904. https://doi.org/10.1073/pnas.1502108112

- Williams, R. J., et al. (2020). Plastics and marine animal health. Environmental Health Perspectives, 128(9), 96001. https://doi.org/10.1289/EHP6174

- Woodruff, M. A., & Hutmacher, D. W. (2010). The return of a forgotten polymer—Polycaprolactone in the 21st century. *Progress in Polymer Science*, 35(10), 1217-1256. https://doi.org/10.1016/j.progpolymsci.2010.04.002

- Wright, S. L., & Kelly, F. J. (2017). Plastic and human health: A micro issue? Environmental Science & Technology, 51(12), 6634-6647. https://doi.org/10.1021/acs.est.7b00423

- Yates, M. R., & Barlow, C. Y. (2013). Life cycle assessments of biodegradable, commercial biopolymers—A critical review. Resources, Conservation and Recycling, 78, 54-66. https://doi.org/10.1016/j.resconrec.2013.06.010

- Zhang, J., Zhang, S., & Yang, R. (2017). Improvement of DNS method for reducing sugar determination. Journal of Agricultural and Food Chemistry, 65(21), 4656-4659. https://doi.org/10.1021/acs.jafc.7b01482

- Zhang, Y.-H. P., et al. (2010). Microbial cellulose utilization: Fundamentals and biotechnology. Microbiology and Molecular Biology Reviews, 74(1), 58-78. https://doi.org/10.1128/MMBR.00046-09

- Zhao, Y., et al. (2018). Statistical analysis strategies for association studies involving rare variants. Nature Reviews Genetics, 19(11), 745-759. https://doi.org/10.1038/s41576-018-0051-5

- Zhao, Q., Sun, L., & Cheng, H. (2025). Application of PHB films in food packaging: Recent developments. *Sustainable Packaging Science*, *3*(1), 25–33.

- Zhu, Q., Geng, Y., & Sarkis, J. (2019). Motivating green public procurement in China: An individual level perspective. Journal of Environmental Management, 250, 109524. https://doi.org/10.1016/j.jenvman.2019.109524

APPENDIX

RESEARCH PUBLICATIONS
AND
CONFERENCES

RESEARCH PUBLICATION

Title

Unlocking sustainable solutions: wood waste as a novel substrate for polyhydroxybutyrate (PHB) production to combat plastic pollution

REFERENCE

Kumar M, Sachan RS, Kauts S, Karnwal A, Mahmoud AE. Unlocking sustainable solutions: wood waste as a novel substrate for polyhydroxybutyrate (PHB) production to combat plastic pollution. Environmental Technology. 2024 Oct 10:1-3.

Unlocking sustainable solutions: wood waste as a novel substrate for polyhydroxybutyrate (PHB) production to combat plastic pollution

Mukesh Kumar, Rohan Samir Kumar Sachan, Simran Kauts, Arun Karnwal & Alaa El Din Mahmoud

View supplementary material

Published online: 10 Oct 2024.

Submit your article to this journal

View related articles

View Crossmark data

CONFERENCES

Participation certificate in oral representation on the title "Isolation of PHA producers from sewage water and production using combined treatment approach" at the international conference "Microbial Bioprospecting for Sustainable Development" held at Lovely Professional University (2023).

Participation certification in oral representation on the title "Isolation and optimization of PHA producers from the waste stream of Jalandhar" at national conference "26th Punjab science

congress on environment, food security and heath with reference to climate change" held at Sri Guru Granth Sahib World University (2023).